GEORGIA INSTITUTE OF TECHNOLOGY
OFFICE OF RESEARCH ADMINISTRATION

Date: November 5, 1970

RESEARCH PROJECT INITIATION

Project Title: Study of Hazards from Burning Apparel and the Relation of Hazards to Test Methods

Project No.: B-1147

Project Director: Dr. S. P. Kezios with Dr. W. Wulff and Dr. N. Zuber, Principal Investigators

Sponsor: National Science Foundat on

Agreement Period: From November 1 1970 until October 31 1971

Type Agreement: Grant No. GK-27189

Amount:
$45,300 NSF Funds (B-1147)
11,653 GIT Contribution (E-1109)
$56,953 Total Budget

NSF Technical Program Director

Dr. Morris S. Ojalvo
Special Engineering Programs
Division of Engineering
National Science Foundation
Washington, D.C. 20550
Phone: (202) 632-4280

Reports Required

Final Technical Letter Report
(See Project Director's Report Schedule)

Final Fiscal Report
(Controller's Office)

Assigned to: School of Mechanical Engineering

COPIES TO:

- [x] Project Director
- [x] School Director
- [x] Dean of the College
- [ ] Director, Research Administration
- [ ] Deputy Controller (2)
- [x] Security-Reports-Property Office
- [x] Patent Coordinator
- [x] Library ✓
- [x] Rich Electronic Computer Center
- [x] Photographic Laboratory
- [ ] EES Machine Shop
- [ ] EES Accounting Office

Other File B-1147

RA-3 (3/70)

GEORGIA INSTITUTE OF TECHNOLOGY

OFFICE OF RESEARCH ADMINISTRATION

RESEARCH PROJECT TERMINATION

Date: February 15, 1972

Project Title: Study of Hazards from Burning Apparel and the Relation of Hazards to Test Methods

Project No: E-25-618 (Old B-1147)

Principal Investigator: Dr. S. P. Kezios, Dr. W. Wulff, Dr. N. Zuber

Sponsor: National Science Foundation

Effective Termination Date: 4-30-72 (Final Report submitted 12/71)

Clearance of Accounting Charges: 4-30-72 (All funds presently committed)

Grant/Contract Closeout Actions Remaining: Final Fiscal Report (within 90 days).

NOTE: Follow-on project is E-25-625.

Assigned to: School of Mechanical Engineering

COPIES TO:

- Principal Investigator
- School Director
- Dean of the College
- Director, Research Administration
- Director, Financial Affairs (2)
- Security-Reports-Property Office
- Patent and Inventions Coordinator
- Library, Technical Reports Section
- Rich Electronic Computer Center
- Photographic Laboratory
- Project File
- Other _____

RA-4 (5-71)

GEORGIA INSTITUTE OF TECHNOLOGY
School of Mechanical Engineering
Atlanta, Georgia

STUDY OF HAZARDS FROM BURNING APPAREL AND THE RELATION OF HAZARDS TO TEST METHODS

FINAL REPORT

By

A. Alkidas
R. W. Hess
W. Wulff
N. Zuber

For

GOVERNMENT-INDUSTRY RESEARCH COMMITTEE
ON FABRIC FLAMMABILITY
Office of Flammable Fabrics
National Bureau of Standards
Washington, D. C. 20234
NSF Grant No. GK-27189

December, 1971

STUDY OF HAZARDS FROM BURNING APPAREL AND THE RELATIONS OF HAZARDS TO TEST METHODS

Final Report

By

A. Alkidas
R. W. Hess
W. Wulff
N. Zuber

School of Mechanical Engineering
Georgia Institute of Technology
Atlanta, Georgia 30332

December 31, 1971

Sponsored by

GOVERNMENT-INDUSTRY RESEARCH COMMITTEE
ON FABRIC FLAMMABILITY
Office of Flammable Fabrics
National Bureau of Standards
Washington, D. C. 20234
NSF Grant No. GK-27189

W. Wulff, Principal Investigator N. Zuber, Principal Investigator

Stothe P. Kezios, Coordinator
Director
School of Mechanical Engineering

GEORGIA INSTITUTE OF TECHNOLOGY
School of Mechanical Engineering

FOREWORD

The research presented here was supported by the National Science Foundation under the RANN program (Research Applied to National Needs), and monitored by the Government-Industry Research Committee on Fabric Flammability. The opportunity to participate in this nationally coordinated research effort is greatly appreciated.

The project was carried out in the Fire Hazard and Combustion Research Laboratory of the School of Mechanical Engineering under the Principal Investigators Dr. Wolfgang Wulff and Dr. Novak Zuber. Dr. Arthur E. Bergles assisted in the supervision of some of the graduate research assistants during the first eight months of the program, specifically in executing fabric ignition temperature measurements, preliminary design from specified concepts and construction on the Ignition Time Apparatus, on the guarded hot plate, as well as initial testing on that equipment.

During the course of the work, the main research assistants involved were Messers. Alexandros Alkidas and Richard W. Hess, both Ph.D. candidates. Mr. Alkidas carried out a large number of property measurements (ignition temperature, enthalpy, conductivity) and assisted in the analysis. Mr. Hess is responsible for the final, successful construction of the Ignition Time Apparatus and the guarded hot plate, as well as the majority of the ignition time measurements.

Also assisting in this research were the M.S. candidates Mrs. Mary J. Kirkpatrick (literature survey on fabric thermal conductivity and specific heat), Mr. Carroll S. Kirkpatrick (design assistance and preliminary construction of the Ignition Time Apparatus), Mr. Edward Champion (fabric enthalpy measurements) and Mr. William Giddens (fabric conductance measurements). Mr. Ronald L. Mays, an undergraduate senior, carried out the optical property measurements.

The participation of the graduate research assistants has been supported in part by the School of Mechanical Engineering under the matching fund provision of the grant. The NSF grant in support of this research is greatly appreciated.

Stothe P. Kezios, Director
School of Mechanical Engineering

December 29, 1971

ABSTRACT

This Final Report presents the research carried out during the time from November 1, 1970 through October 31, 1971, on the portion of the analytical and experimental program administered by the Government-Industry Research Committee on Fabric Flammability (GIRCFF) which has been performed at the Georgia Institute of Technology. The report includes also research carried out between the end of the contract period and the due date of the final report, January 1, 1972.

The hazard from fabric-related burn injuries is shown to be related to the probability of fabric ignition for given exposure to a heat source. The probability of fabric ignition under given exposure depends on the ratio of fabric ignition time to exposure time; hence the ignition time is an important characteristic required to assess the hazards of fabric-related burn injuries. An experimental and analytical program has been carried out to predict the fabric ignition time as function of exposure parameters and fabric properties.

The objective of the experimental phase is two-fold, firstly, to measure the ignition times of a selected set of cotton, nylon, polyester and acetate fabrics and blends, at well defined exposure and fabric conditions, secondly to measure, on the same fabrics, the thermophysical properties which characterize the ignition process. These properties are the thermal conductance, the specific heat, the mass per unit area, the ignition or melting temperature, further the optical properties infrared reflectance and transmittance

and the reaction kinetic parameters activation energy, pre-exponential factor and reaction enthalpy. During the first program period reported herein, ignition time was measured under radiative fabric heating, and all of the properties were measured, except the reaction kinetic parameters.

The objective of the analytical phase is to predict fabric ignition time as a function of fabric properties and exposure conditions. A complete modeling analysis was performed to establish the modeling rules necessary for the prediction of fabric ignition time. Partial modeling rules are discussed, and error estimates appropriate for partial modeling are presented. Modeling experiments are specified which are required to predict ignition time.

Results

Thermal conductance was measured in a guarded hot plate for single layers of fabrics in the temperature range from 70°C to 200°C at the contact pressures of 528,866 and 1,370 N/m^2. The thermal conductance, i.e. the ratio of thermal conductivity to fabric thickness, was found to vary between 60 and 300 W/m^2C) and to increase almost linearly with increasing temperature and pressure, by a factor of up to two.

The specific heat measurements were obtained from enthalpy measurements in a drop calorimeter, carried out in the temperature range between 100°C and 200°C. The enthalpy versus temperature data were graphically smoothed, represented by a power polynomial, and the results were differentiated with respect to temperature. Specific heats were found to vary between 1.2 and 2.5 Ws/(g C) and to agree well with previously published data.

The fabric auto ignition temperature was measured by immersion of the fabric into a modified, preheated Setchkin furnace, flushed by preheated air at the velocity of 0.61 m/S. Pilot ignition temperatures were measured by triggering intermittently a small electric arc near the sample. Melting temperatures are recorded for fabrics which melt prior to ignition. Thermoplastic fabrics were found to melt above 230°C while cellulosic fabrics ignited at temperatures between 280°C and 500°C.

Optical properties were measured in an integrating sphere reflectometer under infrared irradiation. By measuring the apparent reflectance of the fabric, once with a reflecting and once with an absorbing background, both the reflectance and the transmittance were obtained. Most fabrics proved to absorb approximately 20% of the incident radiant flux.

A special Ignition Time Apparatus was designed and constructed, capable of exposing a 1 in.-diameter fabric sample area to a uniform, constant radiant heating pulse of 0.25 to 16.0 W/cm^2 with transients of no more than 5 ms. The energy transmitted through the fabric during the ignition process was monitored by a thermoelectric heat flux meter and the instant of fabric destruction (melt-through or ignition of back face) was sensed by an infrared detector. Ignition times were obtained between 1 and 70 s.

Detailed, distributed-parameter ignition models and simplified analyses based on lumped-parameter models were considered. Governing differential equations were integrated numerically. Seven characteristic groups were established which govern the heating and reaction

processes. Resulting ignition times are compared with experimentally obtained ignition times. The comparison shows the significance of pyrolysis prior to ignition.

TABLE OF CONTENTS

LIST OF FIGURES

LIST OF TABLES

NOMENCLATURE

A	constant in Callendar equation, Equation B-5
A	area
A	pre-exponential factor
B	constant in Callendar equation, Equation B-5
C	waterequivalent of calorimeter
C_o	heat capacity of added water
C_b	heat capacity of basket
c	specific heat
E	activation energy
$E_2(Z)$, $E_3(Z)$	exponential integral of second, third order $E_n(Z) = \int_0^1 y^{n-2} e^{-Z/y}\, dy$
EMF	electrometive force
f	function
ΔH_f	reaction enthalpy
$\bar{h}_c$	convective film coefficient
I	electrical current
I	areal radiant intensity
k	thermal conductivity
k/δ	thermal conductance
m	mass
N_1, N_2	parameters defined by Equations III-10, 21 and 22
$N_{Bi} = h\delta/k$	Biot number of convection
$(N_{Bi})_{rad} = (1-\bar{\delta})\ W/[k/\delta(T_i - T_o)]$,	Biot number of radiation, normalized heating intensity

$N_{Fo} = (k/\delta)t/[c(\rho\delta)]$, Fourier number, normalized time

Q_{if} heat loss from calorimeter

q volumetric heat source

R ohmic resistance

R universal gas constant

T absolute temperature, Kelvin or Rankine scales

t relative temperature, Centigrade or Fahrenheit scale

t time, absolute

U voltage

W radiant heat flux

W* normalized radiant heat flux

x distance

$x^* = x/\delta$ normalized thickness

α radiative absorptance

δ fabric thickness

δ, Δ signal rise, difference

ε mass fraction decomposed by completed pyrolysis

$\theta = (T - T_o)/(T_i - T_o)$ normalized temperature

κ extinction coefficient

$\kappa^* = \kappa\delta$ optical thickness of fabric

λ mass fraction reacted

$\pi_o, \pi_1, \pi_2, \pi_3, \pi_4, \pi_5, \pi_6$ parameters, defined by Equations III-26, 27, 28, 40, 41, 42 and 43

ρ fabric density

$\rho, \tilde{\rho}$ radiative reflectance

τ time, (in Appendix B)

τ non-dimensional time

$\tau, \tilde{\tau}$	radiative transmittance
ϕ	exponent, defined by Equation III-10

subscripts, superscripts:

a	apparent
a	air gap
b	background
c	calorimeter
cl	at center line in fabric, at end of test
e	with empty reflectometer sphere
ex, en	exothermic, endothermic
f	fabric
i	ignition
n	at end of test
r	reference surface
s	sample
w	water
δ	at $x = \delta$
o	incident
0,1,2,I,II	designates particular instances
∞	environment
prime	derivative, slope
*	normalized

I. INTRODUCTION AND PROGRAM OBJECTIVE

A. Introduction

1. Relevance of the Fabric Flammability Hazard Problem

The Flammable Fabrics Act as amended demands that the Secretary of Commerce establish reasonable criteria or standard tests to be imposed on fabrics so as to protect the public from excessive hazards of fabric related burn injuries. In order to establish the technical and scientific foundation for the required legislation, the United States textile industry and the United States Government have initiated a cooperative effort in sponsoring, jointly, research programs designed to lay down this foundation. The task of formulating and administrating these programs has been delegated to the Government-Industry Research Committee on Fabric Flammability.

In initiating the research in support of the Flammable Fabrics Act, the Government-Industry Research Committee made the following statement in Reference [I-1]*:

"The determination of the relationship between fabric behavior in a test method, on the one hand, and the hazard it presents in actual use, on the other, is necessary in order to develop meaningful standards."

The determination of this relation can be considered therefore as the central problem of fabric flammability studies.

---

*Numbers in brackets refer to the Bibliography.

2. Formulation of the Fabric Flammability Hazard Problem

It was proposed, apparently first in Reference [II-2], that the above relation between the behavior of fabric in a laboratory experiment and the hazard it presents in actual use, can be formulated in terms of probabilities. Among the several probabilities shown in the decision tree of Reference [II-2], two probabilities were singled out by the Government-Industry Research Committee as being of particular importance. These were: the probability of ignition given exposure, P(I/E), and the probability of burn injury given ignition (P(B/I).

The primary purpose of the research outlined by the Government-Industry Research Committee in Reference [II-1] was to "determine what properties of a fabric are important in determining the values of P(I/E) and P(B/I)."

In a discussion of the importance of these two probabilities it was noted in Reference [II-1], that the determination of the probability of ignition P(I/E), as function of the time it takes to ignite a fabric "would be an enormous step forward in our understanding of the relationships between material performance and hazard." Whereas it was noted with respect to the probability of burn-injury P(B/I), that "the determination of this function for various levels of fabric flammability would be one of the most desirable outcomes of the present work."

It was first shown in Reference [II-3] how modeling analysis and experiments can be used to obtain the probability of ignition P(I/E) as well as the probability of burn injury P(B/I).

In particular, it was shown in Reference [II-3], how the probability of ignition P(I/E) curve can be obtained and expressed in terms of: 1) physical properties and dimensions of the fabric material, 2) physical processes such as heat and mass transfer, etc., and 3) human responses and reaction.

Similarly, it was discussed and illustrated in Reference [II-3], how the probability of burn injury P(B/I) curve can be obtained and expressed as a function of: 1) physical properties and dimensions of the fabric material, 2) physical processes such as combustion, flame propagation, heat and mass transfer, 3) physical characteristics of human skin, and 4) human responses and reactions.

The investigations which are being carried out in the School of Mechanical Engineering of Georgia Tech under the sponsorship of the Government-Industry Research Committee on Fabric Flammability (GIRCFF), are designed to provide the modeling rules and experimental data which are required for determining the probability of ignition P(I/E) curve.

B. Program Objective

With the ultimate goal of predicting the ignition probability P(I/E) in mind, the objective of the research reported herein has been established [I-3] to be the prediction of fabric ignition time as a function of fabric properties and of exposure conditions. The research consists of an analytical and an experimental phase.

The specific objectives of the analytical program are:

a. a complete modeling analysis for the purpose of determining the relevant modeling rules needed to assess the ignition time; the analysis will be carried out by examining the governing differential equations and will take into account (1) fabric material properties, (2) physical processes such as heating modes and boundary conditions, and (3) different geometries;

b. the development of the rules for partial modeling on the basis of the governing differential equations;

c. an assessment of the errors involved with partial modeling.

The specific objectives of the experimental program are to carry out the partial modeling experiments to determine

d. the fabric ignition time under well-controlled exposure conditions to support the analysis, and

e. all the relevant fabric properties which describe the fabric behavior during the heating process until ignition or melting occurs.

Originally, these fabric properties were anticipated to be

the constant-pressure specific heat c_p
the enthalpy of reaction Δi
the thermal conductivity k normal and parallel to the fabric
the fabric thickness δ
the fabric density ρ
the ignition temperature T_i

but it became evident during the program that, after having chosen radiative heating as the first and simplest heating source, optical properties are most relevant and the above list was changed as discussed in Chapter II.

Chapter II is a presentation of the experimental accomplishments. Details of instrumentation and experimental procedures are presented in Appendix B. The analysis and the comparison between experimental and analytical results are discussed in Chapter III. The conclusions are summarized in Chapter IV. A fabric-by-fabric property summary for the ten primary GIRCFF fabrics, selected by the Government-Industry Research Committee on Flammable Fabrics, is presented in Appendix A. Finally, a summary of the literature survey on fabric properties is given in Appendix C.

II. EXPERIMENTAL PROGRAM

The objective of the experimental program is to measure the thermophysical fabric properties which characterize the fabric behavior during the ignition process and to measure the fabric ignition time itself under well-defined heating conditions so that the analytically predicted ignition time may be verified or the analysis modified and refined until sufficient agreement is reached between analysis and experiment. The particular fabric properties to be measured are density, ignition temperature, thermal conductivity, specific heat at constant pressure, reflectance and absorptance. The ignition time measurement and the measurements of each fabric property are considered separate tasks and discussed below in the above order. Fabric identification for the ten primary GIRCFF fabrics are given in Table II-1.

A. Ignition Time Measurements
(Task 1)

1. Objective

The purpose is to measure the ignition time defined as the time between the instantaneous fabric exposure to a well-known, uniform and time-invariant heat flux and the fabric ignition, or destruction, as recognized through the appearance of a flame or the melt-through of the fabric. The ignition time, considered a key parameter in the definition of ignition probability, must be measured to verify its analytical prediction. An Ignition Time

TABLE II-1. THE TEN PRIMARY GIRCFF FABRICS

GIRCFF No.	Classification	Fiber Composition	Color	Chemical Finish	Weight oz/sq.yd.
2	Textured Woven Blouse	100% Polyester	Yellow	---	2.19
5	T-Shirt, Jersey	100% Cotton	White	---	3.97
8	T-Shirt, Jersey	65/35% PE/C	White	---	4.82
10	Batiste	100% Cotton	Purple	---	2.04
11	Tricot	80/20% Acet./Nylon	White	---	2.67
12	Tricot	100% Nylon	White	---	2.47
13	Tricot	100% Acetate	White	---	2.44
17	Batiste	65/35% PE/C	White	---	2.53
18	Flannel	100% Cotton	White	---	3.69
19	Flannel	100% Cotton	White	Fire Rtd	4.21

Apparatus was designed and constructed with design specifications established to meet the above objective as follows [II-1]:

a. Radiative sample heating at heat fluxes between 0.25 and 15.8 W/cm^2 (800 to 50,000 $Btu/(hr\ ft^2)$).

b. Sample exposure transients of less than two milliseconds to achieve sufficiently time-independent exposures of as low as 20 milliseconds. Maximum exposure time of 60 seconds.

c. Remote infrared flame detection consistent with Item (b).

The operating principle and the design features of the Ignition Time Apparatus are discussed in Appendix B.1, achievements and results are discussed below.

2. Achievements, Ignition Time Measurements

The total of 127 ignitions was carried out and the results are evaluated in nondimensional form as discussed in Section 3 below. The ten primary GIRCFF fabrics were exposed to irradiance levels between 5.73 W/cm^2 (the minimum to achieve ignition in most of the ten primary GIRCFF fabrics) and 20.05 W/cm^2 (the limit of the heating source). Ignition or destruction times were measured successfully in the range of 1 to 90 seconds but are expected to be lower in fabrics which are more opaque than the samples in the primary GIRCFF set. The final design of the Ignition Time Apparatus has exposure transients of less than 10 milliseconds or 1% of the lowest "ignition" time measured.

3. Experimental Results

"Ignition" is defined as either the occurrence of a flame at the heated front face of an igniting fabric or the onset of melting at the heated front face of a fabric which melts before the ignition of its volatile decomposition products. Recorded are, however, the times associated with the occurrence of a flame at the back face of igniting fabrics or with the onset of a break through in the heated zone of the fabric. Both events are sensed by the radiometer placed 0.500 in or less behind the fabric back face.

Ignition time is defined as the time elapsed between the sudden exposure of the fabric to the heating source and ignition as defined above.

The difference between ignition times based on the original definition of ignition on the one hand and the apparent ignition as measured on the other, is small, between 2 and 5% at most. This conclusion is arrived at both by observation and by analysis.

The ignition time data are normalized and presented in the form

$$(N_{Fo})_i = f\{(N_{Bi})_{rad}, \kappa^*\} \qquad \text{(II-1)}$$

which is the normalized ignition time, i.e. the Fourier number of ignition

$$(N_{Fo})_i = \frac{(\frac{k}{\delta})\ t_i}{c(\rho\delta)} \qquad \text{(II-2)}$$

as a function of the normalized heating intensity or the ratio of external to internal thermal conductances, expressed as Biot number of radiation

$$(N_{Bi})_{rad} = \frac{(1-\tilde{\rho})\ W_o}{(\frac{k}{\delta})\ (T_i - T_o)} \qquad \text{(II-3)}$$

and the optical thickness

$$\kappa^* = \kappa\delta \qquad \text{(II-4)}$$

The symbols represent

- (k/δ) thermal conductance (W/cm^2c), or ratio of thermal conductivity k over thickness δ
- $t/_i$ ignition time (s)
- $(\rho\delta)$ mass per unit of fabric area, (g/cm^2), ρ is fabric density
- c specific heat of fabric, (Ws/g K)
- T_i ignition temperature (self ignition) (K)
- T_o initial fabric temperature, equal to environmental temperature, (K)
- $\tilde{\rho}$ radiative fabric reflectance, (-)
- κ radiative extinction coefficient, (-)

This non-dimensional representation, Equation II-1, is based on the analysis presented in Chapter III-C.1 and affords the reduction in the number of variables from nine to three. A family of one-parameter curves describes all fabrics; the optical thickness k* serves as the parameter.

Figures II-1 through 10 show the final results of the experimental ignition data, evaluated with the fabric properties as measured during this research program and reported in Chapter II-B.

Shown are ignition results obtained by Georgia Tech and by Factory Mutual [II-3]. For the Georgia Tech ignition tests all fabrics were dryed in a desiccator for 12 hours or more. Most ignition tests were carried out in 55 to 65% relative humidity environment. The tests were completed within three minutes or less after removal of the dried sample from the desiccator. Doubling this time span gave no noticeable change in ignition time, and it was concluded that the fabric had, at the start of the exposure, the same properties as at the time it was removed from the desiccator.

In Figures II-1 through 10 there are represented the ignition data for the ten primary GIRCFF fabrics, in the order of their respective GIRCFF numbers. Figure II-11 is a summary of data from all ten primary GIRCFF fabrics which shows the trend of ignition time with optical thickness: the fire-retardant cotton fabric absorbs strongest and has the lowest non-dimensional ignition time. The trend toward higher Fourier numbers with decreasing optical thickness or absorption coefficient is demonstrated in principle, although the effects of pyrolysis blank out in part this trend (see GIRCFF Nos. 8, 11, 12 and 17 for example).

The data exhibit basically a deterministic character, their general smoothness suggests unique ignition times under well-controlled circumstances.

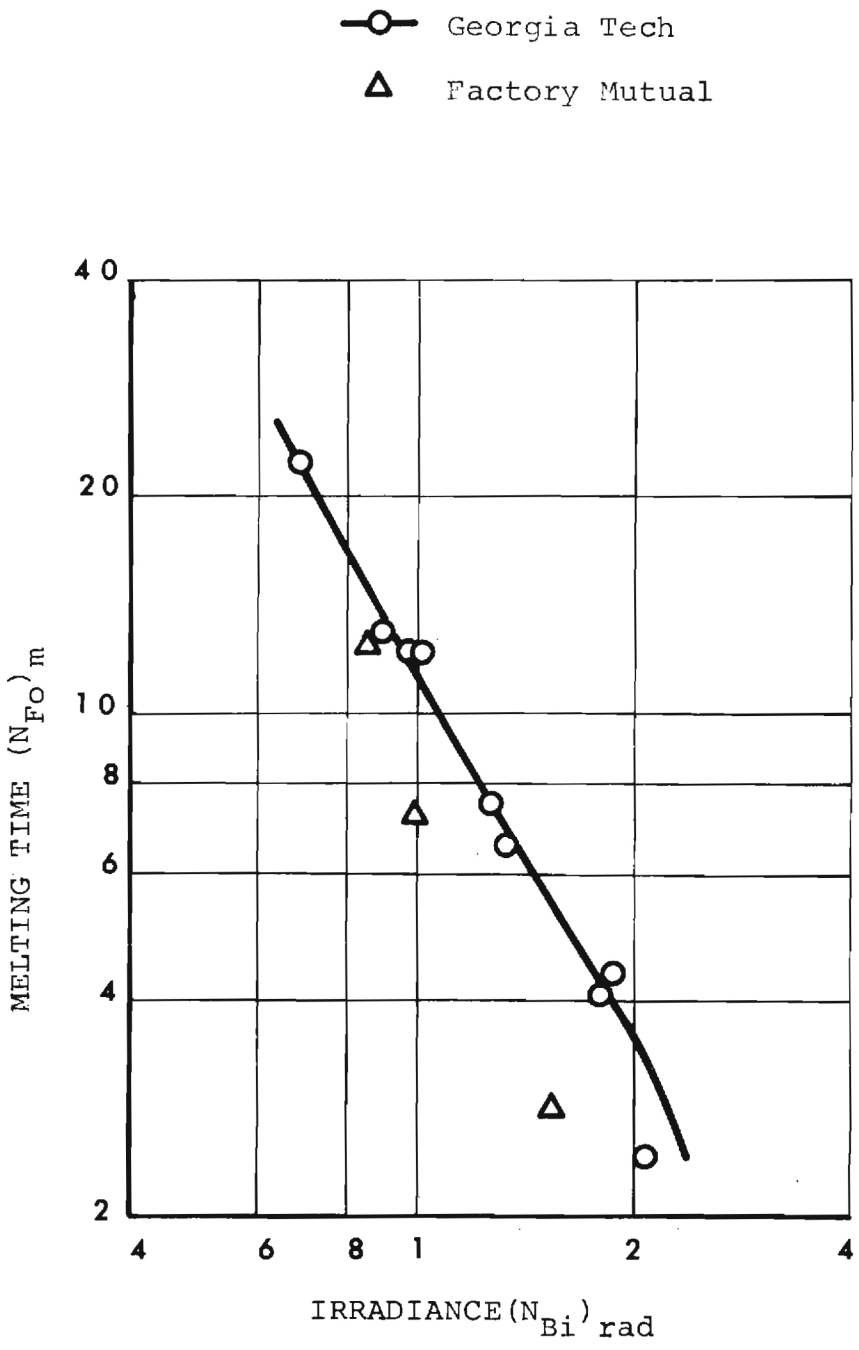

Figure II-1. Non-Dimensional, Experimental Melting Time vs Non-Dimensional Irradiance For 100% Polyester; GIRCFF No. 2

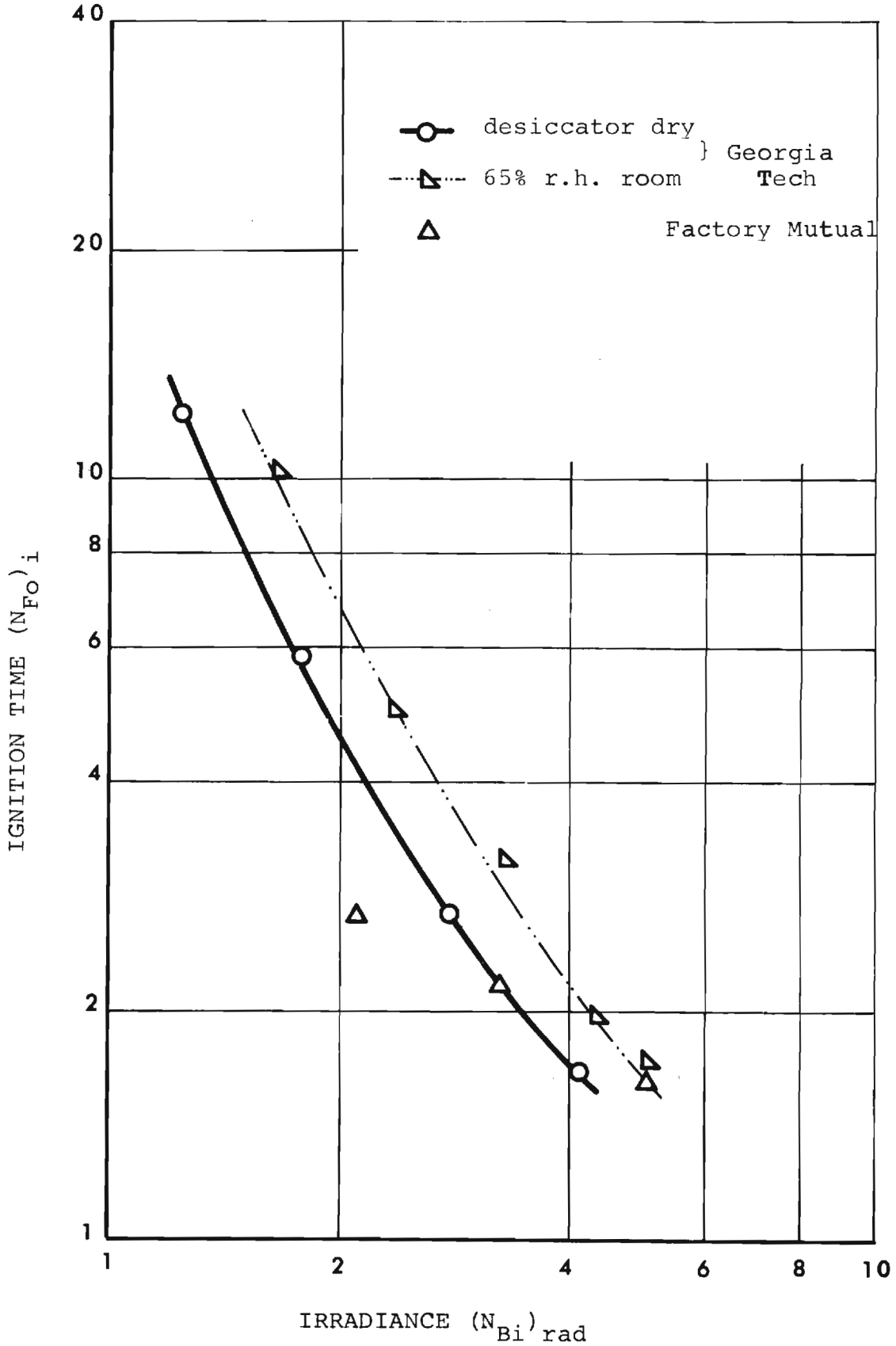

Figure II-2. Non-Dimensional, Experimental Ignition Time vs Non-Dimensional Irradiance For 100% Cotton; GIRCFF No. 5

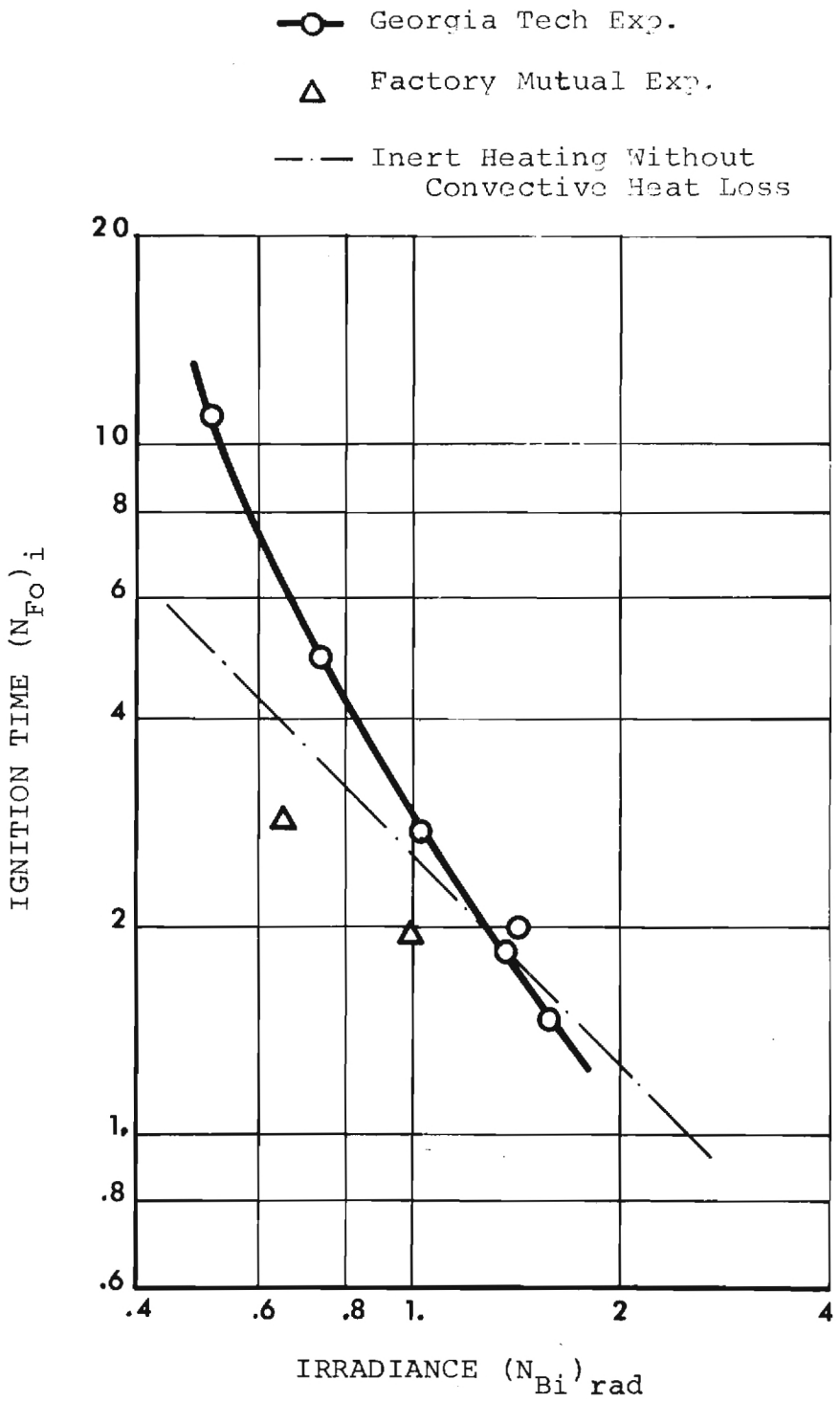

Figure II-3. Non-Dimensional, Experimental Ignition Time vs Non-Dimensional Irradiance for 65/35% Polyester/ Cotton Blend; GIRCFF No. 8

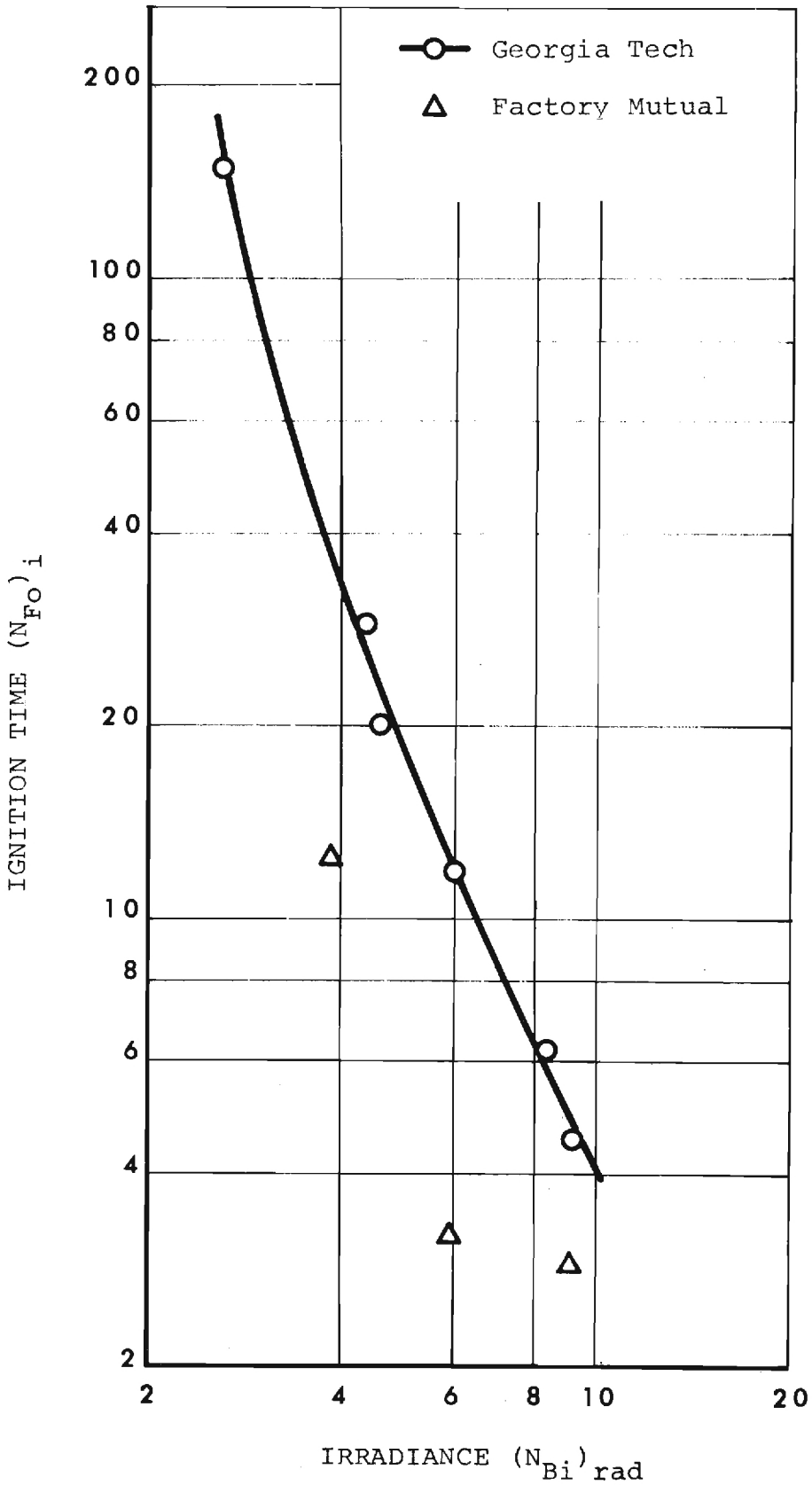

Figure II-4. Non-Dimensional, Experimental Ignition Time vs Non-Dimensional Irradiance For 100% Cotton; GIRCFF No. 10

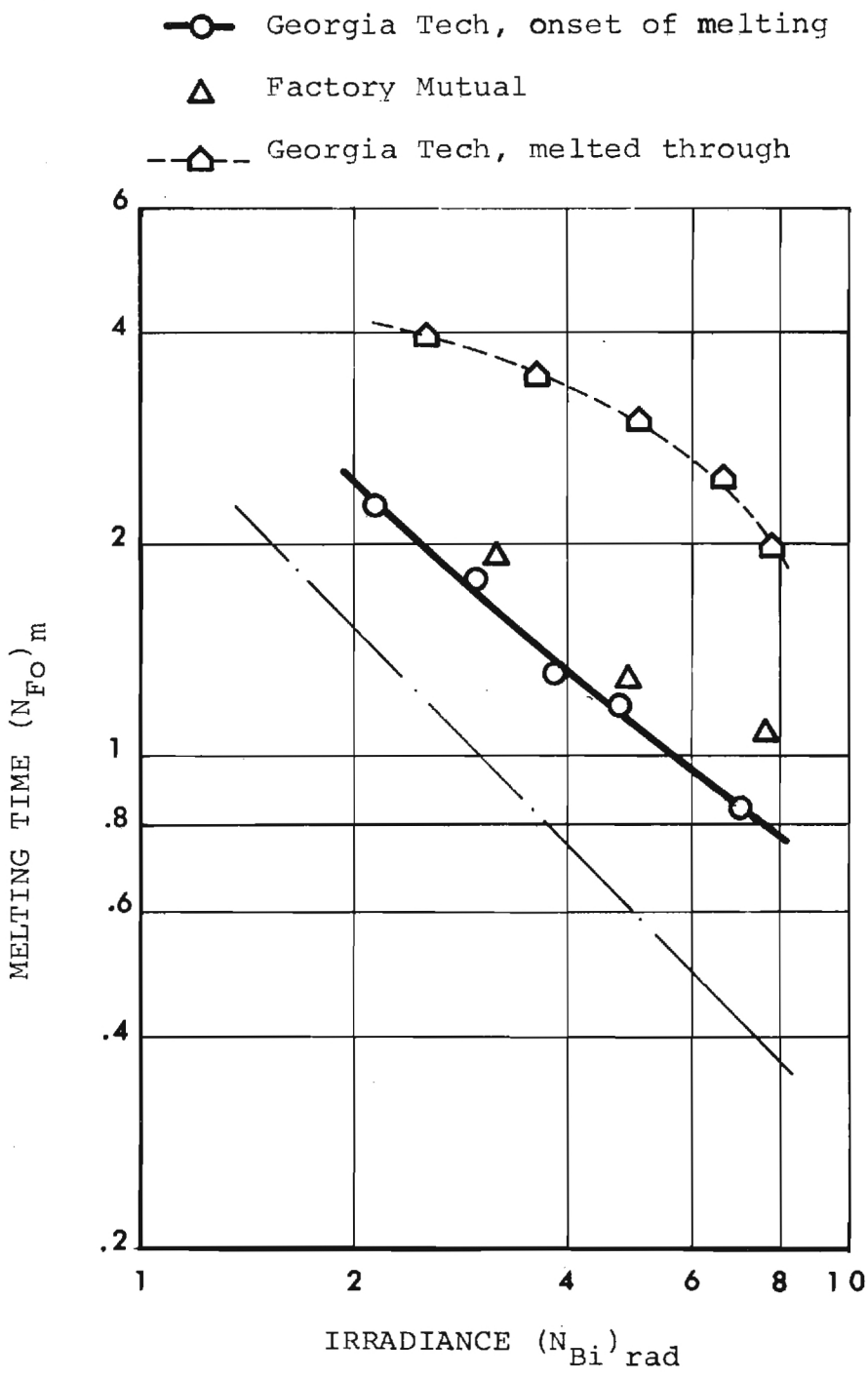

Figure II-5. Non-Dimensional, Experimental Melting Time vs Non-Dimensional Irradiance For 80/20% Acetate/ Cotton; GIRCFF No. 11

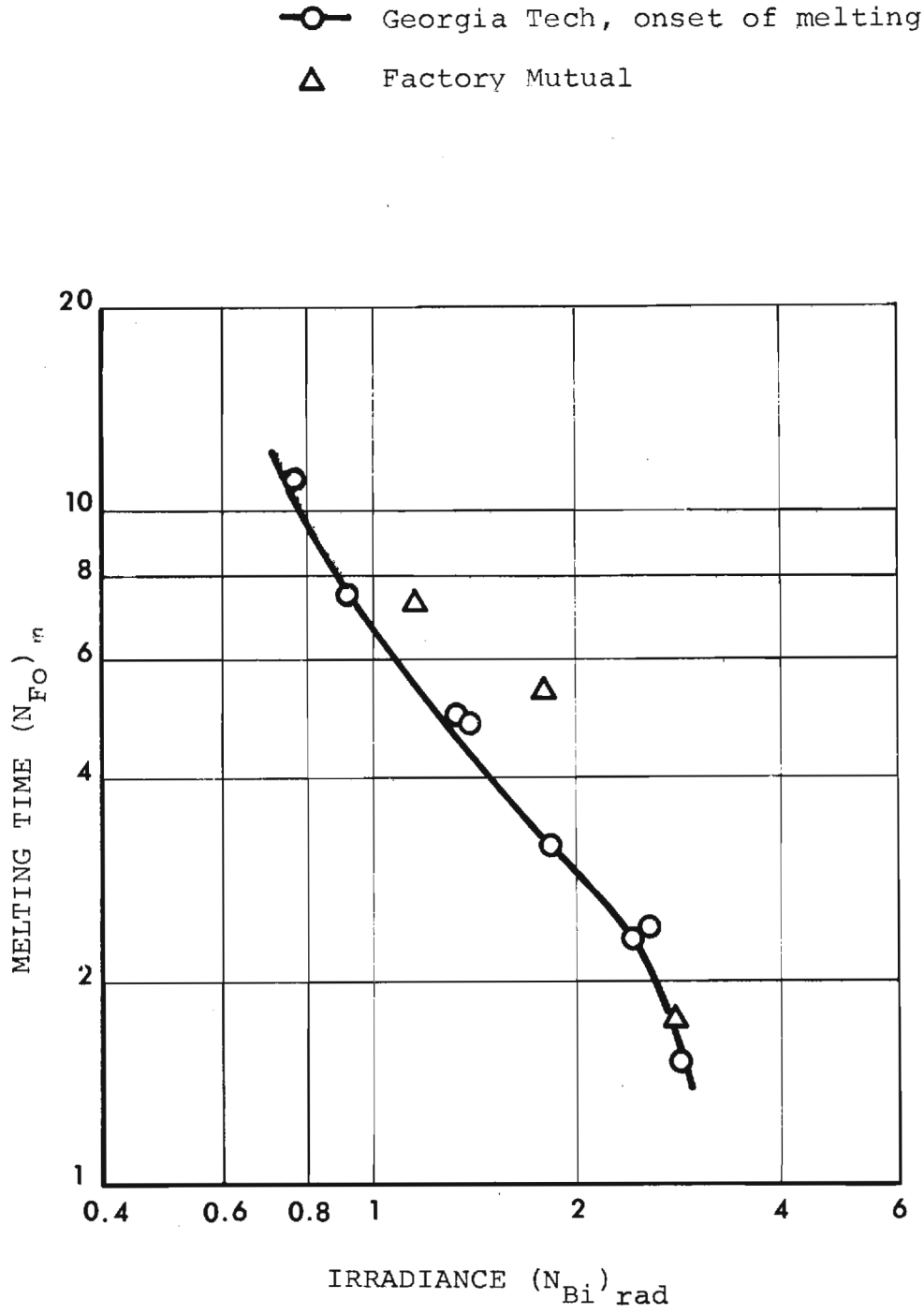

Figure II-6. Non-Dimensional, Experimental Melting Time vs Non-Dimensional Irradiance For 100% Nylon; GIRCFF No. 12

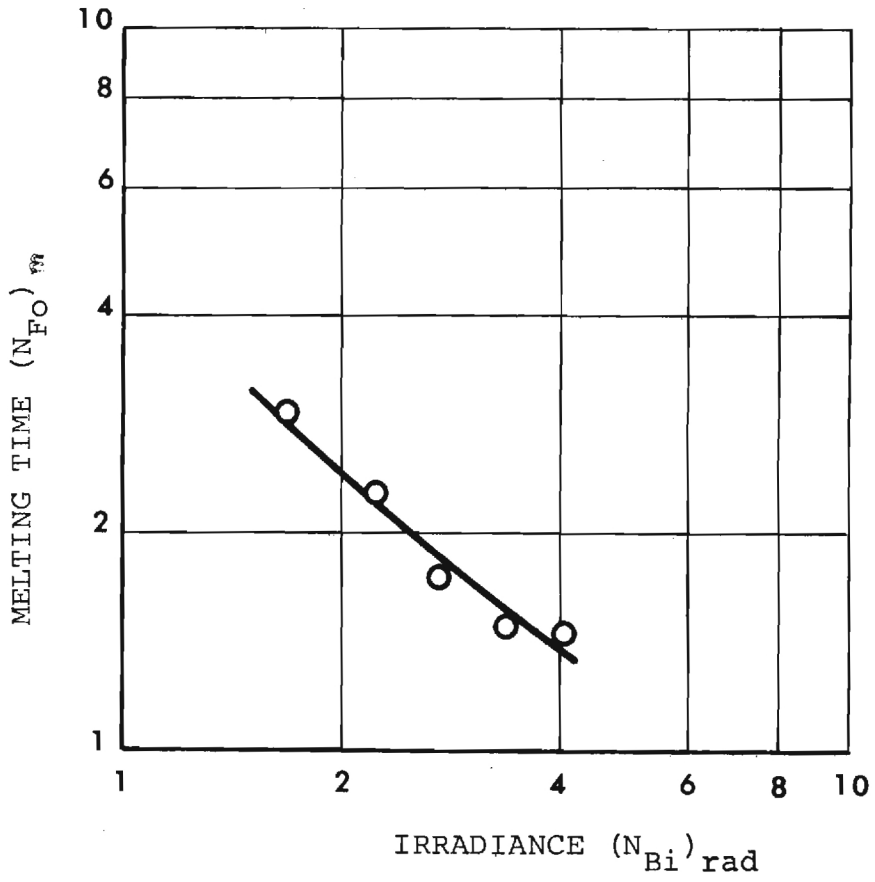

Figure II-7. Non-Dimensional, Experimental Melting Time vs Non-Dimensional Irradiance For 100% Acetate; GIRCFF No. 13

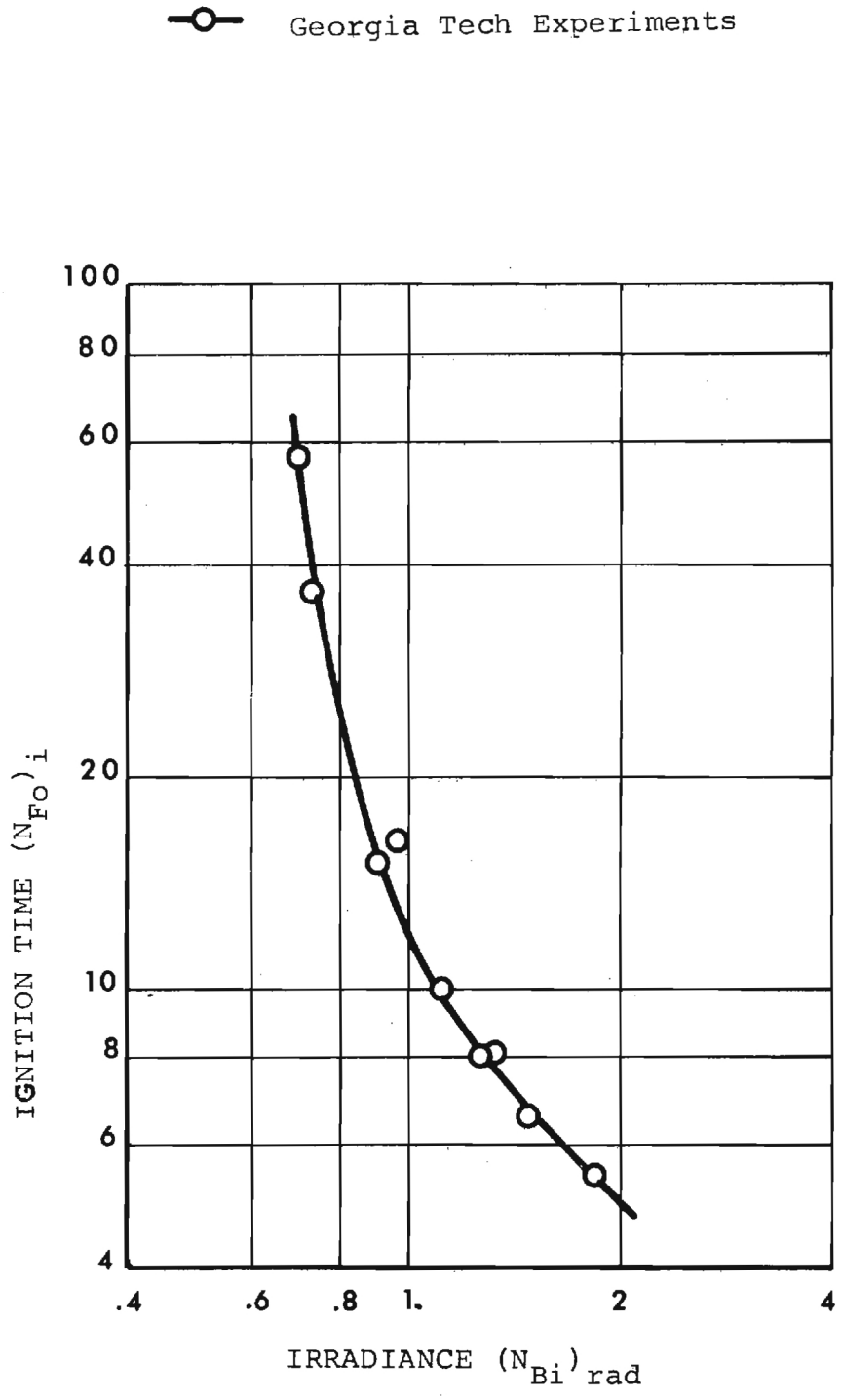

Figure II-8. Non-Dimensional, Experimental Ignition Time vs Non-Dimensional Irradiance For 65/35% Polyester/Cotton; GIRCFF No. 17

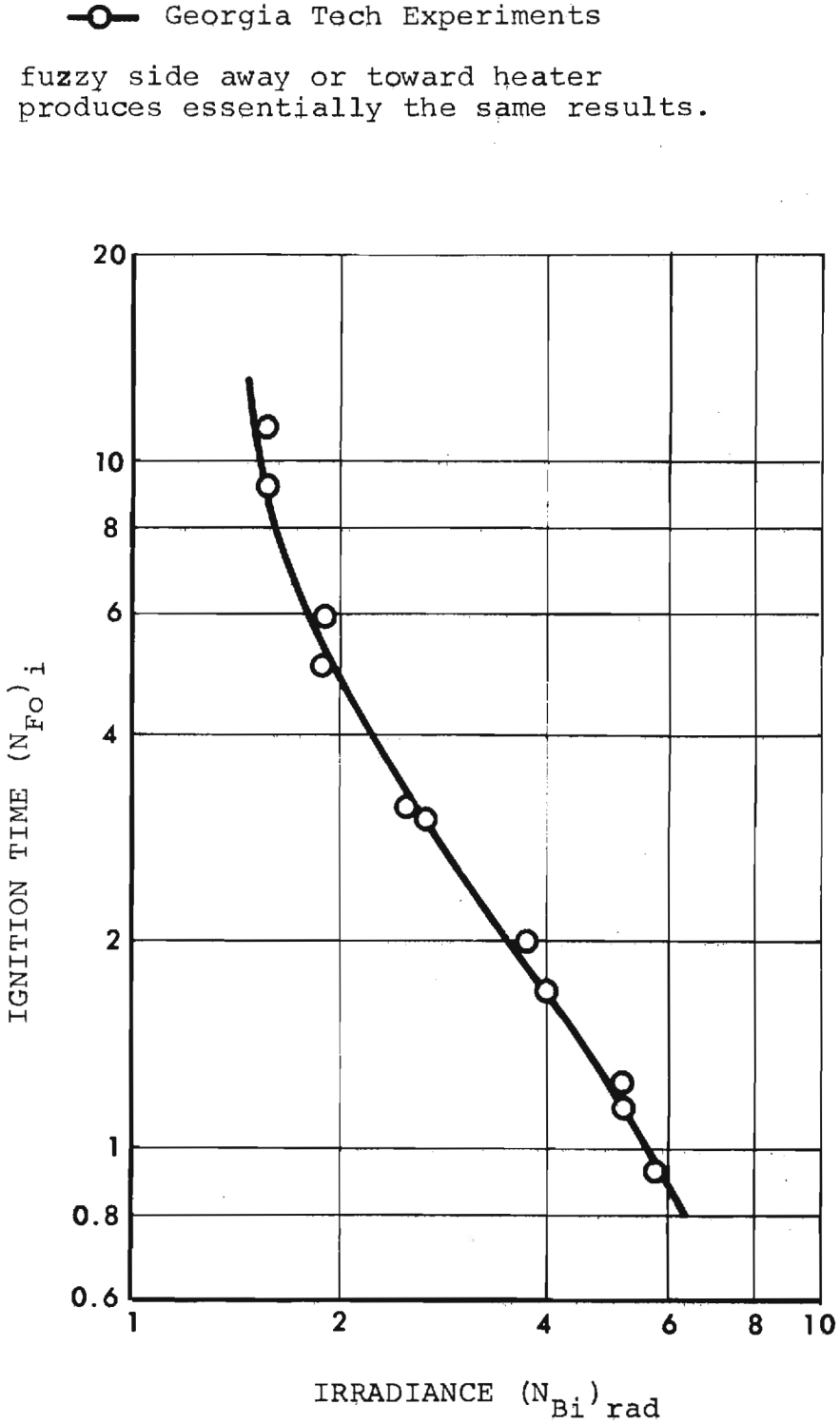

Figure II-9. Non-Dimensional, Experimental Ignition Time vs Non-Dimensional Irradiance For 100% Cotton; GIRCFF No. 17

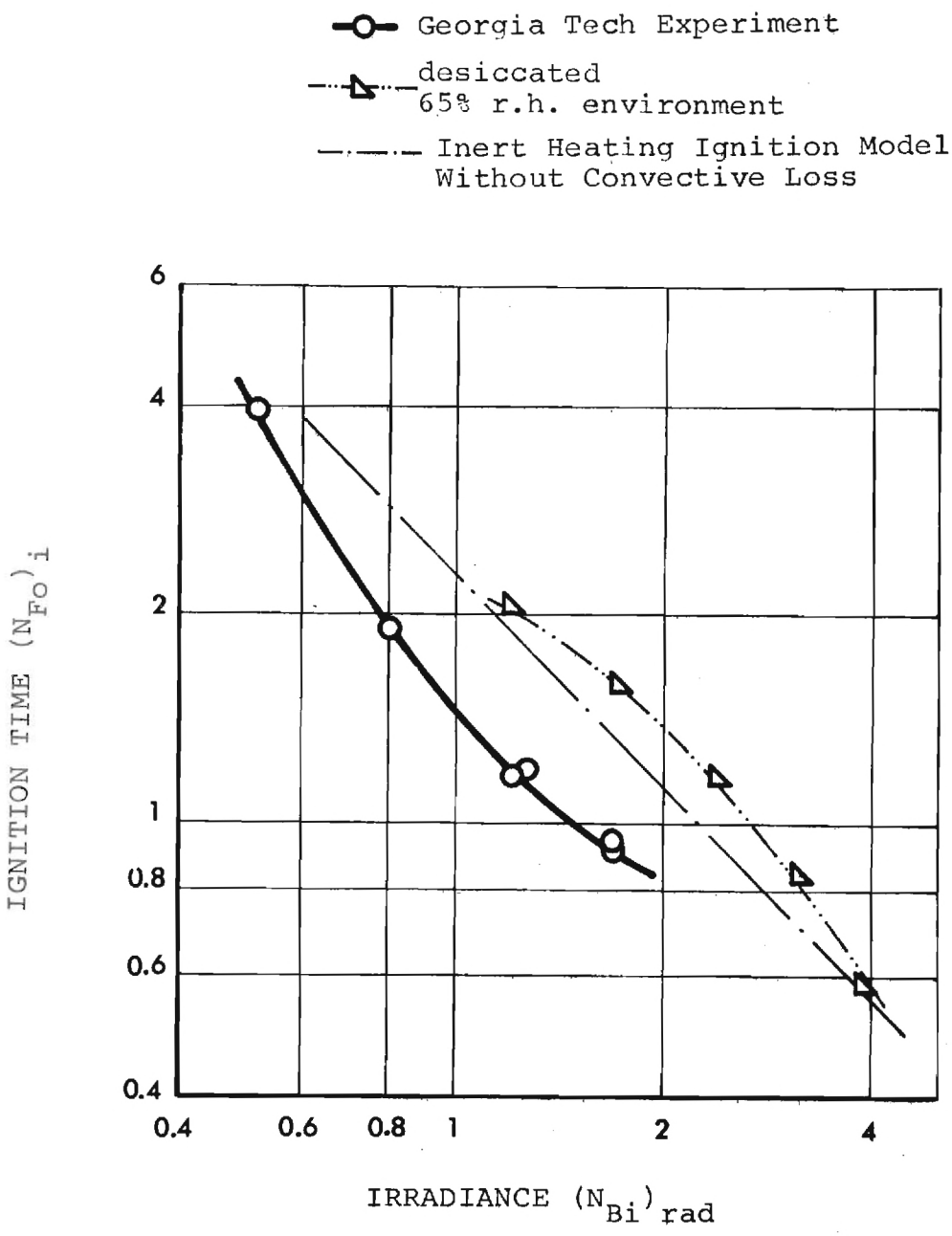

Figure II-10. Non-Dimensional, Experimental Ignition Time vs Non-Dimensional Irradiance For 100% Cotton, Treated With Fire Retardant; GIRCFF No. 19

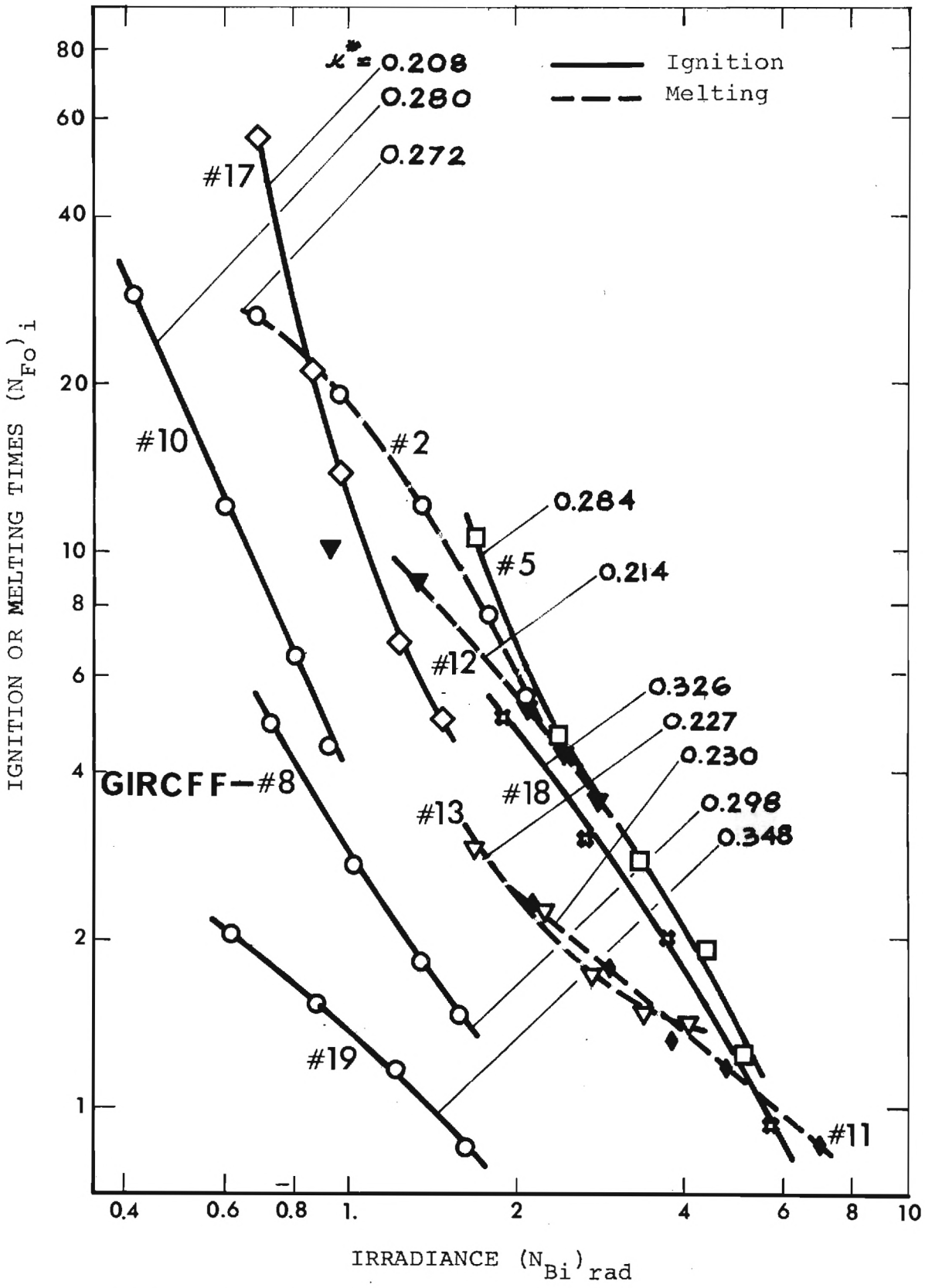

Figure II-11. Summary of Experimental Ignition Data in Non-Dimensional Form

B. Property Measurements
(Tasks 2 through 6)

1. Purpose

A fabric must be heated before it reacts and ignites. The heating process was therefore selected as primary objective during the first program in the study of fabric flammability. The thermophysical properties which characterize fabric behavior during heating are

fabric density, ρ
specific heat of fabric, c
thermal conductivity, k
fabric thickness δ
ignition temperature T_i
radiative properties, reflectance $\tilde{\rho}$, transmittance $\tilde{\tau}$ (for ignition by radiative heating)

The above list of properties lead originally to 6 tasks of property measurements. It was recognized, however, during the program that, firstly, the fabric thickness measurement is not needed, secondly, the fabric density measurement can be replaced by the mass per unit of area measurement and, thirdly, the measurement of thermal conductivity can be replaced by that of the thermal conductance, i.e. of k/δ. All three changes simplify the property measurements significantly. Finally, the thermal conductance measurements were performed in spite of the conclusion reached through analysis (see Chapter III-C.1) that the fabric conductance is insignificant in the description of the ignition process for all ten primary GIRCFF fabrics.

Reaction enthalpy measurements were originally proposed to be included but later eliminated from the program when it became evident that optical properties were far more important to the description of the fabric-heat source interaction then reaction enthalpy was to the prediction of the ignition process. Optical property measurements were not originally proposed. The exclusion of chemical reaction properties was justified on the assumption that reactions prior to ignition contribute only insignificantly to the time requirement for ignition. The assumption is correct for intensive heating levels, but a large number of fabric ignition tests at low and moderate heating levels proved the assumption very restrictive.

With this background, the objective of the property measurement program finally became to establish, on the same fabrics as used in the ignition time measurement, the following five properties

fabric mass per unit area, $\rho\delta$
specific heat of fabric, c
thermal conductance, k/δ
ignition temperature, T_i
radiative properties, reflectance, $\tilde{\rho}$, transmittance, $\tilde{\tau}$.

The property measurement program was accordingly divided into five tasks. The achievements and results of the property measurement program are discussed below for each task. Experimental procedures and test apparatus are described in Appendix B, the literature survey on fabric properties is covered in Appendix C. Finally, a summary of properties, collected for each fabric, is given in Appendix A.

2. Achievements, Property Measurement Program

Task 2. Fabric Mass Per Unit Area.

The total of ten weighings was performed on an analytical balance on samples of 5 in by 5 in large. The results agree well with those obtained by NBS as shown in Section 3 below.

Task 3. Specific Heat of Fabrics.

An existing furnace was modified to serve for the heating of fabric samples. A calorimeter was designed, constructed and calibrated. For details see Appendix B-2.

The total of sixty enthalpy measurements was performed on the ten primary GIRCFF fabrics, in the temperature range from 120°C to 200°C. Not all of the sixty measurements were successful, primarily because of the thermal instability of the fabrics at elevated temperatures. However the specific enthalpy is deemed to be established for all fabrics with a confidence of $\pm$10% except for the GIRCFF Fabric No. 12 which is pure nylon. Here the experimental results were supplemented by published data.

A literature survey was performed to collect published specific heat data of fabrics. Details are given in Appendix C.1.

Task 4. Thermal Conductance of Fabrics.

A guarded hot plate was designed and constructed to measure thermal conductance with the accuracy of $\pm$5%. Details are presented in Appendix B.3.

The total of 56 conductance measurements was performed on the ten primary GIRCFF fabrics between 67°C and 205°C. Of these 56 tests, 34 were performed at the contact pressure of 528 N/m^2, 12 tests at the pressure of 866 N/m^2 and 10 tests at the pressure of 1,370 N/m^2. The results are given in Section 3 below.

An extensive literature search was carried out on fabric properties related to its thermal conductivity. Details are given in Appendix C.2.

Task 5. Ignition Temperature Measurements.

A commercially available Setchkin furnace was extensively modified and improved as discussed in Appendix B.4.

Over 120 ignition temperature measurements were performed, 95 of which after the final improvement was completed on the Setchkin Furnace. Self-ignition or melting temperatures and pilot ignition temperatures of non-melting fabrics were obtained for all of the ten primary GIRCFF fabrics and for six of the ten secondary GIRCFF fabrics. The results are reported in Section 3 below.

Task 6. Radiative Properties.

An existing integrating sphere reflectometer was modified, prepared, calibrated and assembled with a purchased light source, for the purpose of measuring directional-hemispherical infrared reflectance and transmittance. The design details and operating procedures are discussed in Appendix B.5.

Each measurement consists of two test runs and two reference measurements to obtain two properties, reflectance and transmittance.

The total of 32 measurements (64 test runs) was performed. Of these there were 20 measurements carried out on the ten primary GIRCFF fabrics in their original state, each fabric at two wavelength distributions, and 12 measurements were carried out on charred samples. The results are presented in Section 3 below.

Previously published radiative fabric properties are summarized in Appendix C.3.

3. Experimental Results, Fabric Properties

Task 2. Fabric Mass Per Unit Area, $\rho\delta$

This measurement replaces the separate measurements of density ρ and fabric thickness δ, because the analysis discussed in Chapter III requires only the product $\rho\delta$.

Samples of 25 in^2 $\pm 2\%$ were weighed with an analytical balance to within $\pm 1\%$ in dry condition. The results are shown in Table II-2, the first column indicates the results obtained by NBS and reported by Gillette Company Research Institute in their original fabric definition (letter to contractors of January 7, 1971). The second column labeled G.T. are the Georgia Tech results. The third column contains the results of thickness measurements by micrometer, carried out under the contact pressure of 528 N/m^2. The thickness, however, is not required in the analysis.

Table II-2. FABRIC MASS PER UNIT AREA

GIRCFF Fabric Number	Mass Per Unit Area g/cm^2		Fabric Thickness cm
	N.B.S.	G.T.	
2	7.41×10^{3}	7.51	0.0201
5	13.43	13.71	0.0529
8	16.31	16.19	0.062
10	6.91	6.65	0.0177
11	9.05	11.31	0.0614
12	8.36	8.91	0.0271
13	8.26	9.40	0.0304
17	8.56	8.55	0.0193
18	12.49	12.88	0.0713
19	14.25	14.81	0.0692

Task 3. Specific Heat of Fabrics

The results of enthalpy vs temperature measurements are shown in Figures II-12 through 22 for the ten primary GIRCFF fabrics. Curves were fitted graphically to the plotted data points. The resulting curves were read at equal temperature intervals and the ordered pairs of data points obtained were represented by power polynomials of up to fourth degree. The results of differentiating the power polynomial are the specific heats listed in Table II-3.

Results obtained for GIRCFF Fabric No. 12 were not satisfactory as shown by the data points. Specific heat data from Reference II-4 were converted to enthalpy and plotted. Further measurements are in progress. Ignition data were evaluated for Fabric No. 12 with specific heats of pure nylon as taken from Reference II-4 and reported in Table II-3.

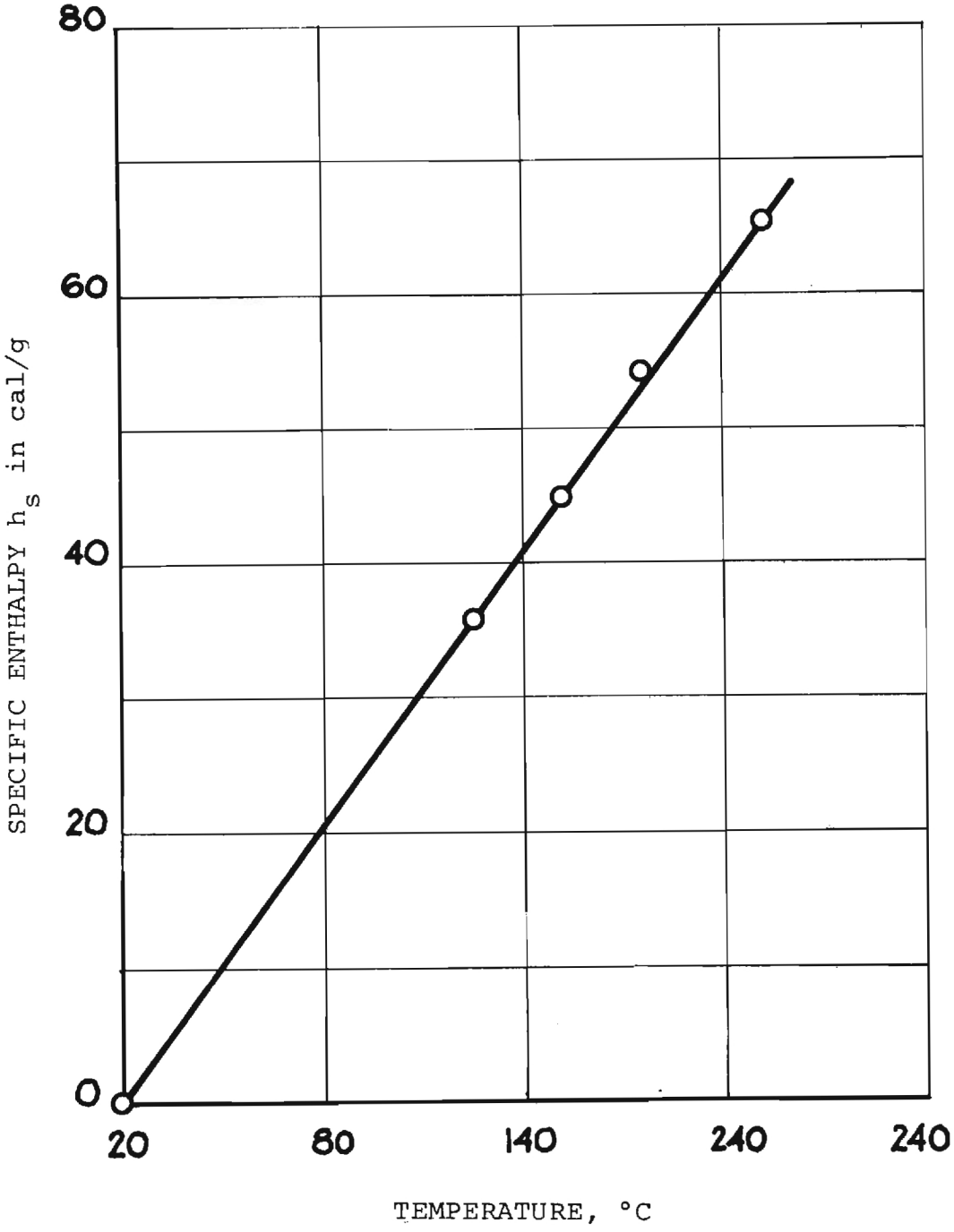

Figure II-12. Enthalpy vs Temperature For 100% Polyester, GIRCFF No. 2

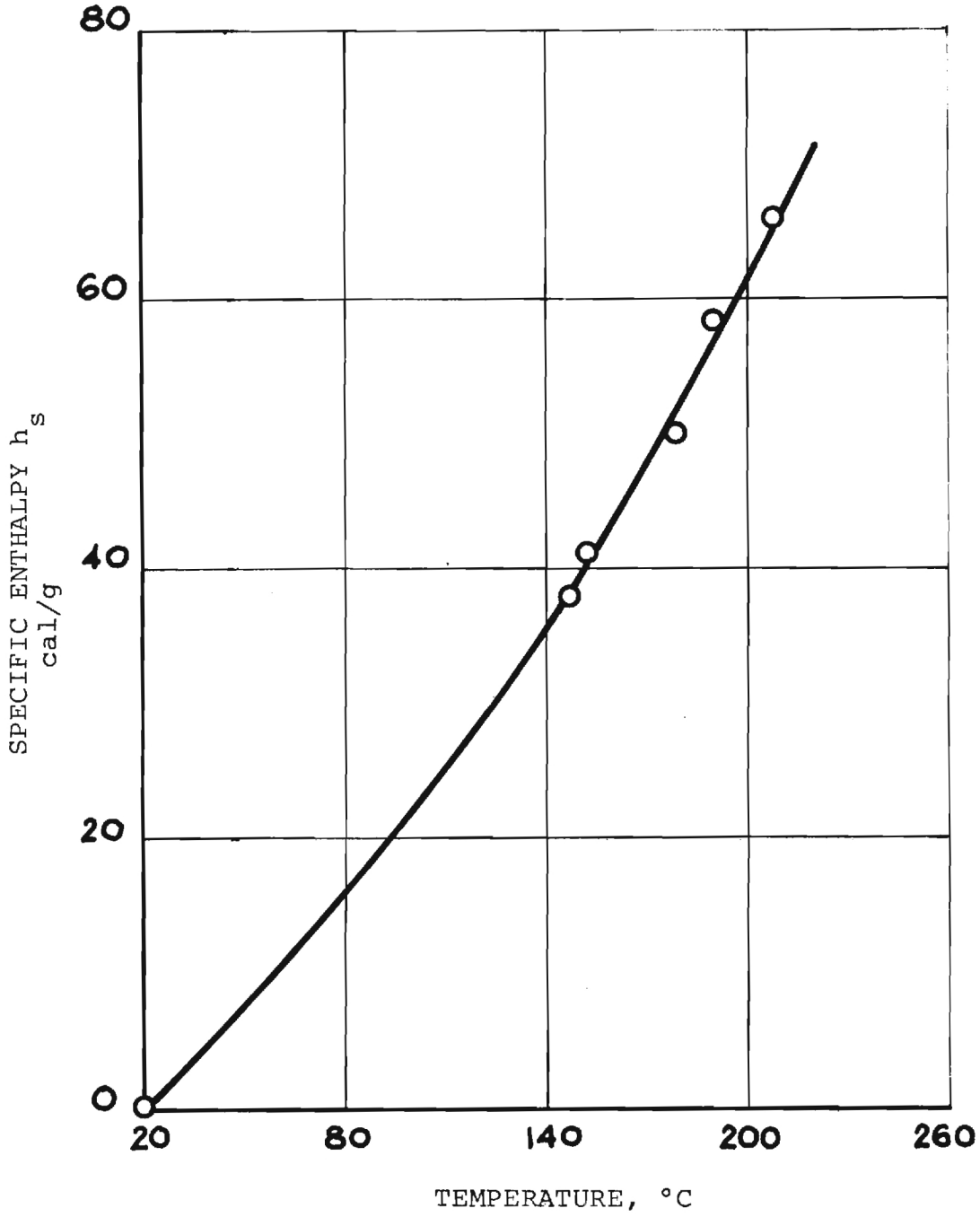

Figure II-13. Enthalpy vs Temperature For 100% Cotton, GIRCFF No. 5

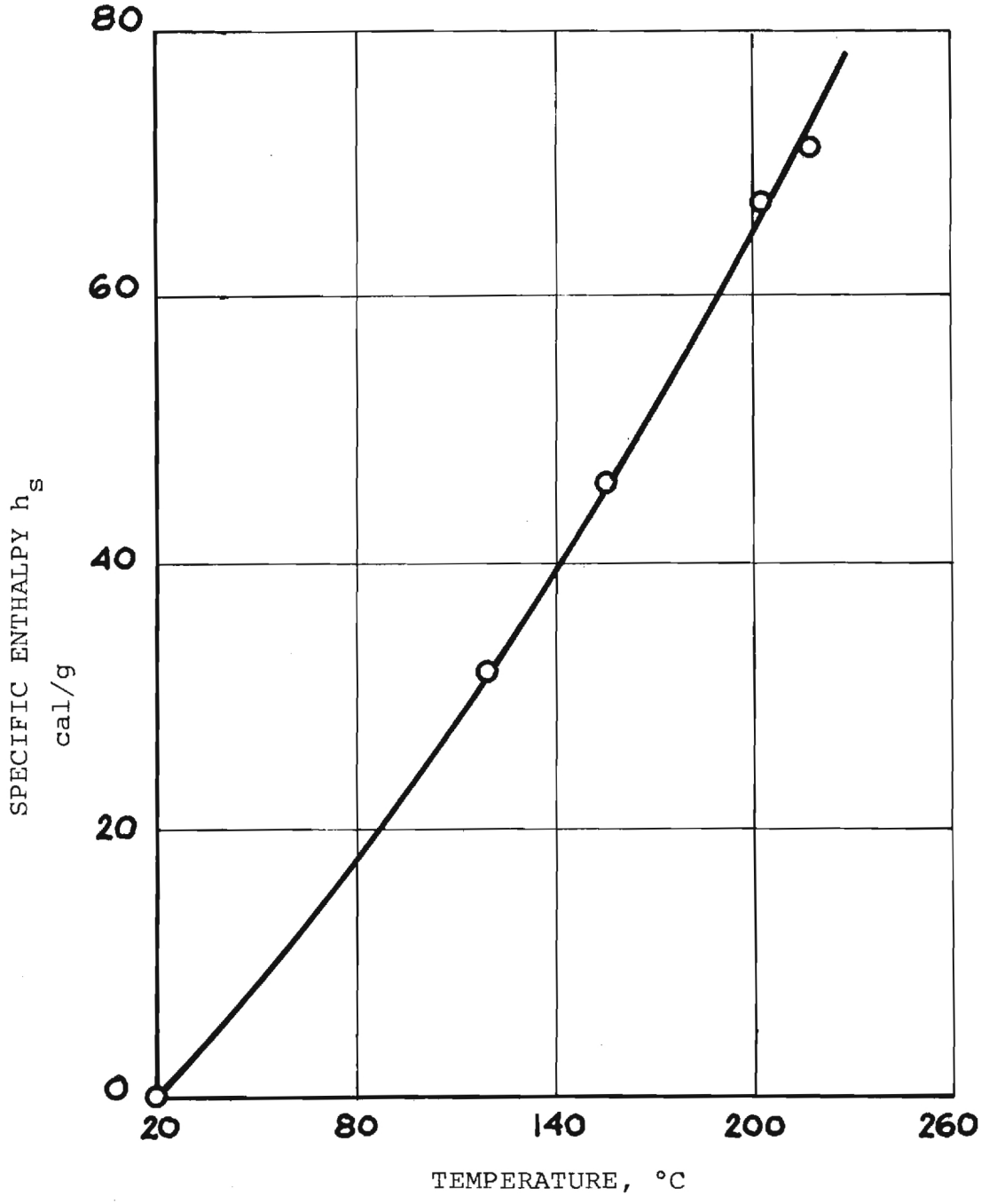

Figure II-14. Enthalpy vs Temperature For 65/35% Polyester/Cotton; GIRCFF No. 8

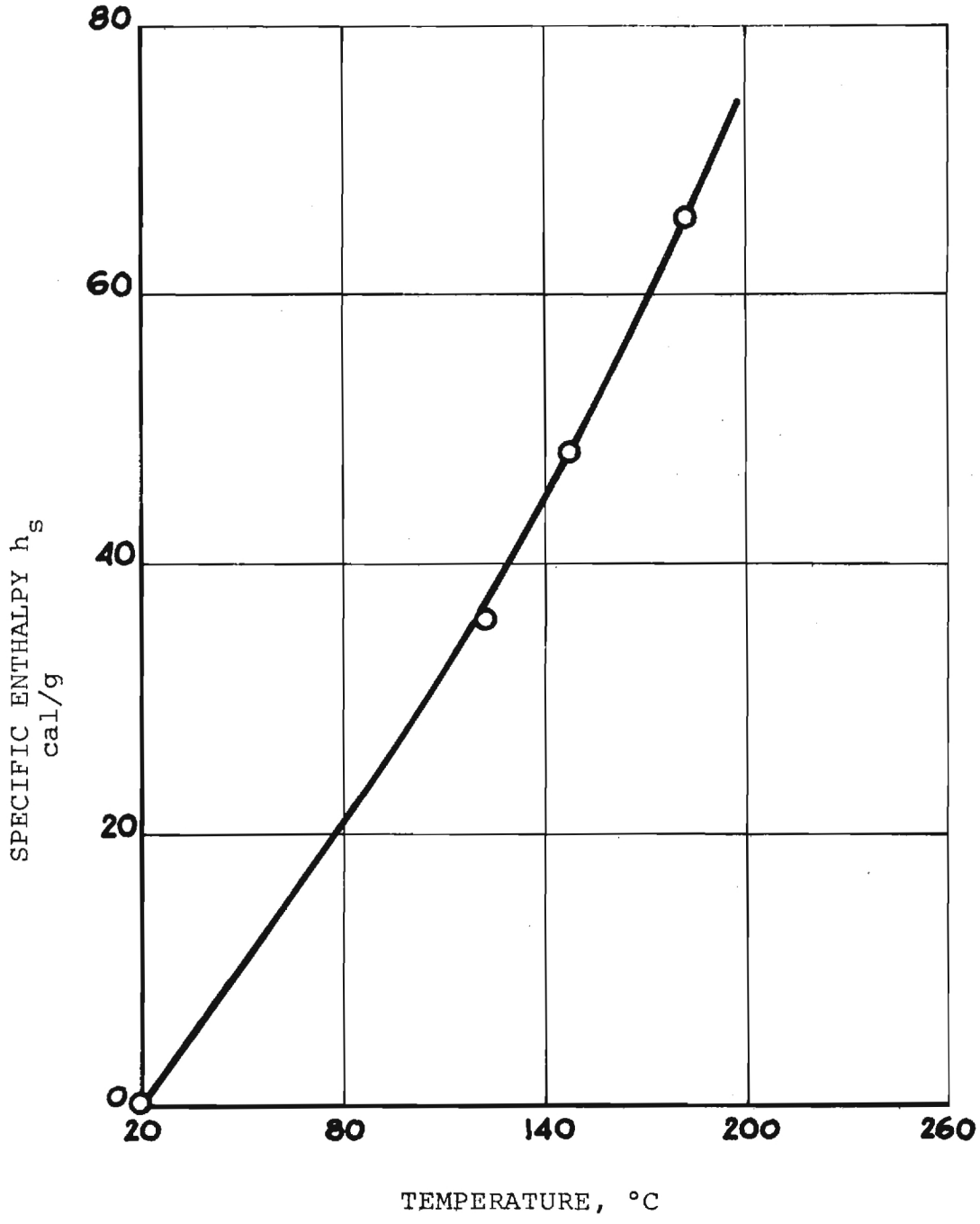

Figure II-15. Enthalpy vs Temperature For 100% Cotton, GIRCFF No. 10

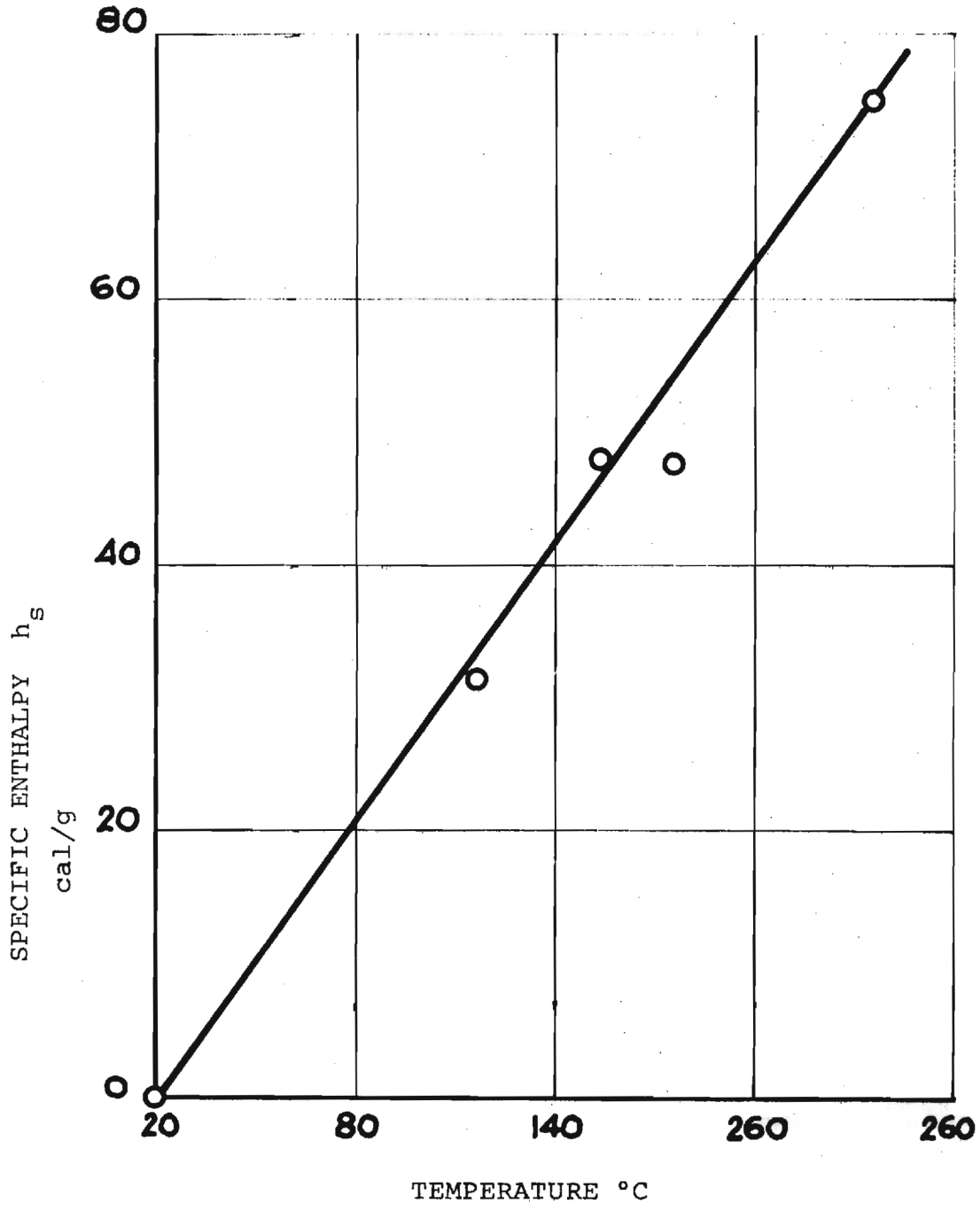

Figure II-16. Enthalpy vs Temperature For 80/20% Acetate/Nylon, GIRCFF No. 11

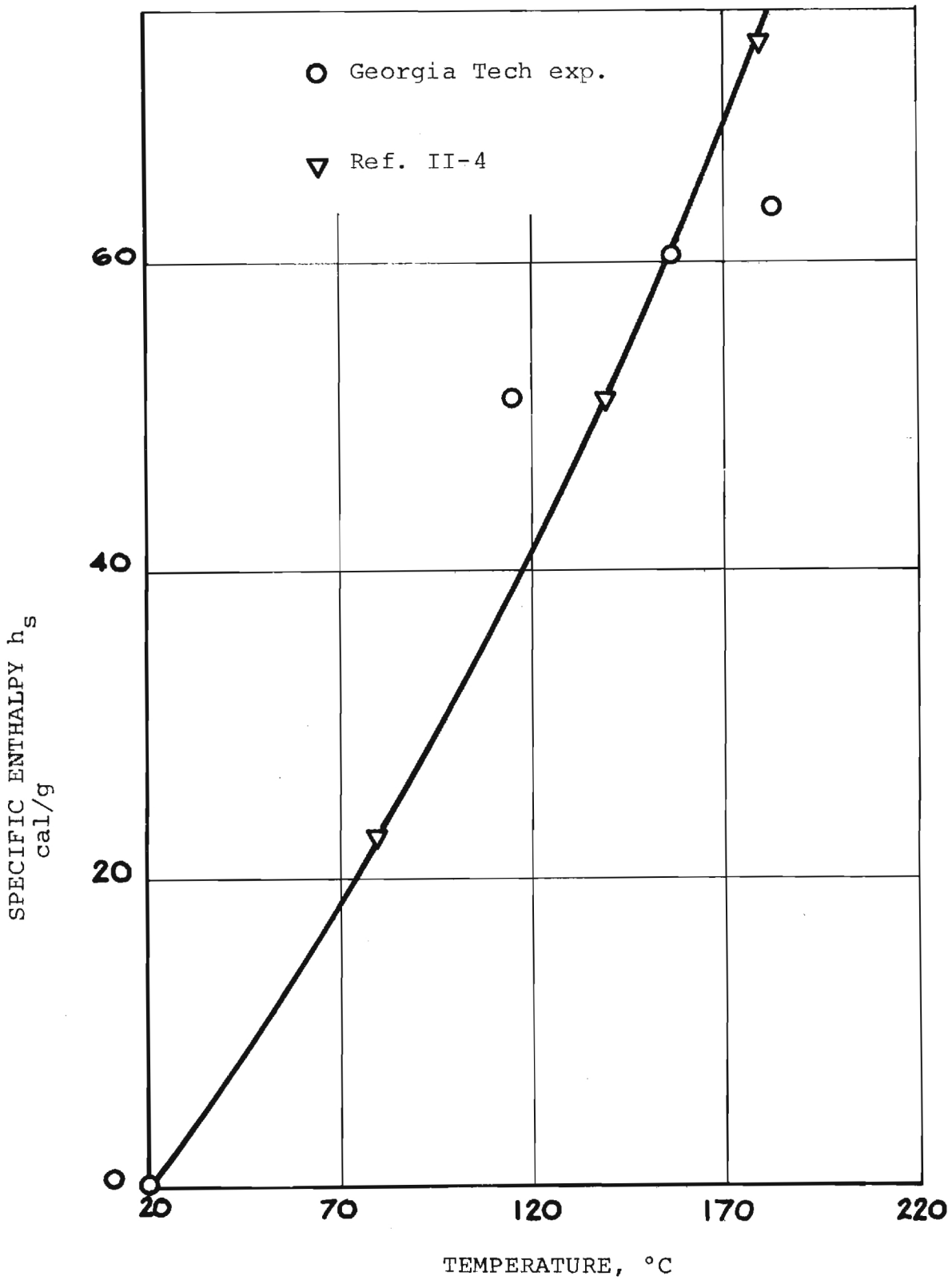

Figure II-17. Enthalpy vs Temperature For 100% Nylon; GIRCFF No. 12

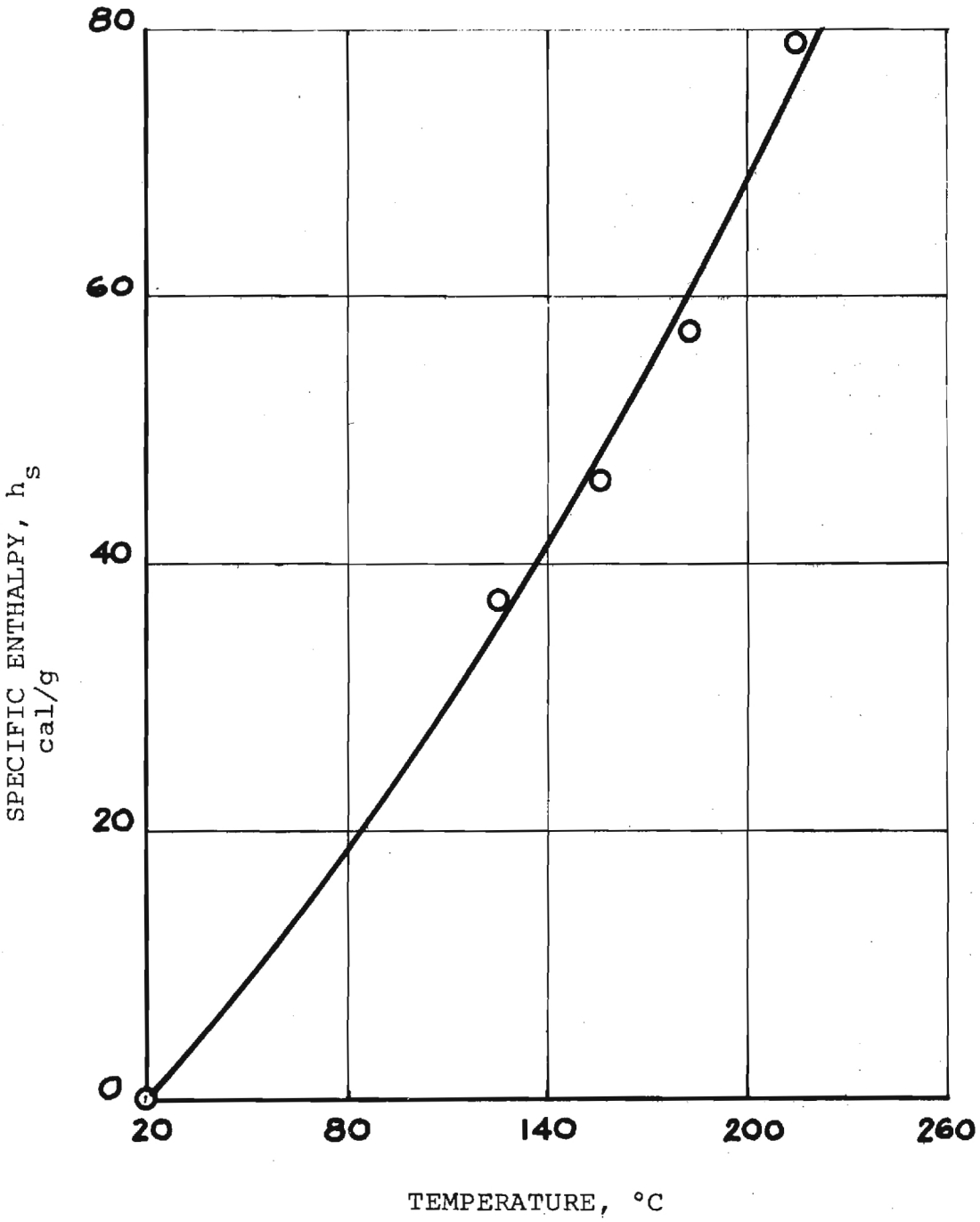

Figure II-18. Enthalpy vs Temperature For 100% Acetate Fabric; GIRCFF No. 13

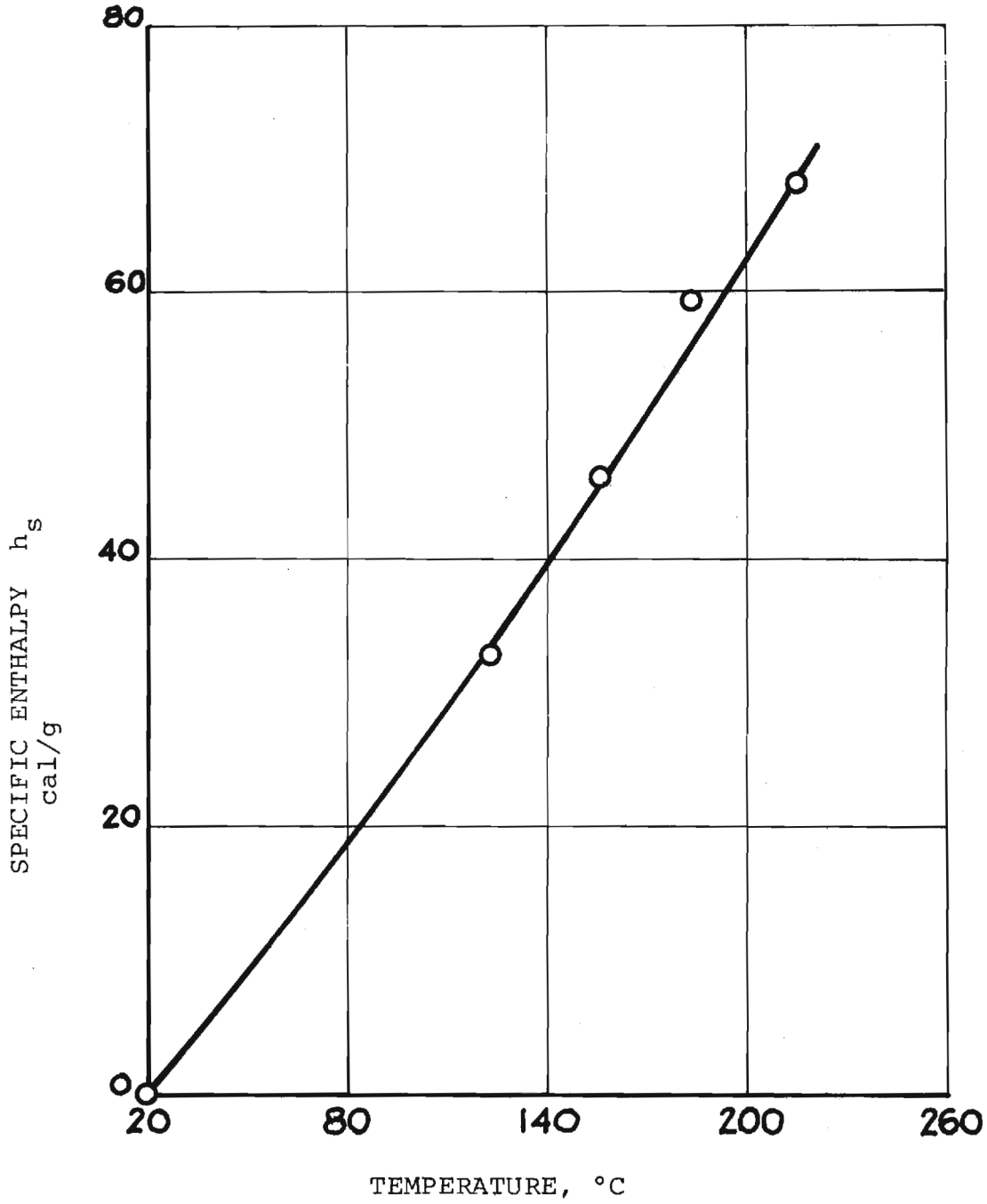

Figure II-19. Enthalpy vs Temperature For 65/35% Polyester/Cotton; GIRCFF No. 17

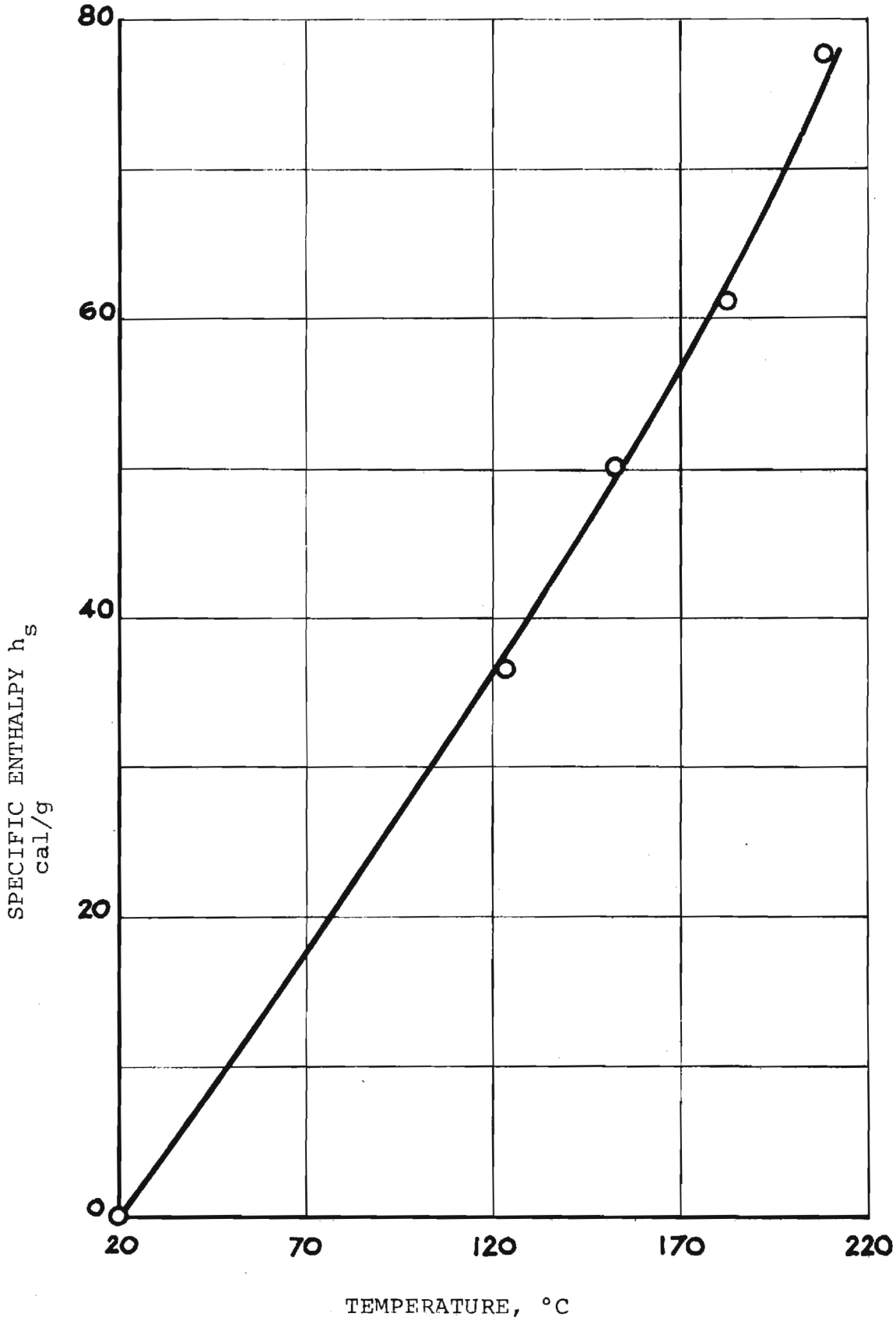

Figure II-20. Enthalpy vs Temperature For 100% Cotton Fabric; GIRCFF No. 18

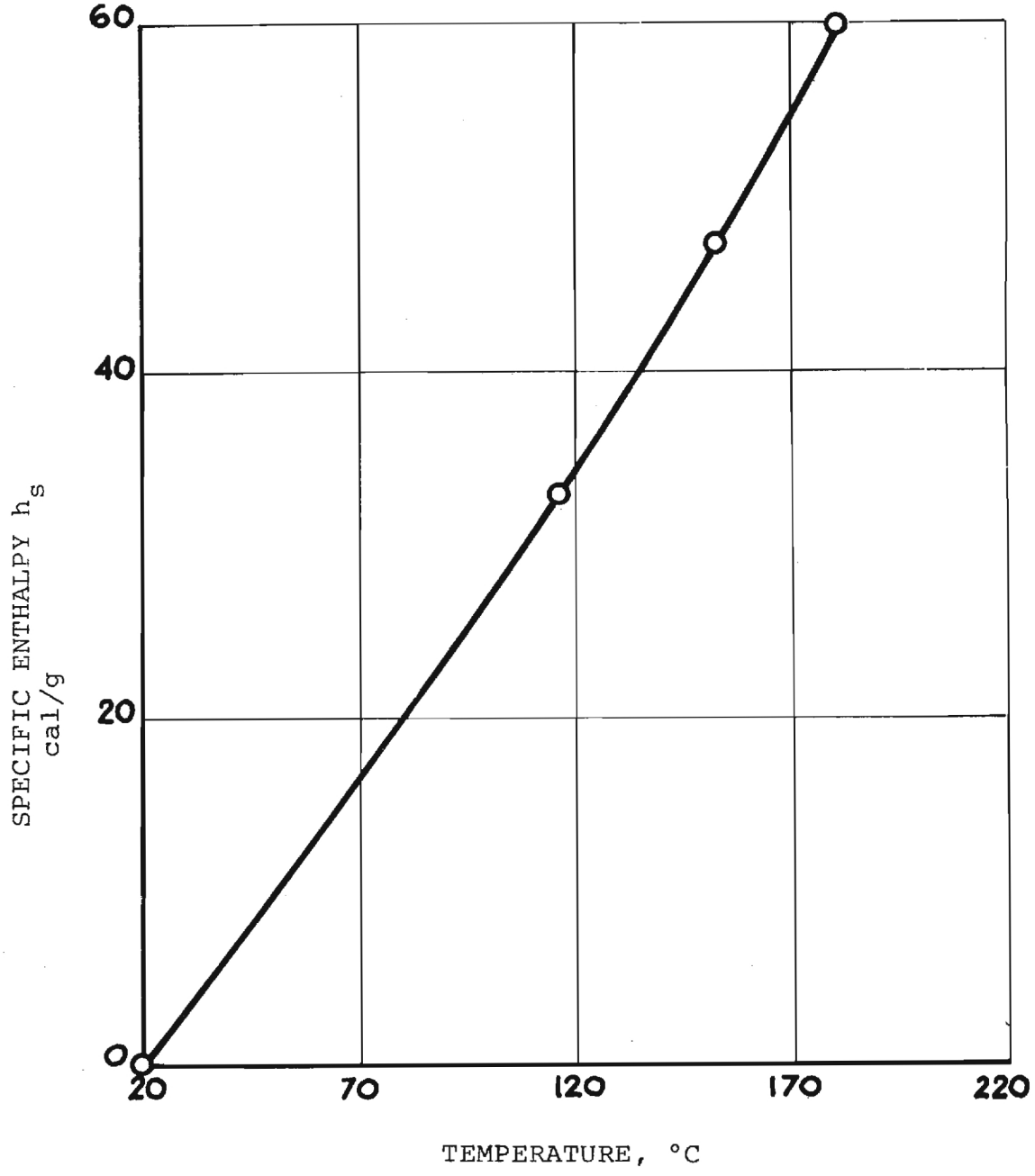

Figure II-21. Enthalpy vs Temperature For 100% Cotton Fabric, Treated With Fire Retardant; GIRCFF No. 19

Table II-3. SPECIFIC HEAT OF FABRICS

GIRCFF Fabric No.	Fabric Temperature in °C						
	50	75	100	125	150	175	200
	Specific Heat in Ws/(gC)						
2	1.42	1.42	1.42	1.42	1.42	1.42	1.42
5	--	1.57	1.65	1.69	1.72	1.73	1.88
8	1.28	1.35	1.43	1.52	1.64	1.78	1.92
10	1.28	1.35	1.65	1.94	1.98	--	--
11	1.45	1.45	1.45	1.45	1.45	1.45	1.45
12	1.72	1.89	2.08	2.25	2.44	2.62	--
13	1.27	1.39	1.53	1.68	1.83	1.97	2.09
17	1.33	1.36	1.39	1.44	1.51	1.61	1.77
18	1.34	11.41	1.58	1.60	1.69	1.82	2.12
19	1.37	1.40	1.46	1.57	1.69	2.17	2.44

Task 4. Thermal Conductance

The thermal conductance was measured in a guarded hot plate apparatus discussed in Appendix B.3. All ten primary GIRCFF fabrics were tested at the minimum contact pressure of 528 N/m^2 in the range of temperatures between 67°C and 205°C or as limited by the thermal instability of the fabric. The results are shown for cotton fabrics in Figure II-22, for plastic polymers in Figure II-23 and for polyester cotton blends in Figure II-24. The results for Fabrics No. 12 and 13 at the temperature of 96°C deviate from the drawn curves because the samples used for these tests had previously been used at the higher temperatures.

The effect of pressure is shown in Figure II-25 for four fabrics, GIRCFF Fabric Nos. 2, 5, 8 and 12. The results are obtained by interpolation of conductance versus temperature at constant pressure data. The results show a general increase of thermal conductance with rising pressure as the effect of compression overwhelms the effect of fiber re-orientation. The exception to this characteristic is GIRCFF Fabric No. 12.

A summary of conductance data is given in Table II-4, together with fabric thickness data so that conductivity can readily be obtained.

It should be observed that the role of conductance was found to be insignificant as a result of the optical properties obtained during this program. This is explained in detail in Chapter III.

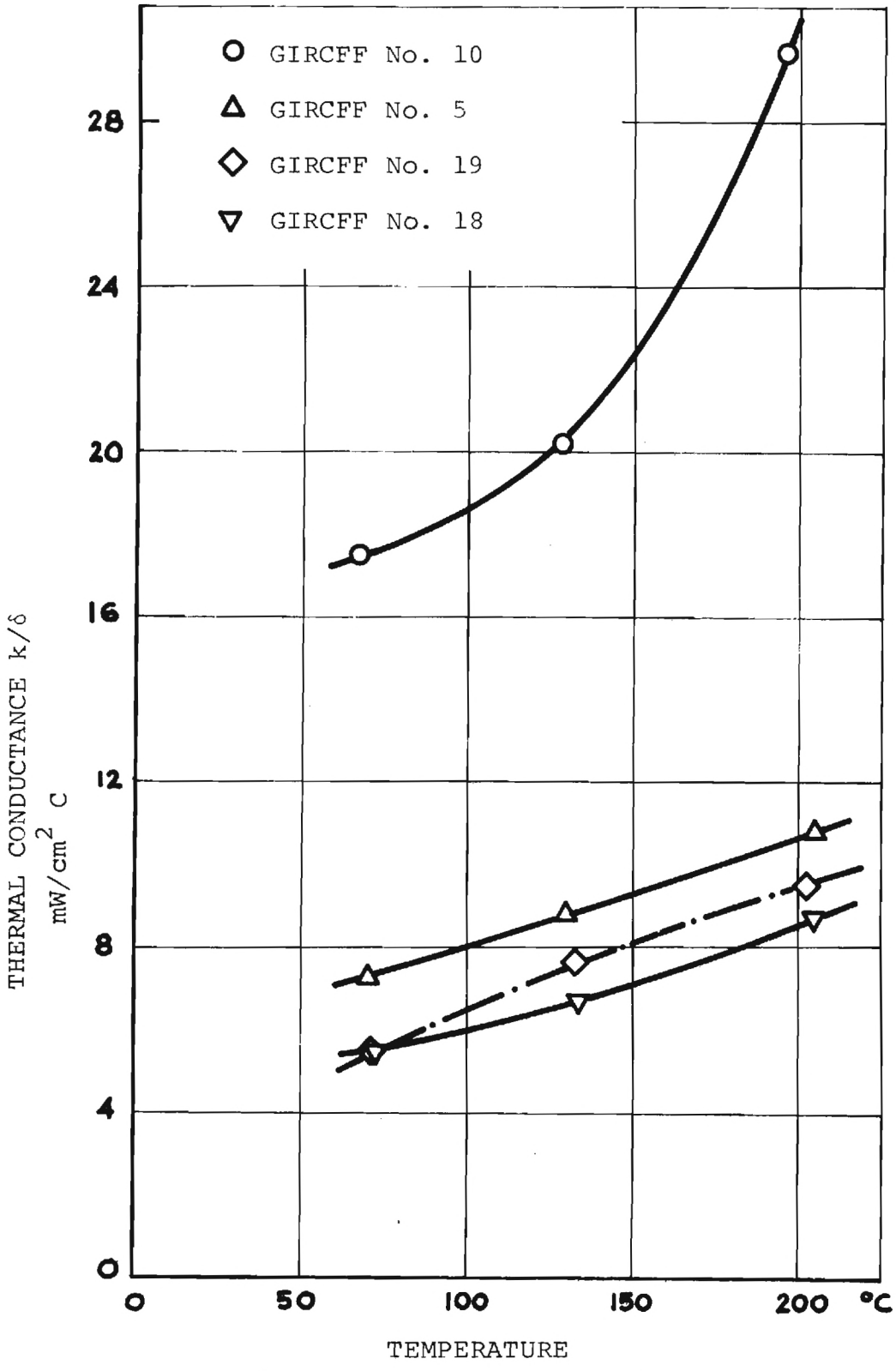

Figure II-22. Thermal Conductance of Cotton Fabrics as a Function of Temperature; Contact Pressure $p = 528\ N/m^2$

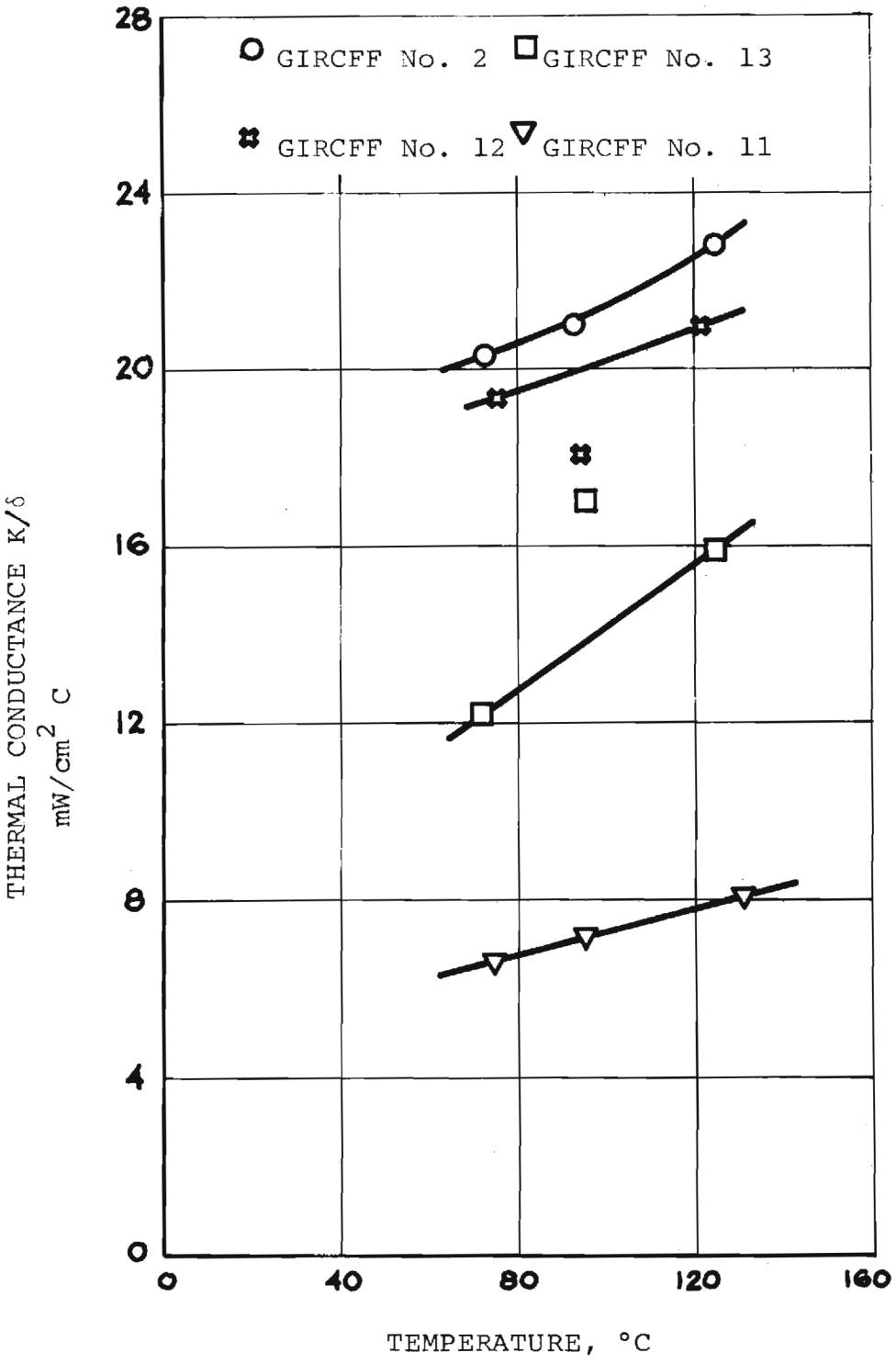

Figure II-23. Thermal Conductance of Plastic Polymers
Contact Pressure p = 528 N/m^2

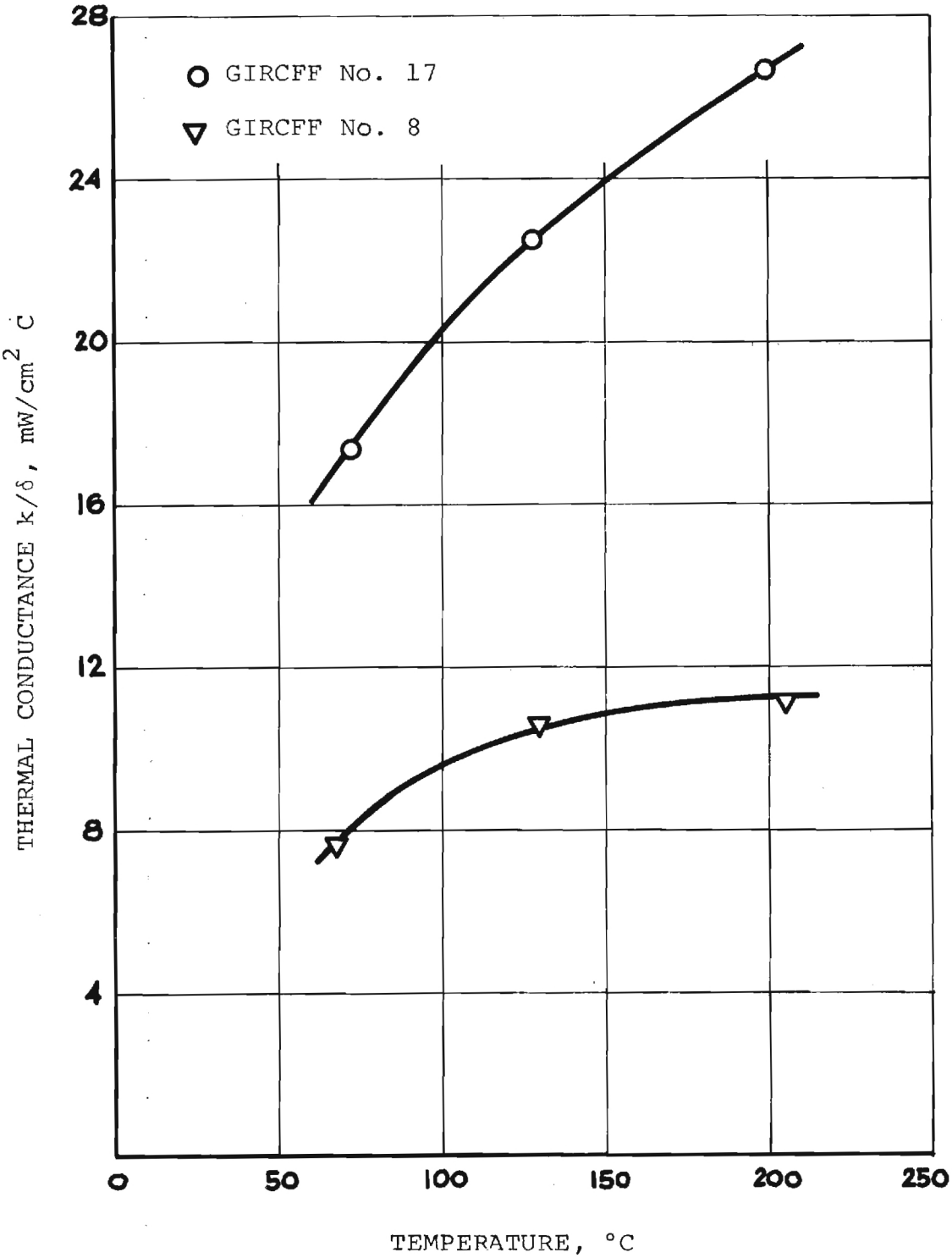

Figure II-24. Thermal Conductance of Polyester-Cotton Blends, Contact Pressure p = 528 N/m^2

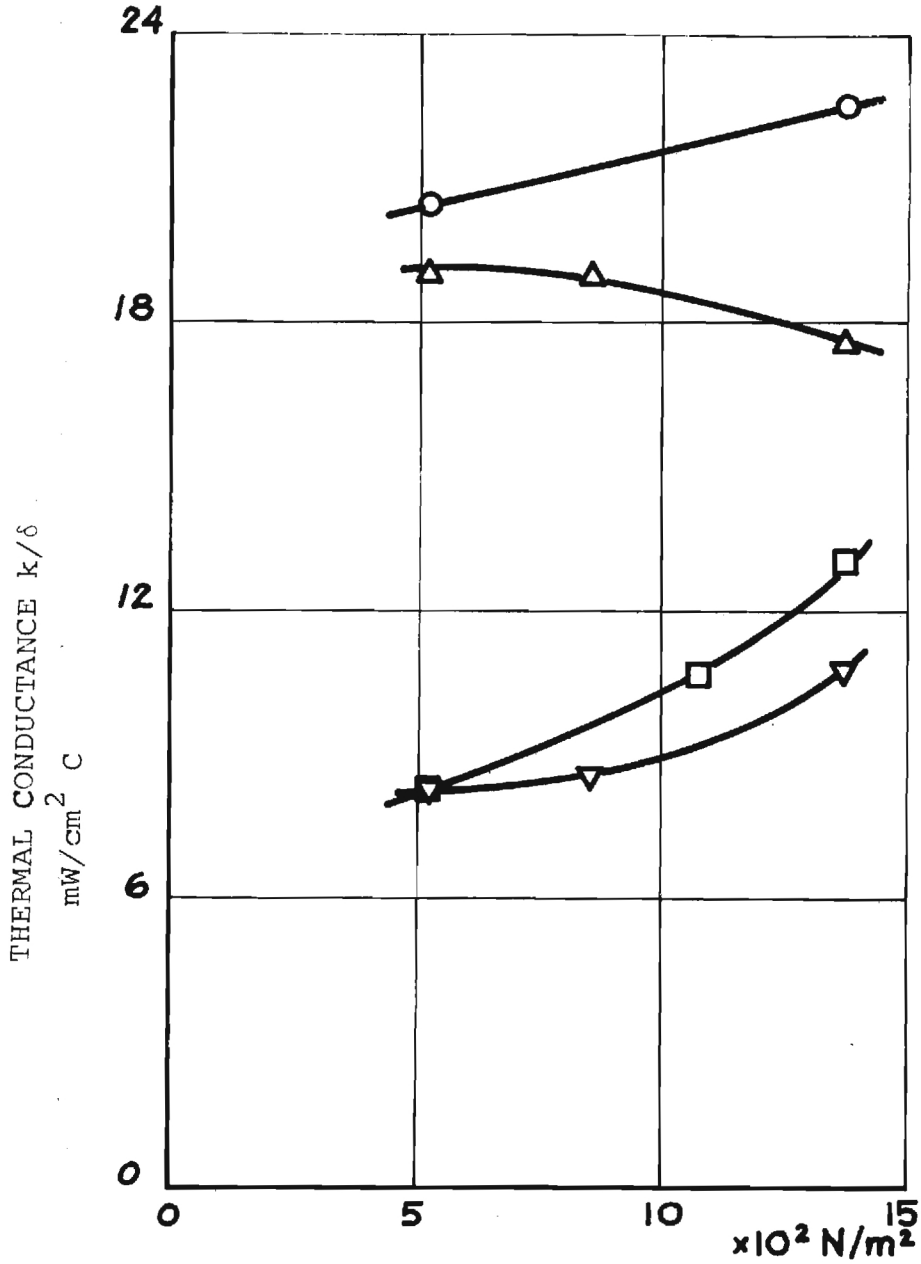

Figure II-25. Contact Pressure Effects on Thermal Conductance

GIRCFF No.		GIRCFF No.	
○	2, @ 75.6°C	□	5, @ 76.5°C
△	12, @ 73.5°C	▽	8, @ 75.4°C

Table II-4. THERMAL CONDUCTANCE OF PRIMARY GIRCFF FABRICS

GIRCFF Fabric Number	Original Fabric Thickness cm	Mass Per Unit Area $g/cm^2 \times 10^3$		Pressure 1 528 N/m^2		Pressure 2 866 N/m^2		Pressure 3 1370 N/m^2	
		N.B.S.	G.T.	k/δ mW $cm^{-2}C^{-1}$	$\bar{T}$ °C	k/δ mW $cm^{-2}C^{-1}$	$\bar{T}$ °C	k/δ mW $cm^{-2}C^{-1}$	$\bar{T}$ °C
2	0.0201	7.41	7.51	20.26 21.02 22.79	73.0 93.1 124.6	29.43 21.03 22.74	62.8 83.3 86.3	22.51	75.8
5	0.0529	13.43	13.71	7.32 8.81 10.82	70.9 130.5 206.0	7.31 11.28	57.4 79.8	13.02	76.5
8	0.062	16.31	16.19	7.63 10.50 11.13	68.4 129.6 205.9	7.99 9.13	56.0 81.7	10.74	75.4
10	0.0177	6.91	6.65	17.48 20.19 29.67	67.8 128.4 195.8			25.36	76.5
11	0.0614	9.05	11.31	6.60 7.08 8.08	75.2 95.2 130.9	7.46	86.2	8.13	77.7
12	0.0271	8.36	8.91	19.30 17.00 20.93	76.1 96.3 122.6	17.35 20.80	56.1 92.2	17.89	73.5

Table II-4 (continued)

GIRCFF Fabric Number	Original Fabric Thickness cm	Mass Per Unit Area $g/cm^2 \times 10^3$ N.B.S.	Mass Per Unit Area $g/cm^2 \times 10^3$ G.T.	Pressure 1 528 N/m^2 k/δ mW $cm^{-2}C^{-1}$	Pressure 1 528 N/m^2 $\bar{T}$ °C	Pressure 2 866 N/m^2 k/δ mW $cm^{-2}C^{-1}$	Pressure 2 866 N/m^2 $\bar{T}$ °C	Pressure 3 1370 N/m^2 k/δ mW $cm^{-2}C^{-1}$	Pressure 3 1370 N/m^2 $\bar{T}$ °C
13	0.0304	8.26	9.40	12.21 18.07 15.86	72.1 94.9 125.1	18.82	91.7	17.56	76.9
17	0.0193	8.56	8.55	17.34 22.48 26.75	72.6 128.0 199.3			30.41	77.3
18	0.0713	12.49	12.88	5.55 6.72 8.74	73.0 134.4 205.3			7.06	78.6
19	0.0692	14.25	14.81	5.38 7.55 9.46	73.0 134.1 203.5			8.55	77.8

Task 5. Ignition Temperature Measurements

Self and pilot ignition temperature data as obtained in a modified Setchkin Furnace (see Appendix B.4 for design features and test procedures) are summarized in Tables II-5 and 6, respectively.

For the total of sixteen fabrics, temperature intervals in which ignition or melting prior to ignition was observed are given in Table II-7 for both self-and pilot-ignition and represented graphically in Figures II-26 and 27, respectively.

Neither self nor pilot ignitions were measured on the molten residue collected in the pan-shaped sample holder as there is presently no interest in the processes following the fabric destruction.

The reproducibility of ignition temperature measurements is demonstrated on GIRCFF Fabrics No. 5, 8 and 10. Repeated measurements produced results within the bracket currently achieved for ignition temperature accuracy (approximately 15°C).

Pilot-ignition temperatures are consistently lower than self ignition temperature as is to be expected.

Table II-5. SELF IGNITION TEMPERATURE DATA OF THE TEN PRIMARY GIRCFF FABRICS

ignition	●	Fabric consumed	⬡
No ignition	○	Fabric not consumed	△
Flash	◇	Melting	■

	GIRCFF FABRIC										
Air Temp. °C	# 2	# 5	# 8	# 10	# 11	# 12	# 13	# 17	# 18	# 19	# 20
317	○ ■	○	○	○	○ ■	○ ■	○ ■	○	○	○	○
328	○ ■	●	○	○	○ ■	○ ■	○ ■	○	●	○	○
396	⬡		○	○	⬡	⬡	⬡	○		○	○
429			○	○				○		○	○
480			● ◇	●				●		○	●
450			● ◇	● ◇ △				○			○
463			● ◇	● ◇ △				○			○
301		○							○		
288		○							○		
311		●							●		
439			○	●							
497										● ◇ △	
249	○				○ ■	○ ■	○ ■				
237					○ ■	○	○ ■				
218					○		○				

Table II-6. PILOT - IGNITION TEMPERATURE OF IGNITING FABRIC

Ignition ● Flash ◇

No Igniton ○ Fabric not consumed △

	GIRCFF FABRIC						
Air Temp. °C	# 5	# 8	# 10	# 17	# 18	# 19	# 20
294	○	○	○	○	●	○	○
339		●	○	○		● △	●
316		●				○	○
329						●	●
355			● △	○			
368				○			
392				● △			
384				●			
217							
299	○						
267					○		
278					○		
304		○					
351			●				

Table II-7. SUMMARY OF SELF AND PILOT IGNITION RESULTS

GIRCFF Fabric No.	Ignition Temperature, °C	
	Self-Ignition	Pilot-Ignition
1	416-409	
2	255-262 M**	
4	297-287	
5	311-301	311-301
	327-318*	
6	416-409	
7	478-467	
8	450-439	316-304
	443-416	
9	308-297	
10	439-429	351-339
	443-434	
11	237-218 M	
12	255-237 M	
13	237-218 M	
17	480-463	384-368
18	311-301	294-278
19	497-480	329-316
20	480-463	329-316

*reported in 2nd Quarterly Report
repeated for check on reproducibility

**M represents melting

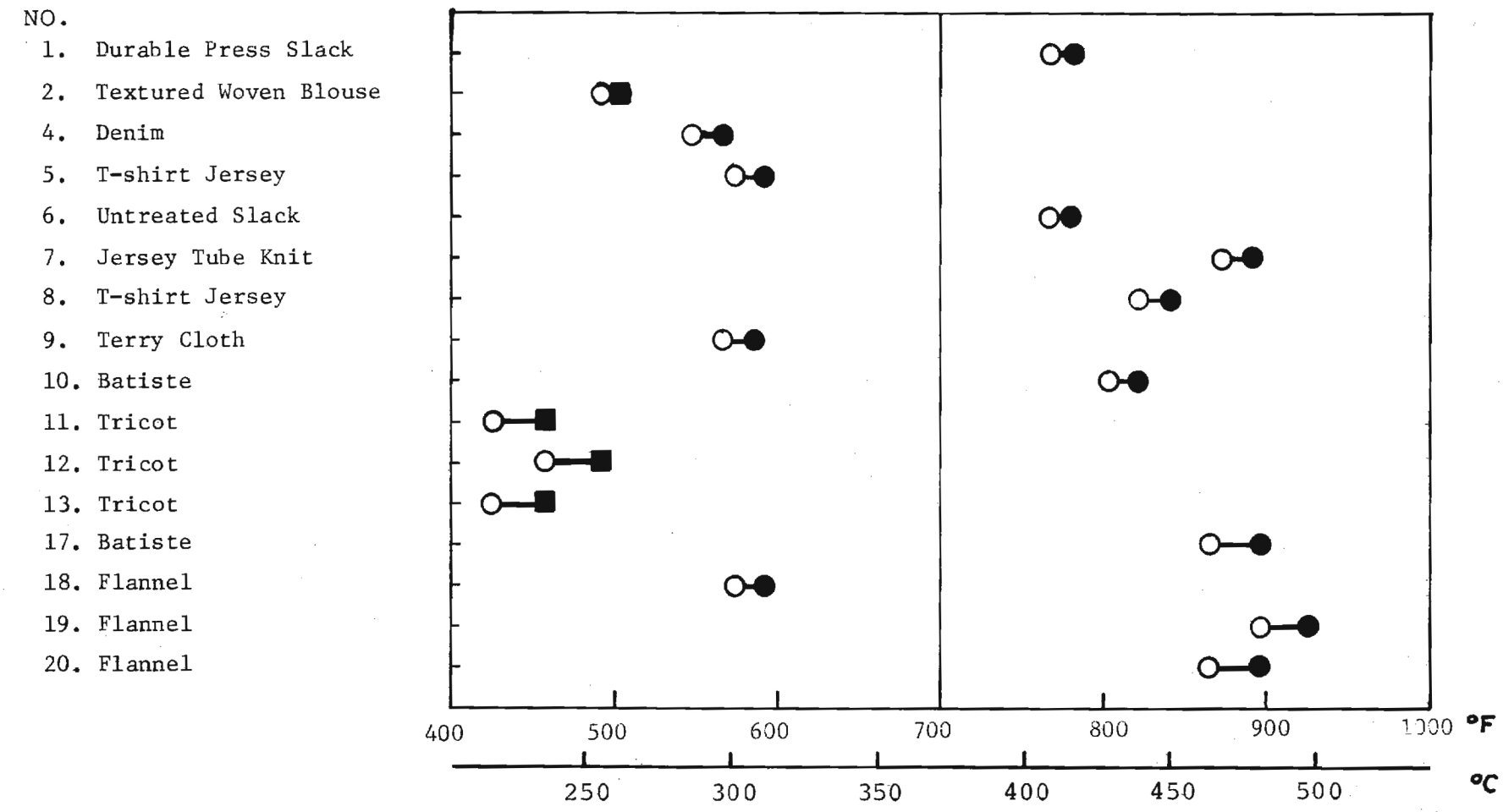

Figure II-26. Self-Ignition Temperatures

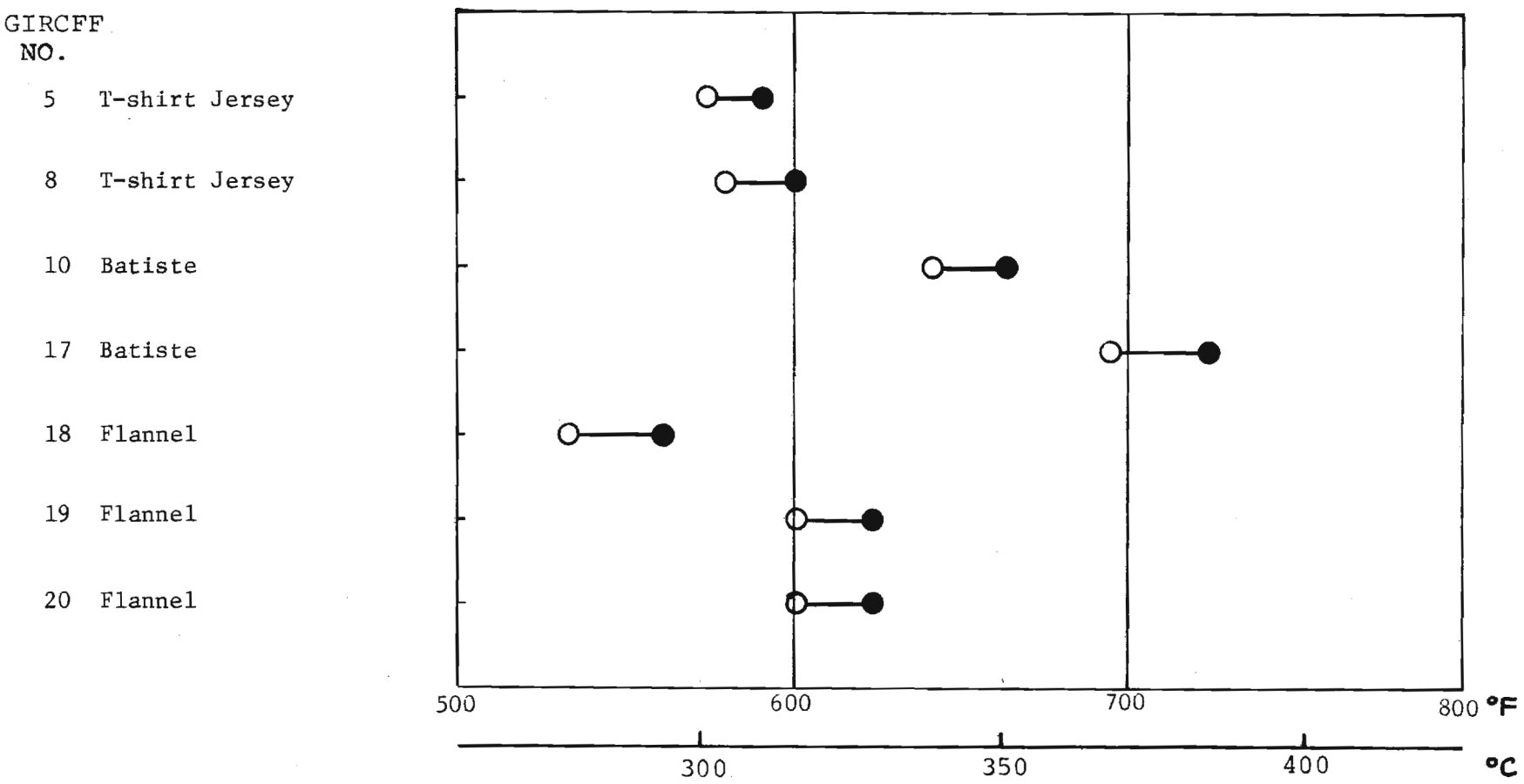

Figure II-27. Pilot-Ignition Temperatures

Task 6. Optical Fabric Properties

The directional-hemispherical reflectance and transmittance were measured in an integrating sphere reflectometer for the purpose of describing the fabric-heater interaction. Details of instrumentation and operating procedures are presented in Appendix B.5.

Measurements were first carried out at incidence of 20° from the normal. Then the effect of incidence was measured at various angles between 0° and 40° and found negligible. The fabrics in the set of primary GIRCFF fabrics can be considered as Lambertian reflectors and transmittors.

Reflectance and transmittance was measured both in the infrared spectrum between 0.6μm and 2.5μm and the combined visible (less than 12%) and infrared spectrum as produced by a tungsten filament projector lamp at 3,200°k filament temperature.

The reflectance, transmittance and absorptance was evaluated for all primary GIRCFF fabrics in their original condition (virgin material). The results are presented in Table II-8 for the irradiation by projector lamp and in Table II-9 for the infrared irradiation.

Six fabrics were charred in air, either in an oven or in the guarded hot plate during conductance measurements. These fabrics are, together with their respective char temperatures

GIRCFF No.	Char Temperature °C
5	124
8	206
10	196
17	199
18	205
19	204

The optical properties of the charred fabrics are listed in Tables II-10 and 11 for the tungsten filament source and the infrared source, respectively. For ease of comparison, all absorptance data obtained are summarized in Table II-12.

The influence of charring is significant as the absorptance is shown to increase by a factor of up to three. The influence of the visible irradiance is shown to affect absorptance by a factor of up to 1.5, however the temperature of the tungsten filaments in the radiant heater of the Ignition Time Apparatus is below 3,000°k in most ignition tests; accordingly the influence of visible radiation is far less in the Ignition Time Apparatus than in the optical property measurements.

Table II-8. OPTICAL FABRIC PROPERTIES

VIRGIN FABRICS

Tungsten Filament Source, Filament Temperature 3,160°K*

FABRIC GIRCFF NO.	Reflectance ρ	Transmittance τ	Absorptance $\alpha = 1-\tau-\rho$	Optical Thickness κ*
2	0.560	0.276	0.164	0.272
5	0.533	0.288	0.179	0.284
8	0.562	0.264	0.174	0.298
10	0.418	0.361	0.221	0.280
11	0.523	0.320	0.157	0.230
12	0.447	0.380	0.173	0.214
13	0.490	0.344	0.166	0.227
17	0.485	0.364	0.151	0.208
18	0.599	0.231	0.170	0.326
19	0.590	0.229	0.181	0.348

*This source produces 11.3% visible and ultraviolet and 88.7% infrared radiation.

Table II-9. OPTICAL FABRIC PROPERTIES

VIRGIN FABRICS

Infrared Irradiation, $0.6\mu m \leq \lambda \leq 2.5\mu m$

FABRIC GIRCFF NO.	Reflectance ρ	Transmittance τ	Absorptance $\alpha = 1-\tau-\rho$	Optical Thickness κ^*
2	0.501	0.346	0.153	0.208
5	0.521	0.296	0.183	0.282
8	0.560	0.276	0.164	0.272
10	0.406	0.394	0.200	0.236
11	0.508	0.329	0.163	0.232
12	0.397	0.433	0.170	0.188
13	0.443	0.390	0.167	0.203
17	0.464	0.372	0.164	0.208
18	0.573	0.251	0.176	0.312
19	0.602	0.197	0.201	0.428

Table II-10. OPTICAL FABRIC PROPERTIES

CHARRED FABRICS

Tungsten Filament Source, Filament Temperature 3,160°K*

FABRIC GIRCFF NO.	Reflectance ρ	Transmittance τ	Absorptance $\alpha = 1-\tau-\rho$	Optical Thickness κ*
5	0.449	0.223	0.278	0.563
8	0.391	0.182	0.427	0.775
10	0.250	0.321	0.429	0.523
17	0.438	0.339	0.223	0.296
18	0.532	0.164	0.284	0.632
19	0.248	0.145	0.607	1.100

*This source produces 11.3% visible and ultraviolet and 88.7% infrared radiation.

Table II-11. OPTICAL FABRIC PROPERTIES

CHARRED FABRICS

Infrared Irradiation, $0.6\mu m \leq \lambda \leq 2.5\mu m$

FABRIC GIRCFF NO.	Reflectance ρ	Transmittance τ	Absorptance $\alpha = 1-\rho-\tau$	Optical Thickness κ^*
5	0.442	0.333	0.225	0.304
8	0.489	0.141	0.370	0.833
10	0.297	0.281	0.422	0.570
17	0.464	0.335	0.201	0.274
18	0.591	0.221	0.188	0.368
19	0.267	0.272	0.461	0.620

Table II-12. COMPARISON OF FABRIC ABSORPTANCE DATA

FABRIC GIRCFF NO.	VIRGIN FABRICS		CHARRED FABRICS	
	Unfiltered Tungsten Source 3,200°K	Infrared Irradiation $0.6\mu m \leq \lambda \leq 2.5\mu m$	Unfiltered Tungsten Source 3,200°K	Infrared Irradiation $0.6\mu m \leq \lambda \leq 2.5\mu m$
2	0.164	0.153		
5	0.179	0.183	0.278	0.225
8	0.174	0.164	0.427	0.370
10	0.221	0.200	0.429	0.422
11	0.157	0.163		
12	0.173	0.170		
13	0.166	0.167		
17	0.151	0.164	0.223	0.201
18	0.170	0.176	0.284	0.188
19	0.181	0.201	0.607	0.461

III. ANALYSIS

A. Objective

Flammability standards must ultimately be defined on the basis of modeling experiments because well-controlled and instrumented experiments on the prototype itself, that is the human, are impossible. Model testing must be reasonably faithful to the conditions of the prototype, so as to yield all the relevant parameters involving the fabric properties characteristic of ignition and burning, and the process parameters such as heating source characteristics and boundary conditions. Of the multitude of possible parameters describing ignition and combustion one must select the important ones to obtain a manageable set of parameters, no more complex than necessary for the adequate determination of fabric flammability. This leads to partial modeling with subsequent assessment of partial modeling errors.

The processes characterizing flammability are essentially transient in nature. Considering pertinent times, the probability of ignition for given exposure should depend primarily on the ratio of the time a person exposes the fabric to a heat source to the time required for ignition. The exposure time can be at most stochastically related to the fabric characteristics, and this doubtful relation is as yet to be established, while the ignition time depends strongly and deterministically on fabric properties. Hence, fabric characterization being the objective, the problem becomes that of predicting the ignition time for a given set of circumstances.

Consequently, the objective of the analysis are

i. a complete modeling analysis for the purpose of determining the relevant modeling rules needed to assess the ignition time; the analysis should take into account (1) fabric material properties, (2) physical processes such as heating modes and boundary conditions, and (3) different geometries;

ii. the development of the rules for partial modeling;

iii. an assessment of the errors involved with partial modeling;

iv. the definition of suitable modeling experiments which are necessary to predict ignition time.

The work presented herein is restricted to radiative heat sources. The more complex convective heat source (gas flame) is considered in a later program phase.

The following section presents the most detailed analysis leading to the complete set of modeling parameters. Section C presents simplified model descriptions and is followed by Section D which illustrates the shortcoming expected from simplifications. Analytical results are compared with experimental results in Section E.

B. Complete Modeling Analysis

Considered is the system consisting of a radiative heat source, the fabric and the human tissue separated from the fabric by an air gap, as depicted in Figure III-1 below.

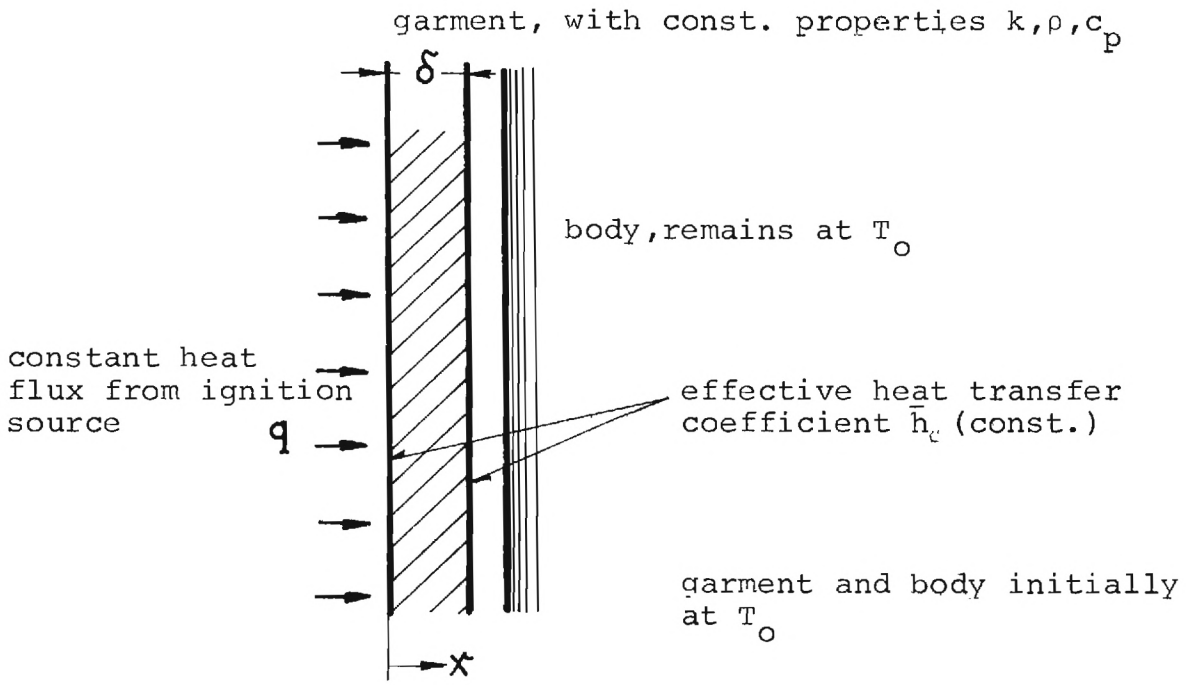

Figure III-1. Geometry of Ignition Model

The fabric response to heating proceeds in four partially overlapping stages

i) inert heating of the fabric

ii) thermal decomposition, change in shape, drying, accompanied by the evolution of combustible, and non-combustible gases, smoke with entrained solid particles, or by melting and shrinking

iii) ignition, that is the appearance of a flame as evidence of exothermal reaction by the volatiles, or the onset of smoldering

iv) combustion, char formation.

Stages i and ii are endothermic while stages iii and iv are exothermic to the extent that the overall process is also exothermic. There are several ignition criteria postulated [III-1]. For auto ignition of thin (cellulosic) materials, Martin [III-2], Lawson and Simms [III-3], Alvares, Blackshear and Murty Kanury [III-4] have suggested that ignition occurs when the material surface temperature reaches a certain fixed value, the ignition temperature T_i. This criterion has been accepted here. Process stage iv is of no interest in the present analysis.

The governing equations are the equations of energy conservation for the fabric interior and the fabric surfaces and the reaction equations.

1. Governing Equations

One dimensional heat transfer, simultaneously by conduction and diffuse radiation, with internal chemical heat sources, is governed by

$$\rho c \frac{\partial T}{\partial t} = \frac{\partial}{\partial x}\left(k \frac{\partial T}{\partial x}\right) + 2(1-\tilde{\rho})\kappa E_2(\kappa x) W_o + q''' \{T(x)\} \qquad \text{(III-1)}$$

where

ρ	fabric density	g/cm^2
c	specific heat of fabric	Ws/(gK)
T	fabric temperature	k
t	time	s
x	coordinate	cm
k	thermal conductivity	W/(cm K)
$\tilde{\rho}$	fabric reflectance	
κ	radiative extinction coefficient	
W_o	incident radiant flux	W/cm^2

$$\text{and} \quad E_2 (\kappa x) = \int_1^\infty t^{-2} \, e^{-(\kappa x) t} dt \qquad \text{(III-2)}$$

arises from the diffuse character of the radiant flux through the fabric. The first term in Equation (III-1) constitutes the storage of thermal energy within the fabric, the second term represents conductive dissipation and the third term describes the internal absorption of radiant energy. The heat generation by chemical reaction is given by

$$q'''(T) = \rho(1-\varepsilon) \{\Delta H_f \, A e^{-\frac{E}{RT}}\}_{ex} + \rho\varepsilon(1-\lambda)\{\Delta H_f \, A e^{-\frac{E}{RT}}\}_{en} \qquad \text{(III-3)}$$

where

ΔH_f	reaction enthalpy	Ws/g
A	pre-exponential factor	1/s
E	activation energy	Ws/mole
λ	degree of reaction	
R	universal gas constant	Ws/(mole K)
ε	maximum mass fraction of endothermic decomposition	

and subscripts ex and en refer to, respectively, exothermic and endothermic reactions. The first term on the right-hand side of Equation III-3 is responsible for the temperature excursion at ignition time t_i while the last term is accounting for the second stage of the ignition process, the thermal decomposition.

The degree of reaction for the first-order decomposition is governed by Arrhenius' law

$$\frac{d\lambda}{dt} = - (1-\lambda) [A e^{-\frac{E}{RT}}]_{en} \qquad \text{(III-4)}$$

with $\lambda = 0$ at time $t = 0$ (III-5)

Finally, the energy conservation equation, Equation III-1 is subject to the initial condition at time $t = 0$

$$T(x,o) = T_o \tag{III-6}$$

and the boundary conditions at the front face, $x = 0$

$$k \frac{\partial T}{\partial x} = (\bar{h}_c)_o \ (T - T_o) \tag{III-7}$$

at the back face, $x = \delta$

$$-k \frac{\partial T}{\partial x} = (h_c)_\delta \ (T - T_a) \tag{III-8}$$

where

$\bar{h}_c$	convective film coefficient	$W/(cm^2{}_K)$
T_o	initial temperature	
δ	fabric thickness	
T_a	representative air gap temperature	

Equation III 7 and 8 describe the convective cooling at the fabric surfaces and may be modified to account also for radiative heat rejection by the fabric.

It should be pointed out for the sake of completeness that convection through the fabric by the volatiles and fabric emission from within the fabric are neglected in Equation III-1. In addition, the exothermic reaction which induces ignition (that is stage iii of the ignition process) is only approximately represented by the zero-order reaction term in Equation III-3. This term would lead to unbounded fabric temperatures, but the objective of the

analysis is reached at the beginning of that reaction, before an appreciable amount of zero-order decomposition has taken place.

The model described by the set of non-linear partial differential equations, Equations III-1 through 8 accounts for all the modes of energy transformation associated with the first three stages listed above:

i. internal absorption of radiant energy

ii. storage of sensible heat

iii. heat loss from the fabric

iv. energy absorption during decomposition or drying

v. energy evolution at the time of ignition.

Of the overall total of 21 parameters describing the system, there are the total of twelve fabric properties ρ, c, k, $\tilde{\rho}$, κ, $(\Delta H_f)_{ex}$, $(\Delta H_f)_{en}$, A_{ex}, A_{en}, E_{ex}, E_{en}, and ε; five process parameters W_o, T_o, T_a, $(\bar{h}_c)_o$, $(\bar{h}_c)_\delta$, together with two dependent variables λ and T, and two independent variables x and t involved in the description of the system. The first five fabric properties are temperature dependent but will be taken as constants, evaluated at suitable temperatures between T_o and T_i. The reaction kinetics parameter are in general a function of the heating rate but are also approximated by constants.

Following this simplification, Equations III-1 and 3 through 8 are recast in nondimensional form to yield, from Equations III-1 and 3

$$\frac{\partial \theta}{\partial N_{Fo}} = \frac{\partial^2 \theta}{\partial (x^*)^2} + 2\kappa^* (N_{Bi})_{rad} E_2(\kappa^* x^*) + q^* \qquad \text{(III-9)}$$

$$q^* = N_1 e^{\phi_1} + N_2(1-\lambda)\ e^{\phi_2} \qquad \text{(III-10)}$$

where

$$\phi_1 = \pi_2 \frac{\psi}{\pi_o + \psi} \qquad \text{(III-11)}$$

$$\phi_2 = \pi_3 \frac{\psi}{\pi_o + \psi} \qquad \text{(III-12)}$$

$$\psi = \theta - 1 \qquad \text{(III-13)}$$

and from Equation III-4

$$\frac{d\lambda}{dN_{Fo}} = -(1-\lambda)\ N_3\ e^{\phi_2} \qquad \text{(III-14)}$$

The initial conditions are, from Equations III-5 and 6 at $N_{Fo} = 0$

$$\lambda = \theta = 0 \qquad \text{(III-15)}$$

The boundary conditions are, from Equations III-7 and 8 at $x^* = x/\delta = 0$

$$\frac{\partial \theta}{\partial x^*} = (N_{Bi})_o\ \theta \qquad \text{(III-16)}$$

at $x^* = 1$

$$-\frac{\partial \theta}{\partial x^*} = (N_{Bi})_\delta\ [\theta - \theta_a] \qquad \text{(III-17)}$$

2. Modeling Parameters

There are eleven parameters, N_{Fo}, $(N_{Bi})_{rad}$, $(N_{Bi})_o$, κ^*, $(N_{Bi})_\delta$, N_1, N_2, N_3, π_o, π_2 and π_4, together with the dependent variables λ and θ and the independent position variable x^*, in Equations III-9 through 17. These parameters are the modeling

parameters and define the solution more compactly than the 21 variables of the original set of equations. The parameters are arbitrary to some extent, in that any combination of parameters yields another parameter that may replace one in the combination. The total number of parameters is unique to the description of the model chosen at the outset (Equations III-1 and 3). Simplification of the model leads to a reduction in parameters and is called partial modeling.

The eleven parameters occuring in Equations III-9 through 17 are defined as

1. the normalized time, $N_{Fo} = \frac{t}{\rho c \delta} \frac{k}{\delta}$ (III-18)

2. the normalized irradiation, $(N_{Bi})_{rad} = \frac{(1-\tilde{\rho})\ W_o}{\frac{k}{\delta}\ (T_i - T_o)}$ (III-19)

3. the optical thickness $\kappa^* = \kappa\delta$ (III-20)

4. the exothermic reaction parameter,

$$N_1 = \frac{(1-\varepsilon)\ (\rho\delta)\ [\Delta H_f A]_{ex}}{\frac{k}{\delta}\ (T_i - T_o)}\ e^{-\pi_2} \qquad \text{(III-21)}$$

5. the endothermic reaction parameters,

$$N_2 = \frac{\varepsilon\ (\rho\delta)\ [\Delta H_f\ A]_{en}}{\frac{k}{\delta}\ (T_i - T_o)}\ e^{-\pi_3} \qquad \text{(III-22)}$$

and

$$N_3 = N_2\ \frac{c(T_i - T_o)}{\varepsilon\ (\Delta H_f)_{en}} \qquad \text{(III-23)}$$

6. the Biot numbers for front and back convection

$$(N_{Bi})_o = \frac{(\bar{h}_c)_o}{(\frac{k}{\delta})} \tag{III-24}$$

$$(N_{Bi})_\delta = \frac{(\bar{h}_c)_\delta}{(\frac{k}{\delta})} \tag{III-25}$$

7. the normalized initial temperature

$$\pi_o = \frac{T_i}{T_i - T_o} \tag{III-26}$$

and, finally,

8. the normalized activation energies

$$\pi_2 = \frac{E_{ex}}{RT_i} \tag{III-27}$$

$$\pi_3 = \frac{E_{en}}{RT_i} \tag{III-28}$$

The nondimensional fabric temperature is defined by

$$\theta = \frac{T-T_o}{T_i-T_o}, \text{ in } o \leq x^* \leq 1 \tag{III-29}$$

and becomes equal to unity at $x^* = 0$ when ignition occurs at the time $N_{Fo} = (N_{Fo})_i$. An order of magnitude comparison performed on the set of coupled equations which govern the time-temperature dependence in both the fabric and the tissue, indicates that $\theta_a = (T_a-T_o)/(T_i-T_o)$ remains insignificant, mainly because the skin temperature rises only moderately during the ignition process so long as the fabric does not touch the skin. Should the fabric touch

the skin then the ignition time would be far too long to be of interest here. Consequently, θ_a is set equal to zero.

Finally, the solution to Equations III-9 and 14, subject to Equations III-15, 16 and 17 yields the ignition time

$$(N_{Fo})_i = f\{(N_{Bi})_{rad}, (N_{Bi})_o, (N_{Bi})_\delta; N_1, N_2, N_3; \pi_o, \pi_2, \pi_3, \kappa^*\} \quad \text{(III-30)}$$

as a function of ten parameters which involve the 21 properties listed above. Every one of the nine parameters involves at least one fabric property. Nevertheless, the normalization of the governing equations has reduced the number of characteristics from 21 to 11 and has revealed that neither the thermal conductivity k nor the fabric thickness occur anywhere by themselves, but rather in the combinations $\rho\delta$, which is mass per unit area and k/δ, the thermal conductance and $\kappa\delta$, the optical thickness. This relevation is extremely helpful for the measurement of fabric properties.

The general solution, Equation III-30, may be found by numerical techniques but its dependence on 10 parameters renders it unwieldy. Thus it becomes necessary to identify and eliminate the parameters to which the solution is insensitive. This leads to partial modeling.

C. Partial Modeling Analysis

Depending on how many of the five processes listed in Chapter III-A dominate ignition under a given set of circumstances one can reduce the number of, or modify, the terms in the governing differential equations, Equations III-9, 10 and 14 so as to retain only

the dcminating terms. The relative significance of any term may be determined either from known fabric properties by an order-of-magnitude comparison, or by comparing experimental results with solutions to the simplified differential equations. The latter method was used since no reaction kinetics properties were known during the program phase reported herein.

When pre-ignition reactions are insignificant then one ignores the last term in Equation III-9 to obtain the inert ignition model. The fabric may be opaque and then represented by an inert, pure conduction model, or the fabric may be semitransparent as were all fabrics in the primary GIRCFF set. Then the fabric is represented by the inert, conductive and radiative model. These inert models are discussed below. All models described by partial differential equations such as Equation III-9 shall be called distributed parameter models. When details in the fabric interior are ignored then ordinary differential equations are used and the resulting class of models is called lumped-parameter models.

1. Distributed-Parameter Model Without Chemical Reaction

Setting the reaction term $q^* = 0$ in Equation III-9 leads to the description of the inert model. Analytical solutions exist in the literature for the cases of pure conduction through an opaque slab [III-5] and of conduction and radiation following Beer's law [III-6].

Pure conduction through an opaque slab implies $\kappa^* \to \infty$ and $E_2 (\kappa^* x^*) \to 0$. In the limit, the appropriate equations become

$$\left.\begin{aligned} &\frac{\partial\theta}{\partial N_{Fo}} = \frac{\partial^2\theta}{\partial (x^*)^2} \\ &\theta\ (x^*,\ O) = O \\ &\text{at } x^* = o\text{: } \frac{\partial\theta}{\partial x^*} = -\ (N_{Bi})_{rad} + (N_{Bi})_o \\ &\text{at } x^* = 1\text{: } -\frac{\partial\theta}{\partial x^*} = (N_{Bi})_\delta \end{aligned}\right\} \qquad \text{(III-31)}$$

The solution θ is presented in Figure III-2 for the front face, $\theta(O, N_{Fo})$ when $(N_{Bi})_o = O$ and for an adiabatic back face, that is $\theta\ (1, N_{Fo})$ when $(N_{Bi})_\delta = O$.

The diagram in Figure III-2 is used by first evaluating three of the four non-dimensional groups (with only two choices for $x^* = x/\delta$) listed above and then selecting the curve corresponding to the value of $N_{Bi} = \bar{h}_t\delta/k$ (if this group is known), either from the family of curves for the front face (heated) or from that for the back face to find the unknown fourth group, either $\theta/(N_{Bi})_{rad}$ or N_{Fo}. Once the unknown group is found one can readily compute the unknown parameter itself, such as the temperature T corresponding to a specific time t or the time at which a specific temperature is reached. Two possible applications are depicted in the figure.

Allowing for convective cooling from both sides, the ignition time

$$(N_{Fo})_i = f\ \{(N_{Bi})_{rad},\ (N_{Bi})_o,\ (N_{Bi})_\delta\} \qquad \text{(III-32)}$$

depends on <u>three</u> parameters, and when the heating is intense convection becomes insignificant; the ignition time of opaque

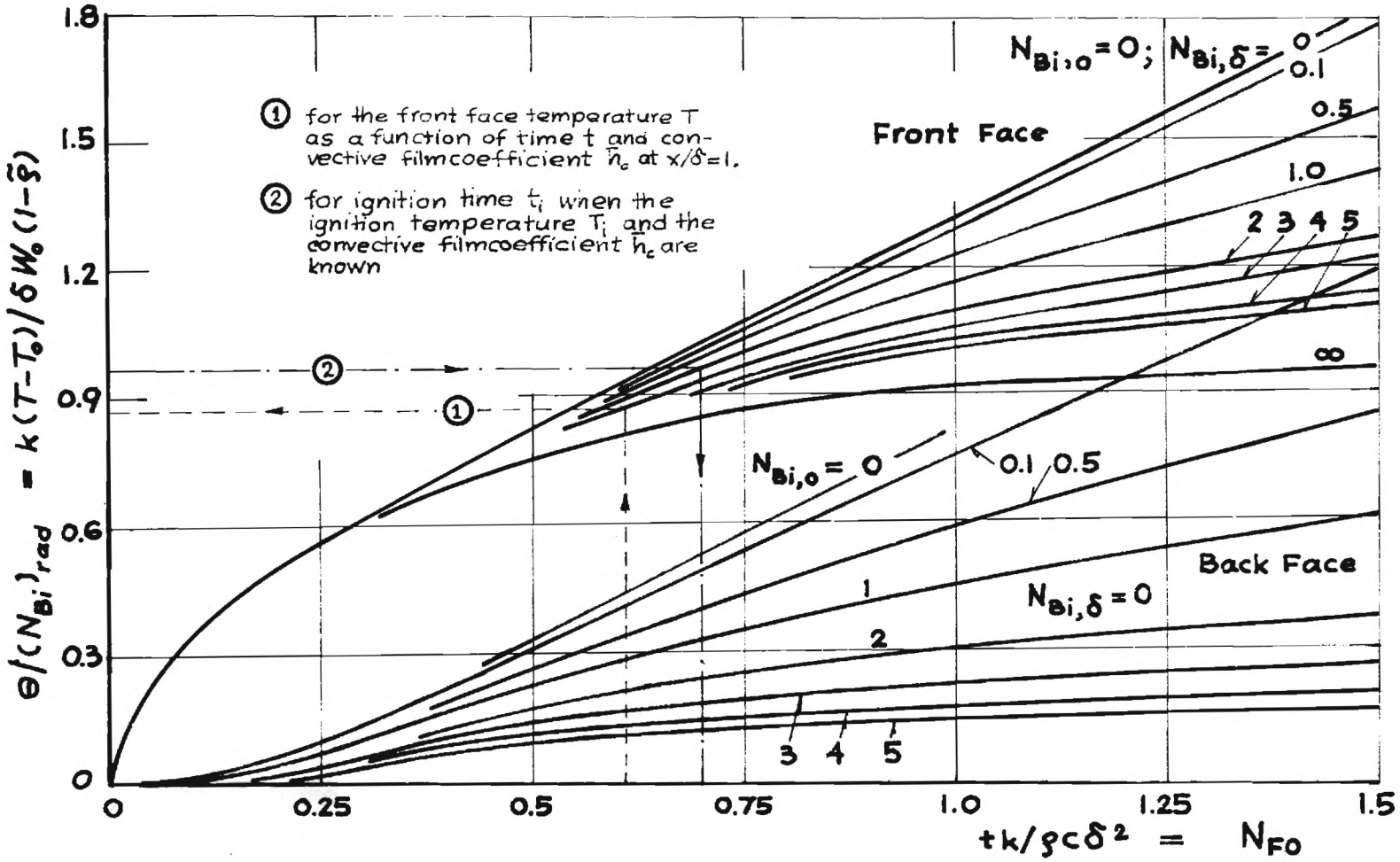

Figure III-2. Solution Chart For Conductive Slab With Constant Heat Flux at One Face and Convective Boundary at the Other

ordinary differential equation was integrated by a fifth-order Runge-Kutta procedure with automatic time step selection. The convection parameters $(N_{Bi})_o$ and $(N_{Bi})_\delta$, which characterize fabric sample size, geometry and the fabric's ability to conduct heat, were evaluated for the test conditions in the Ignition Time Apparatus and found to be $(N_{Bi})_o = (N_{Bi})_\delta = 0.05$. Comparing the solution calculated with $(N_{Bi})_o = (N_{Bi})_\delta = 0$ with that computed with $(N_{Bi})_o = (N_{Bi})_\delta = 0.05$ for $\kappa^* = 0.284$ (cotton) one finds that convection retards ignition only slightly at the moderately strong irradiation of $(N_{Bi})_{rad} = 3.0$ ($W_o = 12$ W/cm^2). The ignition time is increased by ≈5% as the result of convection. Convection becomes effective only at low heating levels and can prevent the fabric from ever reaching ignition.

For the case of strong heating one may set $(N_{Bi})_o = (N_{Bi})_\delta = 0$ to obtain the solution

$$(N_{Fo})_i = f\{(N_{Bi})_{rad}, \kappa^*\} \qquad \text{(III-35)}$$

as shown in Figure III-3. The integrations were performed for $0.1 \leq (N_{Bi})_{rad} \leq 100$ and $0.1 \leq \kappa^* \leq 2.0$ although the domain of interest is much smaller as indicated in the diagram.

The most important conclusion drawn from Figure III-3 is that, for the fabrics of interest, i.e. $0.1 \leq \kappa^* \leq 0.5$, the slope of the curve $(N_{Fo})_i$ versus $(N_{Bi})_{rad}$ has the value of nearly -1. This means that the product $(N_{Fo})_i \cdot (N_{Bi})_{rad}$ equals a constant,

$$\frac{(1-\tilde{\rho})\, W_o t_i}{\rho c \delta\, (T_i - T_o)} = \text{const.} = \frac{1-\tilde{\rho}}{\alpha} \qquad \text{(III-36)}$$

(heavy) fabrics under intense heating and in the absence of chemical reactions depends on a single parameter, $(N_{Bi})_{rad}$.

None of the ten primary GIRCFF fabrics is opaque. Radiative heat transfer is superimposed on conductive transfer. The governing equations for the inert semitransparent slab are derived from Equation III-9 by setting $q^* = 0$

$$\left.\begin{aligned}
&\frac{\partial\theta}{\partial N_{Fo}} = \frac{\partial^2\theta}{\partial(x^*)^2} + 2\kappa^* (N_{Bi})_{rad} E_2(\kappa^* x^*) \\
&\text{at } x^* = 0 \\
&\quad -\frac{\partial\theta}{\partial x^*} = (N_{Bi})_o \theta \\
&\text{at } x^* = 1 \\
&\quad \frac{\partial\theta}{\partial x^*} = (N_{Bi})_\delta \theta \\
&\text{at time } N_{Fo} = 0 \quad \theta = 0 \\
&\text{at ignition} \qquad \theta = 1 \\
&\qquad\qquad N_{Fo} = (N_{Fo})_i
\end{aligned}\right\} \qquad \text{(III-33)}$$

The ignition time $(N_{Fo})_i$ for semitransparent, conducting inert fabrics depends on four parameters

$$(N_{Fo})_i = f\{(N_{Bi})_{rad}, k^*, (N_{Bi})_o, (N_{Bi})_\delta\} \qquad \text{(III-34)}$$

The system of Equations III-33 was numerically integrated. Spatial derivatives were discretized, and the resulting first-order

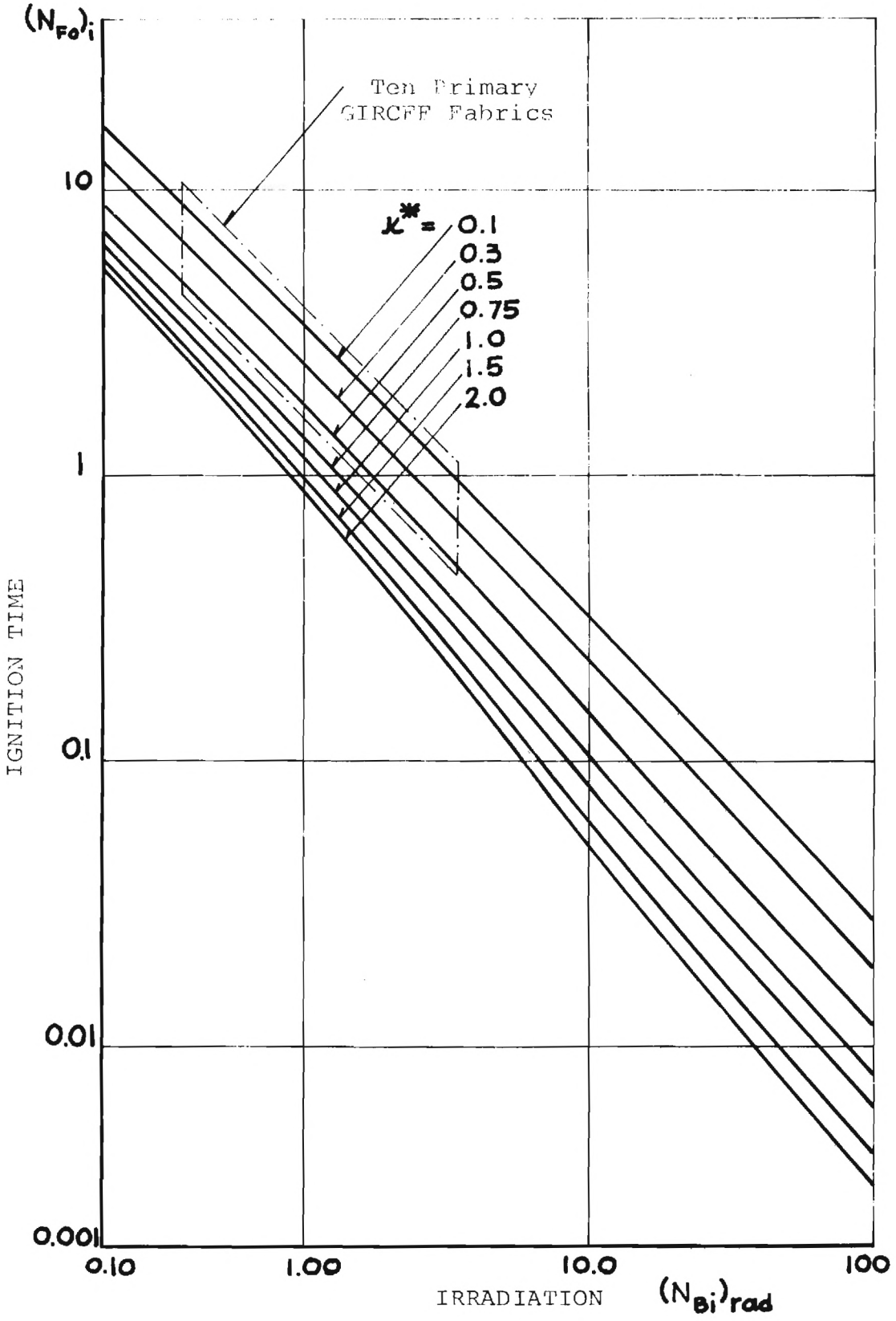

Figure III-3. Ignition Time Chart for Semitransparent Slab of Optical Thickness κ^*, Without Convective Loss

and that the thermal conductance is insignificant. Close inspection of the computer results reveals that, very early in the heating process, a temperature profile establishes itself which compensates for the non-uniform radiant heat absorption in such a way that the local energy storage and with it the time rate of temperature rise are uniform. Then, under constant heating, the temperature rises linearly with time. The difference between front and back face temperatures is less than 10% except when $(N_{Bi})_{rad} > 5.0$ which is beyond the capability limit of the Ignition Time Apparatus. Hence the energy stored per unit area, $\rho c\delta\ (T_i - T_o)$ is essentially equal to the energy absorbed during the ignition period, $\alpha W_o t_i$, where α is the fabric absorptance. But that is precisely what is expressed by Equation III-36.

The thermal conductance is equally insignificant even in the presence of free convection. Moreover, chemical reaction rates are dictated primarily by fabric temperature, and when the fabric temperature is uniform the reaction rate will also be uniform. Detailed, distributed parameter analyses are not called for in the study of fabric ignition, except in the case of heavy, opaque fabrics where appreciable temperature gradients can develop.

In summary, the distributed parameter analysis of the semi-transparent, conducting slab with in-depth radiative energy absorption has shown that the ignition process is

i. generally independent of the fabric conductance k/δ

ii. associated with uniform heating within the fabric, except in heavy, opaque fabrics

iii. associated with uniformly distributed chemical reactions, if any.

This shows that a lumped parameter analysis is adequate, the most significant result of the distributed parameter analysis.

2. Lumped-Parameter Model with Chemical Reaction

Integrating Equation III-1 with respect to x, from x = o to x = δ and combining the result with the boundary conditions, Equation III-7 and 8 one obtains, after setting $T_a = T_o$, $(\bar{h}_c)_o = (\bar{h}_c)_\delta$ and after normalization

$$\dot{\theta} = 1 + \pi_4 e^{\phi_1} + \pi_5 (1-\lambda) e^{\phi_2} - \pi_1 \theta \qquad \text{(III-37)}$$

$$\dot{\lambda} = -(1-\lambda)\ \pi_6 e^{\phi_2} \qquad \text{(III-38)}$$

where the superscripted dot represents differentiation with respect to the non-dimensional time τ

$$\tau = \frac{\alpha\ W_o\ t}{\rho c \delta\ (T_i - T_o)} \qquad \text{(III-39)}$$

The exponents ϕ_1 and ϕ_2 have been defined by Equations III-11 through 13 and III-26 through 28. The parameter of relative heat loss by convection is

$$\pi_1 = \frac{2\ \bar{h}_c\ (T_i - T_o)}{\alpha\ W_o} \qquad \text{(III-40)}$$

while π_4, π_5 and π_7 replace N_1, N_2 and N_3, respectively

$$\pi_4 = \frac{(1-\varepsilon)\ \rho\delta\ [\Delta H_f\ A]_{ex}}{\alpha\ W_o}\ e^{-\pi_2} \qquad \text{(III-41)}$$

$$\pi_5 = \frac{\varepsilon\rho\delta\ [\Delta H_f\ A]_{en}}{\alpha\ W_o}\ e^{-\pi_3} \qquad \text{(III-42)}$$

$$\pi_6 = \pi_5\ \frac{c\ (T_i - T_o)}{\varepsilon\ (\Delta H_f)_{en}} \qquad \text{(III-43)}$$

In Equation III-37 the first term on the left-hand side represents energy storage, the first on the right-hand side constitutes the energy absorption, the second the exothermic reaction, the third represents the energy absorbing $[(\Delta H_f)_{en} < 0]$ first-order reaction, and the last term stands for the convective heat loss. Equations III-37 and 38 are subject to the initial conditions

$$\text{at } \tau = 0: \qquad \theta = \lambda = 0 \qquad \text{(III-44)}$$

and the ignition time τ_i is reached when $\theta = 1$ and, therefore

$$\tau_i = f\ \{\pi_o,\ \pi_1,\ \pi_2,\ \pi_3,\ \pi_4,\ \pi_5,\ \pi_6\} \qquad \text{(III-45)}$$

depends now on <u>seven</u> parameters, a reduction by three relative to the distributed parameter analysis. Equations III-37, 38 and 44 have been integrated numerically with the parameters π_o, π_1, π_2, π_3, π_4, π_5, and π_6 evaluated for α-cellulose on the basis of reaction kinetic properties published by Akita and Kase [III-7]. The preliminary results indicate the proper ignition delay by the endothermic reaction, they check against limiting cases discussed later and they reveal weak dependence on the parameters π_2 and π_3. Further studies are in progress and final verification must await the measurement of reaction kinetics.

3. Limiting Cases of the Lumped-Parameter Model

Three closed-form solutions will demonstrate the significance of the parameter τ_i and the effects of individual processes.

a. Inert Heating. Setting π_4, π_5 and π_6 equal to zero in Equations III-37 and 38 yield the inert heating process. In the absence of free convection, $\pi_1 = 0$, one obtains simply $\tau_i = 1$ and the real ignition time

$$t_i = \frac{\alpha W_o}{\rho c (T_i - T_o)} \qquad \text{(III-46)}$$

depends on four fabric characteristics: α, ρ, c and T_i and two process parameters, W_o and T_o. When $\pi_1 \neq 0$ then

$$\tau_i = -\frac{1}{\pi_1} \ln (1-\pi_1) \qquad \text{(III-47)}$$

This result is shown in Figure III-4 and demonstrates the effect of free convection. Free convection prolongs the ignition time at decreasing irradiance levels until ignition is no longer possible for $\pi_1 \to 1$, that is as the convective losses at ignition temperature approach the incident heat flux. For a fixed sample size and geometry π_1 increases with decreasing heating intensity. Moving in the positive abscissa direction in Figure III-4 corresponds to increasing radiant intensity. The operating range of the Ignition Time Apparatus lies between $\pi_1 = 0.2$ and $\pi_1 > 1$ where ignition occurs due to the exothermic effects. Most data were obtained in $0.2 < \pi_1 < 0.99$. The curve in Figure III-4 shows that convection can increase the ignition time by a factor 4.5 over

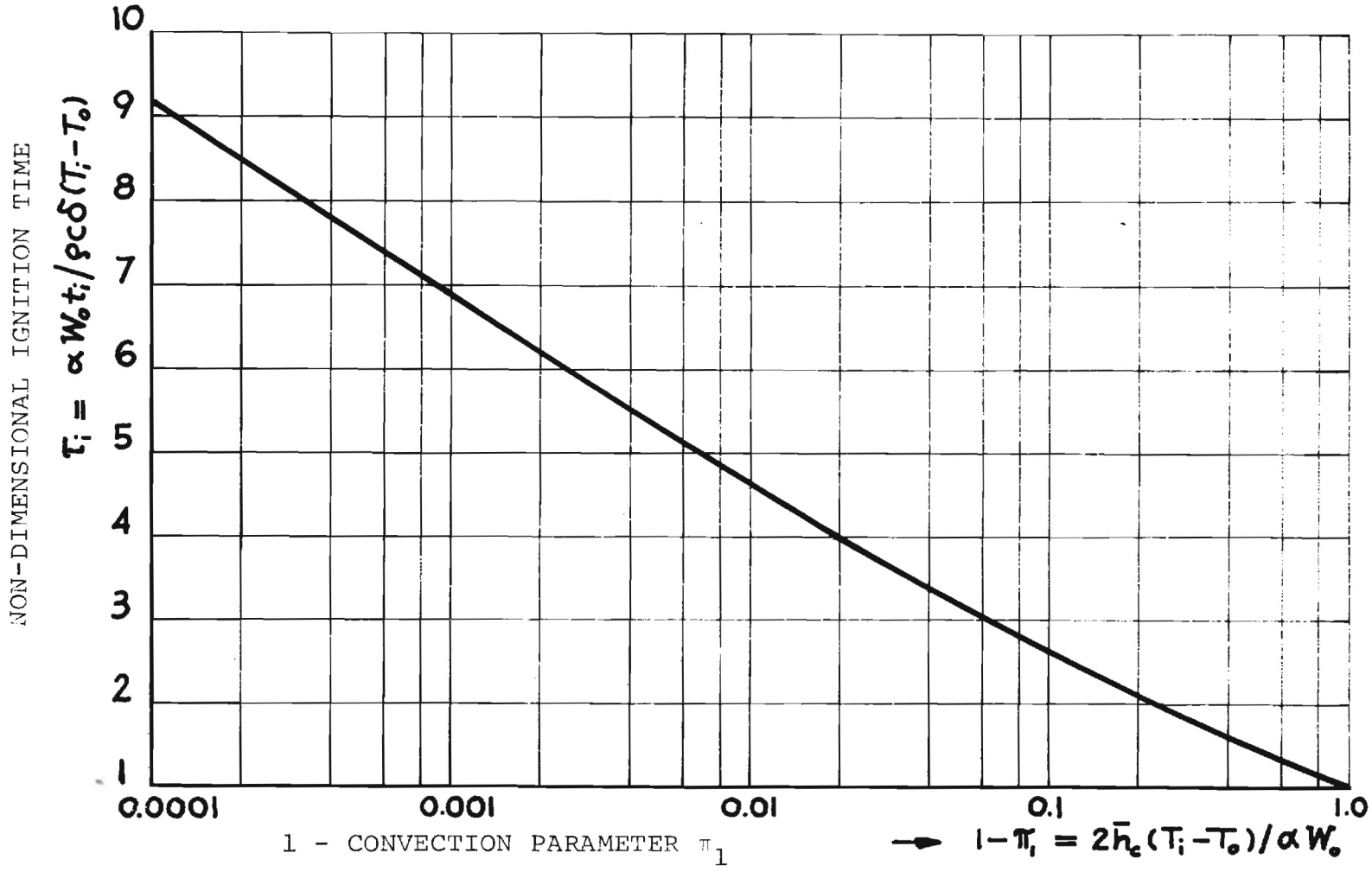

Figure III-4. Effect of Free Convection on Ignition Time

that given by Equation III-46, at very low heating levels.

b. Zero-Order Reactions. The significance of the zero-order reaction (with both exothermic or endothermic effects) can be demonstrated by integrating Equation III-37 after setting $\pi_1 = \pi_5 = 0$. The closed-form, analytical integration is possible when

$$\pi_o >> (\theta-1) \tag{III-48}$$

that is, for fabrics with low ignition or melting temperatures then $\phi_1 \tilde{=} \pi_2 (\theta-1)/\pi_o$ and the ignition time

$$\tau_i = 1 + \frac{\pi_o}{\pi_2} \ln \frac{1 + \pi_4 e^{-\pi_2/\pi_o}}{1 + \pi_4} \tag{III-49}$$

depends on two parameters, namely π_4 and (π_2/π_o) where

$$\frac{\pi_2}{\pi_o} = \frac{E (T_i - T_o)}{R T_i^2} \tag{III-50}$$

This contraction of parameters is the result of ignoring $\theta-1$ in the sum $\pi_o + \theta - 1$.

When $\pi_4 > 0$ (exothermic reaction) then τ_i is less than unity as it should on account of the fabrics deliberation of heat. When $\pi_4 = 0$ (inert heating) then $\tau_i = 1$ and Equation III-46 applies. However, when $\pi_4 < 0$ (endothermic zero-order reaction) singularities occur in the solution, Equation III-49. The first singularity occurs when no ignition takes place because $\pi_4 = -1$ and, at some

fabric temperature, the incident energy is totally absorbed by the endothermic reaction. Should that occur at the initial temperature, then Equation III-49 would degenerate into its second singularity, that is, ignition is also impossible when $1 - \pi_4 \exp(-\pi_2/\pi_o) = 0$. The entire range of possible τ_i in accordance with Equation III-49 is $0 \leq \tau_i \leq 1$ for exothermic reactions and $1 \leq \tau_i < \infty$ for endothermic reactions with $-1 < \pi_4 \leq 0$. There are no solutions for $-1 > \pi_4 > -\exp(\pi_2/\pi_o)$ and the mathematically possible solutions for $\pi_4 < -\exp(\pi_2/\pi_o) < -1$ cannot be expected to be physically meaningful.

All the conclusions drawn from this analysis of a zero-order reaction are subject to the rather restrictive condition that there be no significant depletion of decomposable material. One would therefore expect the zero-order reaction model without convective losses to apply only to those cases of intense heating where ignition occurs <u>early</u> during pyrolysis or drying, or where ignition occurs without endothermic reaction.

D. Errors Associated With Partial Modeling

There are two methods to estimate the errors associated with partial modeling of the fabric ignition process. The first method is the comparison of analytical results calculated from the simplified ignition model with experimental ignition data. The comparison may produce disagreement between calculated and experimental results in which case the model is inadequate to the extent of the disagreement, provided that the experiments are reliable.

If agreement is found with a particular model which includes a set of processes (such as sensible heat storage, convection losses) and if disagreement is shown between experimental data and another model which includes only the processes neglected in the first model, then one concludes that the first model is adequate. But if only the first condition is met then there remains some doubt concerning the correctness of the simplifications or partial modeling. As an example, ignition may be delayed either by convective losses or by endothermic effects or by both with partial compensation by exothermic effects. Conceivably, there could be three partial modeling analyses in acceptable agreement with experiments.

The comparison of experimental data with the computed results is presented in Section III-E and shows that the error associated with partial modeling depends on the fabric properties.

The second method is based on the presupposition that all the fabric properties are known and that the complete mathematical description, Equations III-9 through 17, is adequate. Then one can either estimate the relative magnitude of each term in the governing equation and conclude as to the error associated with the omission of a term, i.e. a set of parameters, or one can execute the integration of both the complete and the simplified equations and calculate the error from the difference of the results.

A complete and vigorous discussion of the errors associated with partial modeling involves the combination of both methods and appears impossible without reaction kinetics data of fabrics available. However, the analyses carried out on the basis of

inert heating reveal nevertheless when certain simplifications can be made. These are discussed below.

1. Error of Lumped-Parameter Analysis

All fabrics in the primary GIRCFF set have optical thicknesses κ^* below 0.4, all but one fabric have $\kappa^* < 0.3$. Numerical solutions to Equations 33 have shown that the ignition time error introduced by the lumped-parameter analysis ranges between 4% and 7%. This result was obtained by integrating Equations III-33 for $\kappa^* = 0.284$ (cotton fabric GIRCFF #5) for the irradiance levels $1.0 \leq (N_{Bi})_{rad} \leq 6.00$ or $4.5 \leq W_o \leq 28.0$ W/cm^2, and no convective losses. The higher discrepancy (7%) was obtained for the high heating rate.

The inclusion of chemical reactions and of free convection is not expected to alter the error estimate because chemical reactions are as uniformly distributed throughout the fabric as its temperature, and convection alters the temperature distribution insignificantly. The lumped-parameter description merely replaces the inherently flat temperature distribution by a constant, mean temperature throughout.

2. Error of Ignition Models Without Convective Losses

The convection parameter π_1, defined by Equation III-40, represents mainly the shape and size of the heated fabric area. It is the ratio of convective heat loss over incident heat fluxes. At intense heating with $\pi_1 < 0.2$ the ignition time calculation is affected by less than 12%. As the heating intensity decreases and

π_1 increases to 0.9, the ignition time increases by a factor of 2.6. With further decreases in heating intensity convection becomes rapidly overwhelming and eventually prevents ignition as the ignition time tends toward infinity, $\tau_i \rightarrow \infty$.

Within the range of experimental heating intensities in the Ignition Time Apparatus, $0.1 < \pi_1 < 0.9$, and the influence of convection on ignition time causes the ignition time to grow by a factor between 1.1 and 2.6 at most.

3. Error of Ignition Models Without Chemical Reaction

This error cannot be clearly identified for the fabrics tested since no reaction parameters are known. Of greatest interest for the ignition time measurements is the ignition delay found in cotton fabrics. Activation energy, pre-exponential factor and enthalpy of pyrolysis for α-cellulose have been published by Akita and Kase [III-7] and may be used to estimate the order of magnitude of the parameters describing the chemical reaction of cotton.

These parameters are π_o, π_1, π_2, π_3, π_4, π_5, and π_6 defined by Equations III-26, 27, 28, 41, 42 and 43. Knowing the ignition temperature is essentially equivalent to the knowledge of the parameters π_2 and π_4, together with π_o. Consequently there remains the assessment of the effects from parameters π_3, π_5, and π_6.

With regard to endothermic reactions such as drying, pyrolysis and melting, one can say summarily that whenever the endothermic reaction is completed prior to ignition, then the normalized

ignition time τ_i increases due to endothermic reaction by the quantity $\rho\delta\varepsilon(\Delta H_f)_{en}/(\alpha W_o t_i)$, that is the ratio of energy consummed by the reaction to the energy absorbed by the fabric. Whether or not the reaction is completed prior to ignition depends on A and E, the pre-exponential factor and the activation energy. The above ratio is equivalent to π_5.

When the endothermic reaction is essentially incomplete at ignition time (ignition of pyrolysis products when rate of evolution and gas temperature are sufficiently high), or when partial melting precedes ignition, or when ignition occurs at the beginning of an exothermal reaction then ignition delay or acceleration can be estimated by means of Equation III-49. Taking $\pi_2/\pi_o = 15$ as for α-cellulose one obtains for the non-dimensional ignition time τ_i the following reductions and increases as a function of π_4:

Table III-1. Estimate of Error Due to Neglecting Zero-Order Reaction

	Reaction parameter* π_4	Non-dimensional ignition time τ_i	Error from setting $\pi_4 = 0$
Endothermic	-0.999	1.461	-46%
	-0.900	1.153	-15%
	-0.800	1.107	-11%
	-0.600	1.034	- 3.4%
	-0.200	1.015	- 1.5%
Inert	-0.000	1.000	--
Exothermic	1.0	0.9538	+ 4.6%
	2.0	0.9314	+ 6.9%
	3.0	0.9076	+ 9.2%
	5.0	0.8805	+12%
	10.0	0.8400	+16%
	100.0	0.6910	+31%

*π_4 is defined by Equation III-41

This table indicates the possible errors resulting from neglecting chemical reaction for a particular value of (π_2/π_o). General error estimates are readily evaluated from Equation III-49.

E. Comparison of Analytical with Experimental Results

Ignition time and thermophysical properties were measured for the ten primary GIRCFF fabrics as discussed in Chapter II. These ten fabrics are listed in the order of their GIRCFF numbers in Table II-1, but are divided here into three groups:

1. 100% Cotton, GIRCFF Fabric Nos. 5, 10, 18, 19 (cellulose)
2. Plastic Polymers, GIRCFF Fabric Nos. 2, 11, 12, 13
3. Blends of Cotton and Polyester, GIRCFF Fabric Nos. 8, 17

Figures III-5, 6 and 7 show, respectively the experimental ignition data for Groups 1, 2 and 3. The non-dimensional ignition time τ_i is plotted versus $1-\pi_1$, where π_1 is the convective heat loss parameter that characterizes sample size and geometry and that is the only independent parameter appearing in the ignition model without chemical reactions. In Figure III-5 are indicated the contributions to the ignition time by sensible heating, convective heat losses and endothermic reaction. The parameter π_1 is evaluated with the convective film coefficient $\bar{h}_c = 3.82 \times 10^{-3}$ W/(cm^{2}c).

All cotton fabrics, except the five retardant treated GIRCFF Fabric No. 19, show the same behavior. Energy requirements for ignition are up to twice as large as can be accounted for by sensible heat storage and convective losses, the balance being

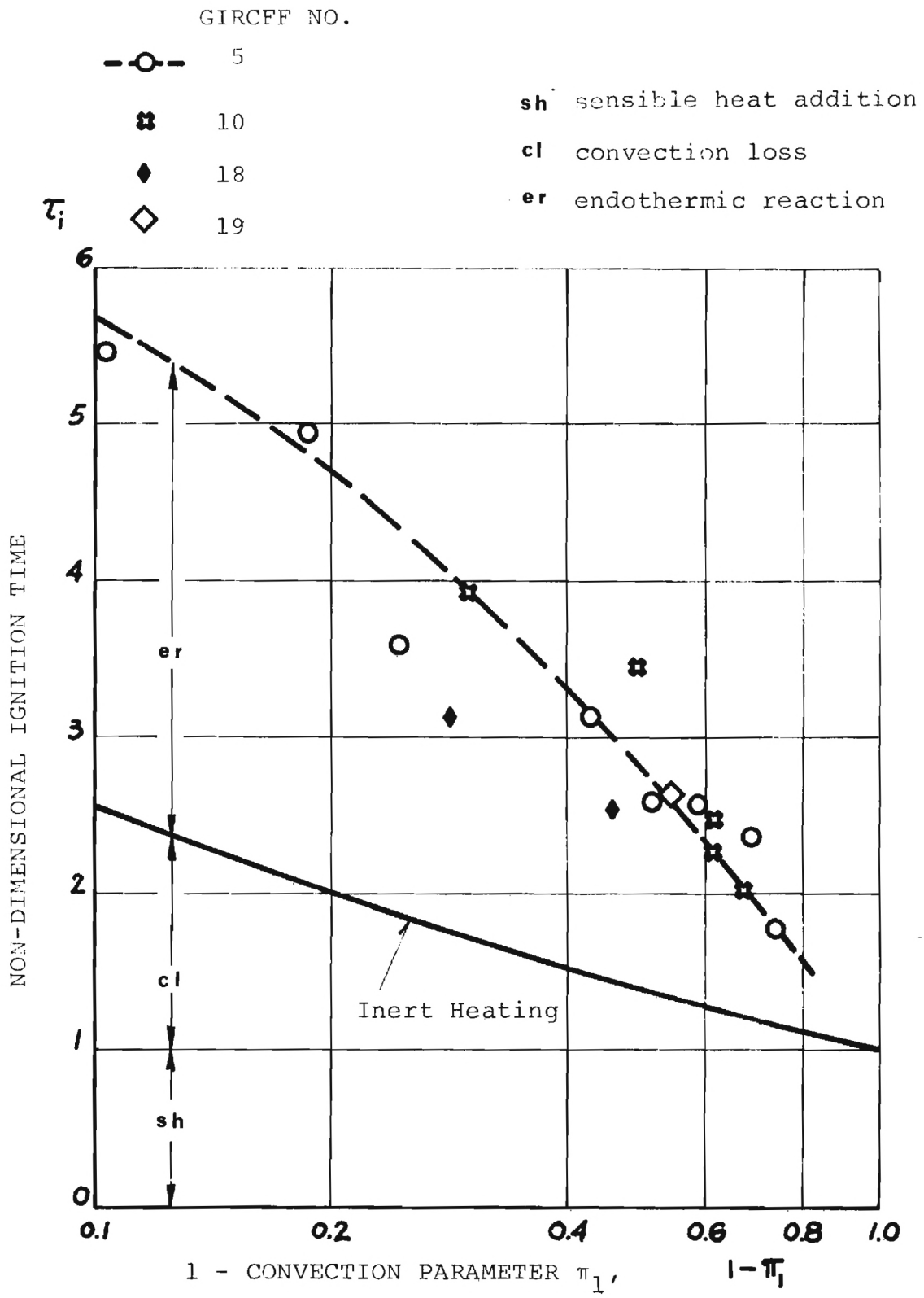

Figure III-5. Comparison of Experimental Ignition Data With Inert Heating Ignition Model For Four Cotton Fabrics

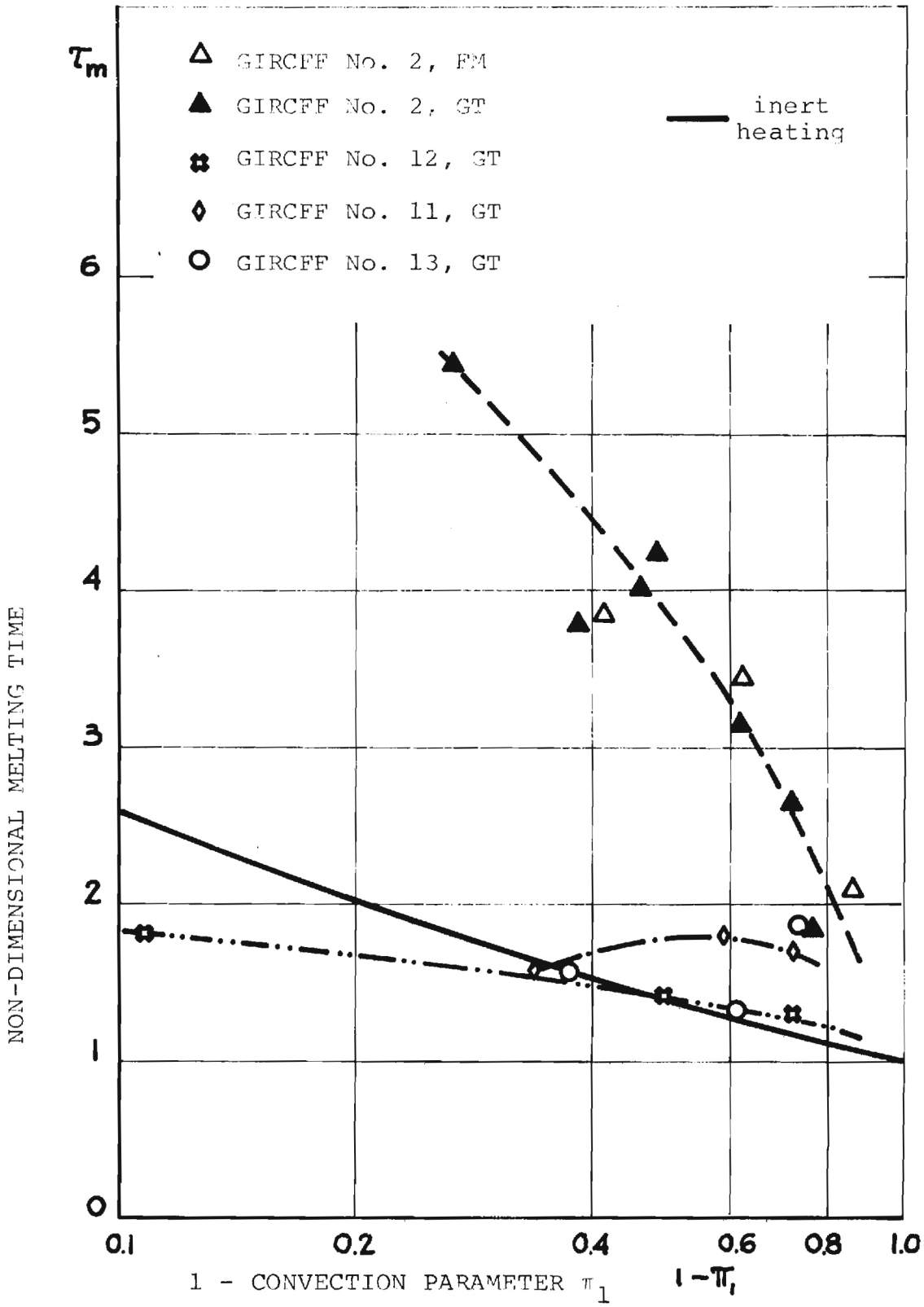

Figure III-6. Comparison of Experimental Melting Data With Inert Heating Model For Plastic Polymeric Fabrics

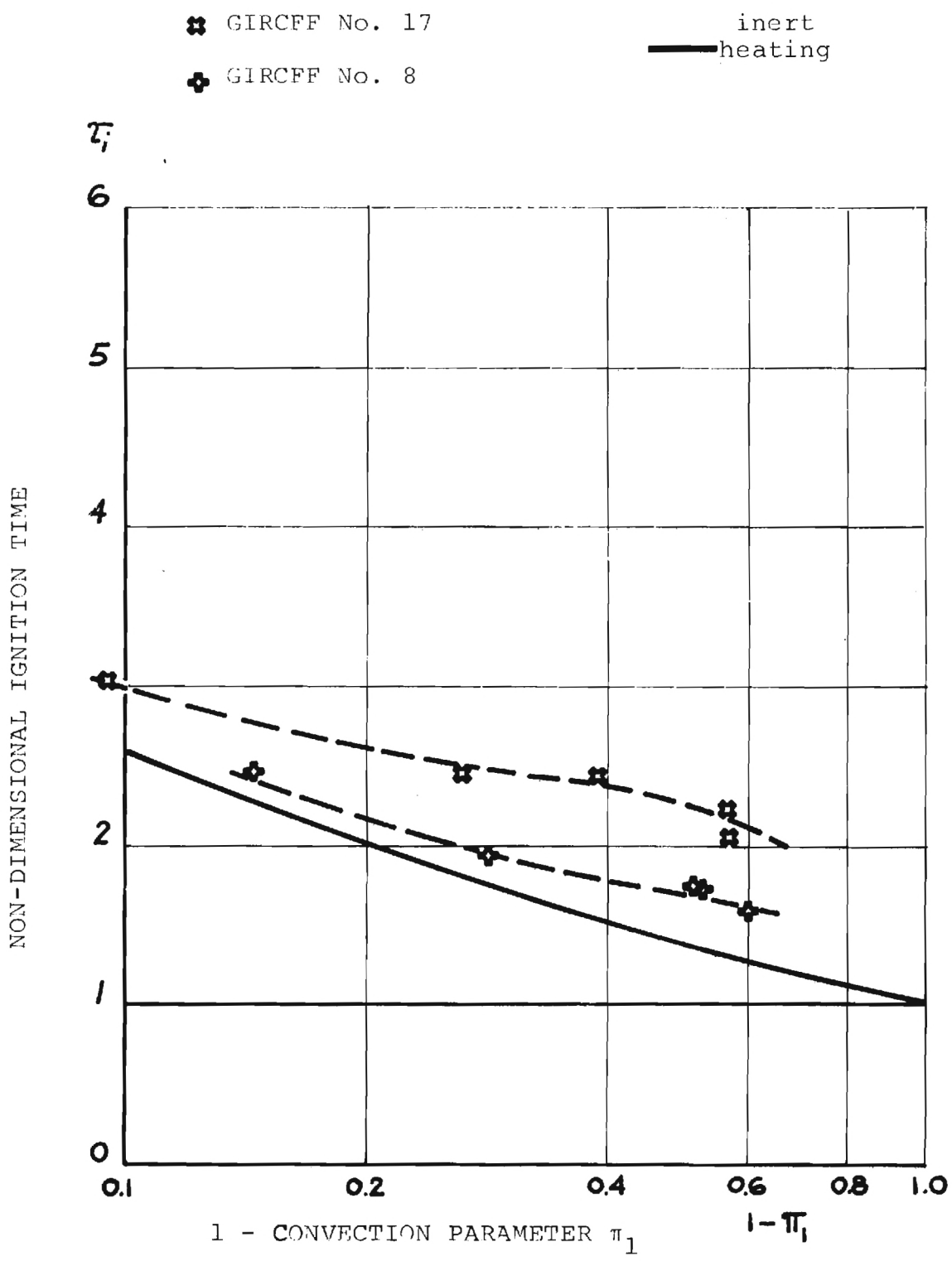

Figure III-7. Comparison of Experimental Ignition Data With Inert Heating Ignition Model For Blends of Cotton and Polyester

considered necessary for pyrolysis. The significance of pyrolysis decreases with increasing heating intensity. Fabric No. 19 does not fit this pattern. Its non-dimensional ignition time is less than unity, suggesting ignition accelerating energy deliberation from exothermic reactions. One point each for Fabrics No. 5 and 10 and two points each for Fabrics No. 18 and 19 are not reported since the π_1 parameter evaluation resulted for these fabrics in values greater than unity. The inert-heating ignition model cannot predict ignition for $\pi_1 > 1$ ($\tau_1 \rightarrow \infty$ for $\pi_1 \rightarrow 1$), and negative values of $(1-\pi_1)$ cannot be reported in the semi-logarithmic chart.

Plastic polymeric fabric ignition data are plotted in Figure III-6. Polyester shows strong influence by endothermic reactions prior to ignition, with the same general pattern as for cotton fabrics. Both the results from Factory Mutual [III-8] and Georgia Tech are represented. The other plastic polymers show relative small deviations from the inert-heating ignition model.

Cotton-polyester blends show ignition characteristics that differ from both those of cotton and of polyester, as may be seen in Figure III-7. With decreasing heating intensity both blends approach the ignition pattern of inert fabrics. Also, with increasing irradiance $\tau_i \rightarrow 1.0$, while there is approximately 100% deviation at $\pi_1 \simeq 0.6$.

In general, it may be concluded, that reaction kinetics are as important as sensible heat storage and convective losses during the ignition process. Based on inert heating, the self ignition analysis under-estimates ignition time by a factor of up to two in the case of eight fabrics, by a factor of up to three in the case

of one fabric, and over-estimates ignition time by 50% in the case of one fabric. Pyrolysis enthalpies of approximately $2\rho c\delta\ (T_i - T_o)$ are suggested by the experimental data to be associated with endothermic reactions prior to ignition of nine fabrics.

Figure III-8 is the original plot of non-dimensional ignition time $(N_{Fo})_i$ versus non-dimensional irradiation $(N_{Bi})_{rad}$ as presented in Chapter II but with two inert-heating ignition models included. The two models are inert heating with and without convective heat losses, and the chosen fabric is GIRCFF No. 10. This figure demonstrates the significance of convection losses at low radiative heating levels.

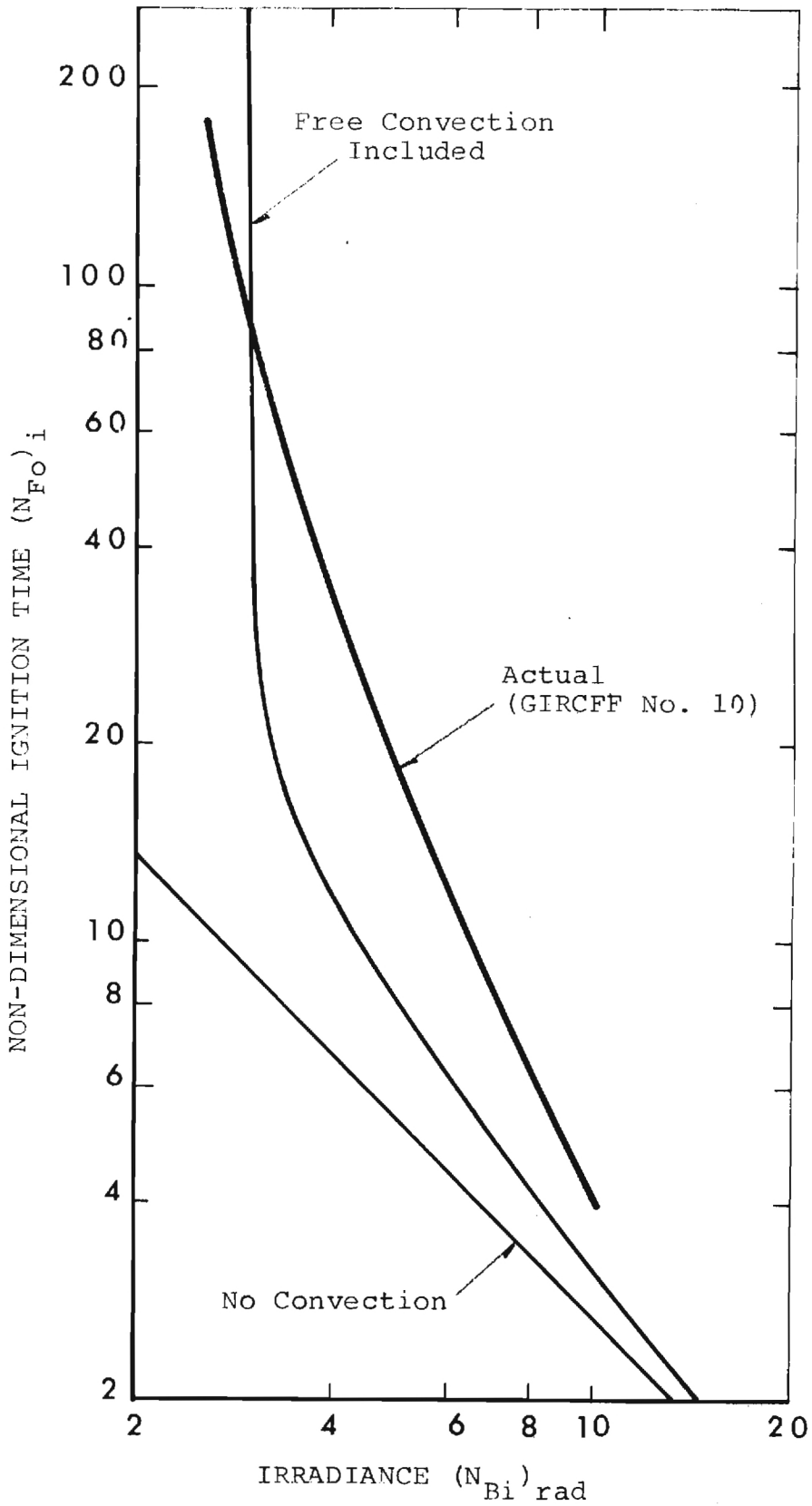

Figure III-8. Inert Heating Models and Experimental Ignition Data in the $(N_{Fo})_i$ - $(N_{Bi})_{rad}$ Plane. See Figure II-4

IV. CONCLUSIONS

The Analysis has lead to the conclusion that under radiative heating and free convection heat losses

1. for fabrics whose optical thickness (product of physical fabric thickness and radiative extinction coefficient) is less than 0.5, a lumped-parameter analysis describes sufficiently well the ignition process to predict ignition time,
2. for fabrics with optical thickness less than 0.5 (all primary GIRCFF fabrics), conduction within the fabric plays an insignificant role, thermal conductivity measurements are not necessary.

This most important conclusion simplifies significantly the modeling analysis.

Considering inert heating by a radiative heat source, fabric ignition time is related to fabric properties such that

3. fabric ignition time increases proportionally to the product of fabric mass per unit area ($\rho\delta$) times specific heat (c) times excess of ignition temperature over initial temperature ($T_i - T_o$), divided by the radiative absorption coefficient (α), or

$$t_i \sim \rho c \delta \, (T_i - T_o)/\alpha \qquad \text{(IV-1)}$$

4. the proportionality coefficient implied in (IV-1) increases with decreasing heating intensity and with increasing ratio of excess of ignition over initial temperatures, $(T_i - T_o)$, to the radiative absorption coefficient, (α).

5. Convective heat losses during radiant heating to ignition increase ignition time significantly, except during intensive heating (with ignition times of less than five seconds in the case of the primary GIRCFF fabrics).

6. Pre-ignition pyrolysis may significantly retard or even prevent ignition (see Chapter III-C.3b for estimate of conditions.)

7. Exothermal reaction effects are indirectly prescribed at least in part, through the specification of ignition temperature; the effects may be responsible for ignition to occur even in limiting cases where convective heat losses would prevent the fabric from reaching ignition temperature.

The Experiments have shown that for the primary GIRCFF fabrics

8. Fabric properties that are essential to the ignition process can tentatively be identified as:

    mass per unit area
    specific heat
    ignition temperature
    radiative absorptance
    enthalpy of pyrolysis

    the measurements of these fabrics may be considered to be part of the partial modeling process.

9. Specific heat varies widely, between 1.2 (acetate) and 2.4 Ws/gC (cotton) from fabric to fabric and between 1.4 and 2.4 Ws/gC as a function of temperature.

10. Thermal conductance is found to increase with temperature and to increase generally with increasing contact pressure (the only exception is nylon tricot); conductance was found

to vary between 6.5 and 30 mW/cm^2c, over all fabrics, as a result of both temperature and pressure variations.

11. Melting fabrics melt all in the narrow temperature range between 218 and 255°C, self-ignition temperatures range between 300 and 500°C, with cotton batiste having the lowest, cotton flannel the highest self-ignition temperatures.

12. Only approximately 20% of the radiative energy incident on the fabric is absorbed by the fabric.

13. Ignition time depends strongly on chemical reactions prior to ignition. Cellulosic fabrics ignite up to three times slower than predicted by inert reaction models. For plastic polymers the retardation factor is less, about 1.5. One fabric showed a 20% reduction in ignition time due to exothermic reaction.

APPENDIX A

THERMOPHYSICAL PROPERTY SUMMARY

Appendix A.1

Thermophysical Property Summary

Textured Woven Blouse

GIRCFF Fabric No.2

1. Description

   Fiber Composition: 100% polyester

   Color: Yellow

2. Mass Per Unit Area: 7.51 mg/cm^2

3. Specific Heat

Temperature	50	125	200	°C
Spec. Heat	1.42	1.42	1.42	Ws/gC

4. Thermal Conductance

(i)	Contact Pressure	528 N/m^2			
	Temperature	73.0	93.1	124.6	°C
	Conductance	20.3	21.0	22.8	W/cm^2K
(ii)	Contact Pressure	866 N/m^2			
	Temperature	83.3	86.3		°C
	Conductance	21.0	22.7		W/cm^2K
(iii)	Contact Pressure	1,370 N/m^2			
	Temperature	75.8			°C
	Conductance	22.5			W/cm^2K

5. Melting Temperature, self 255°C, pilot °C

6. Infrared Optical Properties

	Original	Charred at °C
Absorptance	0.153	
Reflectance	0.501	
Transmittance	0.346	
Optical Thickness	0.208	

Appendix A.2

Thermophysical Property Summary

T-shirt, Jersey

GIRCFF Fabric No. 5

1. Description

   Fiber Composition: 100% cotton

   Color: White

2. Mass Per Unit Area: 13.71 mg/cm^2

3. Specific Heat

Temperature	50	125	200	°C
Spec. Heat		1.69	1.88	Ws/gC

4. Thermal Conductance

(i)	Contact Pressure	528 N/m^2			
	Temperature	70.9	130.5	206.0	°C
	Conductance	7.32	8.81	10.82	W/cm^2K
(ii)	Contact Pressure	866 N/m^2			
	Temperature	57.4	79.8		°C
	Conductance	7.31	11.28		W/cm^2K
(iii)	Contact Pressure	1,370 N/m^2			
	Temperature	76.5			°C
	Conductance	13.02			W/cm^2K

5. Ignition Temperature, self 311°C, pilot 311°C

6. Infrared Optical Properties

	Original	Charred at 206°C
Absorptance	0.183	0.225
Reflectance	0.521	0.442
Transmittance	0.296	0.333
Optical Thickness	0.282	0.304

Appendix A.3

Thermophysical Property Summary

T-shirt, Jersey

GIRCFF Fabric No. 8

1. Description

   Fiber Composition: 65/35% Polyester/Cotton

   Color: White

2. Mass Per Unit Area: 16.91 mg/cm^2

3. Specific Heat

Temperature	50	125	200	°C
Spec. Heat	1.28	1.52	1.92	Ws/gC

4. Thermal Conductance

(i)	Contact Pressure	528 N/m^2			
	Temperature	68.4	129.6	205.9	°C
	Conductance	7.63	10.50	11.13	W/cm^2K
(ii)	Contact Pressure	866 N/m^2			
	Temperature	56.0	81.7		°C
	Conductance	7.99	9.13		W/cm^2K
(iii)	Contact Pressure	1,370 N/m^2			
	Temperature	75.4			°C
	Conductance	10.74			W/cm^2K

5. Ignition Temperature, self 439 °C, pilot 304 °C

6. Infrared Optical Properties

	Original	Charred at 206°C
Absorptance	0.164	0.370
Reflectance	0.560	0.489
Transmittance	0.276	0.141
Optical Thickness	0.272	0.833

Appendix A.4

Thermophysical Property Summary

Batiste

GIRCFF Fabric No. 10

1. Description

   Fiber Composition: 100% Cotton

   Color: Purple

2. Mass Per Unit Area: 6.65mg/cm^2

3. Specific Heat

Temperature	50	125	200	°C
Spec. Heat	1.28	1.94		Ws/gC

4. Thermal Conductance

   (i) Contact Pressure 528 N/m^2

Temperature	67.8	128.4	195.8	°C
Conductance	17.48	20.19	29.67	W/cm^2 K

   (ii) Contact Pressure 866 N/m^2

Temperature				°C
Conductance				W/cm^2 K

   (iii) Contact Pressure 1,370 N/m^2

Temperature	7.65			°C
Conductance	25.36			W/cm^2 K

5. Ignition Temperature, self 429 °C, pilot 339 °C

6. Infrared Optical Properties

	Original	Charred at 196°C
Absorptance	0.200	0.422
Reflectance	0.406	0.297
Transmittance	0.394	0.281
Optical Thickness	0.236	0.570

Appendix A.5

Thermophysical Property Summary

Tricot

GIRCFF Fabric No. 11

1. Description

   Fiber Composition: 80/20% Acetate/Nylon

   Color: White

2. Mass Per Unit Area: 11.31 mg/cm^2

3. Specific Heat

Temperature	50	125	200	°C
Spec. Heat	1.45	1.45	1.45	Ws/gC

4. Thermal Conductance

   (i) Contact Pressure 528 N/m^2

Temperature	75.2	95.2	130.9	°C
Conductance	6.60	7.08	8.08	W/cm^2K

   (ii) Contact Pressure 866 N/m^2

Temperature	86.2	°C
Conductance	7.46	W/cm^2K

   (iii) Contact Pressure 1,370 N/m^2

Temperature	77.7	°C
Conductance	8.13	W/cm^2K

5. Melting Temperature, self 218°C, pilot °C

6. Infrared Optical Properties

	Original	Charred at °C
Absorptance	0.163	
Reflectance	0.508	
Transmittance	0.329	
Optical Thickness	0.232	

Appendix A.6

Thermophysical Property Summary

Tricot

GIRCFF Fabric No. 12

1. Description

   Fiber Composition: 100% Nylon

   Color: White

2. Mass Per Unit Area: 8.91mg/cm^2

3. Specific Heat

Temperature	50	125	200	°C
Spec. Heat	1.72	2.25		Ws/gC

4. Thermal Conductance

(i)	Contact Pressure	528 N/m^2			
	Temperature	76.1	96.3	122.6	°C
	Conductance	19.3	17.00	20.93	W/cm^{2}K
(ii)	Contact Pressure	866 N/m^2			
	Temperature	56.1	92.2		°C
	Conductance	17.35	20.8		W/cm^{2}K
(iii)	Contact Pressure	1,370 N/m^2			
	Temperature	73.5			°C
	Conductance	17.89			W/cm^{2}K

5. Melting Temperature, self 237°C, pilot °C

6. Infrared Optical Properties

	Original	Charred at °C
Absorptance	0.170	
Reflectance	0.397	
Transmittance	0.433	
Optical Thickness	0.188	

Appendix A.7

Thermophysical Property Summary

Tricot

GIRCFF Fabric No. 13

1. Description

   Fiber Composition: 100% Acetate

   Color: White

2. Mass Per Unit Area: 9.40mg/cm^2

3. Specific Heat

Temperature	50	125	200	°C
Spec. Heat	1.27	1.68	2.09	Ws/gC

4. Thermal Conductance

   (i) Contact Pressure 528 N/m^2

Temperature	72.1	94.9	125.1	°C
Conductance	12.21	18.07	15.86	W/cm^{2}K

   (ii) Contact Pressure 866 N/m^2

Temperature	91.7	°C
Conductance	18.82	W/cm^{2}K

   (iii) Contact Pressure 1,370 N/m^2

Temperature	76.9	°C
Conductance	17.56	W/cm^{2}K

5. Melting Temperature, self 218°C, pilot °C

6. Infrared Optical Properties

	Original	Charred at °C
Absorptance	0.167	
Reflectance	0.443	
Transmittance	0.390	
Optical Thickness	0.208	

Appendix A.8

Thermophysical Property Summary

Batiste

GIRCFF Fabric No. 17

1. Description

   Fiber Composition: 65/35% Polyester/Cotton

   Color: White

2. Mass Per Unit Area: 8.55 mg/cm^2

3. Specific Heat

Temperature	50	125	200	°C
Spec. Heat	1.33	1.44	1.77	Ws/g^C

4. Thermal Conductance

   (i) Contact Pressure 528 N/m^2

Temperature	72.6	128.0	199.3	°C
Conductance	17.34	22.48	26.75	W/cm^2K

   (ii) Contact Pressure 866 N/m^2

Temperature				°C
Conductance				W/cm^2K

   (iii) Contact Pressure 1,370 N/m^2

Temperature	77.3			°C
Conductance	30.41			W/cm^2K

5. Ignition Temperature, self 463 °C, pilot 368 °C

6. Infrared Optical Properties

	Original	Charred at199°C
Absorptance	0.164	0.201
Reflectance	0.464	0.464
Transmittance	0.372	0.335
Optical Thickness	0.208	0.274

Appendix A.9

Thermophysical Property Summary

Flannel

GIRCFF Fabric No.18

1. Description

   Fiber Composition: 100% Cotton

   Color: White

2. Mass Per Unit Area: 12.88 mg/cm^2

3. Specific Heat

Temperature	50	125	200	°C
Spec. Heat	1.34	1.60	2.12	Ws/gC

4. Thermal Conductance

   (i) Contact Pressure 528 N/m^2

Temperature	73.0	134.4	205.3	°C
Conductance	5.55	6.72	8.74	W/cm^2K

   (ii) Contact Pressure 866 N/m^2

Temperature		°C
Conductance		W/cm^2K

   (iii) Contact Pressure 1,370 N/m^2

Temperature	78.6	°C
Conductance	7.06	W/cm^2K

5. Temperature, self 301 °C, pilot 278 °C

6. Infrared Optical Properties

	Original	Charred at 205°C
Absorptance	0.176	0.188
Reflectance	0.573	0.591
Transmittance	0.251	0.221
Optical Thickness	0.312	0.368

Appendix A.10

Thermophysical Property Summary

Flannel

GIRCFF Fabric No.19

1. Description

   Fiber Composition: 100% Cotton

   Color: White

   Finish: Fire Retardant

2. Mass Per Unit Area: 14.81 mg/cm^2

3. Specific Heat

Temperature	50	125	200	°C
Spec. Heat	1.37	1.57	2.44	Ws/gC

4. Thermal Conductance

   (i) Contact Pressure 528 N/m^2

Temperature	73.0	134.1	203.5	°C
Conductance	5.38	7.55	9.46	W/cm^2K

   (ii) Contact Pressure 866 N/m^2

Temperature				°C
Conductance				W/cm^2K

   (iii) Contact Pressure 1,370 N/m^2

Temperature	77.8			°C
Conductance	8.55			W/cm^2K

5. Temperature, self 463 °C, pilot 316 °C

6. Infrared Optical Properties

	Original	Charred at 204°C
Absorptance	0.201	0.461
Reflectance	0.602	0.267
Transmittance	0.197	0.272
Optical Thickness	0.428	0.620

APPENDIX B

INSTRUMENTATION AND PROCEDURES

Appendix B.1

The Ignition Time Apparatus

The Ignition Time Apparatus, designed to meet the specifications listed in Chapter II-A.1, is shown schematically in Figure B-1 and the assembly in Figures B-2 through B-6. The device consists of four major components discussed in Part b of this Appendix.

i) the shutter system
ii) the radiant heater
iii) the sample support
iv) the instrumentation for timing and flame detection.

a. Operating Principle of Ignition Time Apparatus. The radiant heater is first energized to reach radiative equilibrium while the fabric sample is shielded from the heater by the first shutter plate. The release solenoid (near the front edge of the table in Figures B-5 and B-6) releases the first shutter plate which rapidly exposes the fabric sample to the radiant heater and triggers two dual-channel oscilloscopes shown in Figure B-10. When ignition occurs the infrared flame emission activates the infrared detector shown in Figure B-9 which deflects one of the four oscilloscope beams. Ordinarily this completes the principal ignition time test. The heater is deactivated, the shutter spring recocked and a new sample inserted.

The energy transmitted through the fabric sample is monitored by a thermoelectric radiant heat flux meter maintained essentially at constant temperature. The second oscilloscope beam traces this transmitted radiant heat flux behind the fabric while the other two beams serve for the timing references. Furthermore, the shutter

system is capable to expose the fabric for a limited time interval in that a second shutter plate can be released to interrupt the radiant flux after a selected time interval (0.2 to 60 seconds) following the exposure by the first plate. This procedure affords the detailed study of thermal degradation on the fabrics.

b. Design Features of Ignition Time Apparatus. As shown in Figure B.1 the first three major components as listed above are mounted onto the 1 in x 12 in x 66 in base plate made from 6061-T651 aluminum tooling plate. The 1.500 in wide and 1/8 in deep slot milled lengthwise along the centerline serves to line up accurately the subassemblies of the shutter system.

i. The Shutter System

consists of the shutter, the shutter release and catch system and the cock and uncock system, one each for exposure and subsequent closing actions. Figure B-1 shows only one half of the system; the other half is essentially symmetric.

Each shutter consists of the shutter plate which is held vertically in the plate guides and connected to a heavy, helical spring by the slender operating rod. The operating rod engages, at its necked-down sections, with the release and catch mechanisms. After being cocked and released the spring accelerates the shutter plate. Then the rod is caught by the catch mechanism when it reaches, for the first time, the instant of zero velocity and extreme spring deformation opposite to its starting position. While sweeping across the fabric sample center with its exposing or shielding edge, the shutter plate reaches its maximum velocity and its edge traverses the fabric sample in approximately 5 milliseconds.

The shutter plates are made from 0.032 in thick, stainless steel and travel in pairs of slotted brass assemblies bolted to aluminum "T" extrusions (6061-T651) one of which is fitted into the base plate slot and the other one is mounted to the top protrusions machined on the spring housing supports. The operating rods which connect shutter plates and springs are made from drill rod and heat treated to maximum hardness. They travel in bronze bearings pressed into cylindrical blocks at the shutter side of the tubular spring housing. The outer ends of the operating rods are connected to the inner, mobil spring terminals which are made from hot-rolled steel and machined to screw tightly into a spring end. Similar but larger spring terminals, flanged to the outer, jack side ends of the spring housings hold the stationary ends of the heavy, primary springs. The primary springs are 8.50 in long, have the helix diameter of 1.75 in, 20 turns and are wound from 0.250 in diameter wire. Their spring constant is 100 lbf/in and their maximum deformation is 2.50 in. The spring mass is approximately 1.20 lbm and comprises fifty percent of the effective translating mass. Each of the primary springs is enclosed in the tubular spring housing which is flanged axially against the outer, jack side spring housing support and also supported by the inner, shutter side spring housing support.

The shutter release and catch mechanisms serve to release in selected time intervals the exposing and shielding shutter plates under dual shutter operating mode and to catch the rod at the proper time as discussed above. Both mechanisms are similar and mounted to the base plate as well as the inner spring housing

support blocks. Each of the four mechanisms consists of a brass yoke carried by a pair of hardened rods (tool steel) which are attached to a Model 446-1, AC push-pull solenoid of 608 oz capacity. The brass yoke engages with the operating rod at its necked-down sections. The steel rods travel in sintered bronze bushings pressed into the aluminum blocks which support the release and catch mechanisms. The catching yoke is held against the large-diameter section of the operating rod by two small compression springs, the secondary springs, which push the yoke into the reduced diameter section of the operating rod at its end position. The catch yoke is released from the primary spring load by the cocking jack.

The cock and uncock systems serve to expand or compress the primary springs for cocking and to return the springs to their neutral positions. These systems consist each of one heavy duty automotive screw-type jack and a steel rod which connects the jack to the mobil spring terminal. The jack is bolted to the base plate via two "L" profiles as can be seen in Figure B-9.

ii. The Heating Source

necessary to produce the fabric sample irradiation between 800 and 50,000 Btu/(hr ft^2) or 0.25 to 15.8 W/cm^2 consists of a Model 5208-5 High Density Modular Radiant Heater purchased from Research, Inc. and a variable autotransformer suitable to adjust the power level continuously from zero to full power at 7.2 kW. The heater contains six tungsten filament tubular quartz lamps, Model 1200 T3/CL from General Electric. The lamps have the active length of

6 in, produce 1.2 kW and are air-cooled. The highly reflective, aluminum lamphousing is water-cooled and emits the radiant heat flux through its 6 in x 3 in quartz window at the rate of 37.8 W/cm^2 or 120,000 Btu/(hr ft^2). An insulated shield with a 1-1/2 in opening separates the heater from the shutter.

The heater is mounted to the base plate of the Ignition Time Apparatus via a transite block, such that the distance between the heater window and the shutter plates is 0.25 in. The resulting distance between fabric and heater window is approximately 1 in.

iii. The Sample Support

as shown in Figure B-7 is designed to position the fabric sample parallel to and at most one inch away from the heater window and to expose a 1 in diameter circle of the fabric to the heater while the back face of the irradiated sample is free to accommodate the radiometer which senses the heat transmitted through the fabric. The principle arrangement of the fabric sample with respect to the heater, the shutter and the sensors is shown in Figure B-8.

iv. The Timing and Sensing Instrumentation

consists of a microswitch, activated by the exposing shutter plate and signaling the start of the exposure, further of a Mark 1 Infrascope by Barnes Engineering to signal ignition, of a Hy-Cal Model C-1301-A thermoelectric heat flux meter to measure the energy transmitted through the fabric and, finally, of two dual channel oscilloscopes equipped with Polaroid cameras to record the signals from the microswitch, the Infrascope and the flux meter. Typical oscillograms are shown below. Ignition or melting is taken to occur where the extensions of the flat and step-rise curve portions intersect.

The timing circuit necessary to activate the release solenoids for dual shutter operation is not yet designed but will consist of commercially available, electronic (short-time action) and electro-mechanical timers.

IGNITION TIME OF FABRICS

Experimentors RWH & A.A. Date Oct. 19, 71

Run No. 37, S. H. No. 10 Fabric No. 10

Voltage Supplied to Heat Source (U_o) 110 Volts

Incident Heat Flux (W_o) 6.58×10^4 Btu.hr.$^{-1}$ft^{-2}, 20.78 w/cm^{-2}

Biot Number $(N_{Bi})_{rad}$ 0.841

INFRASCOPE TRACE

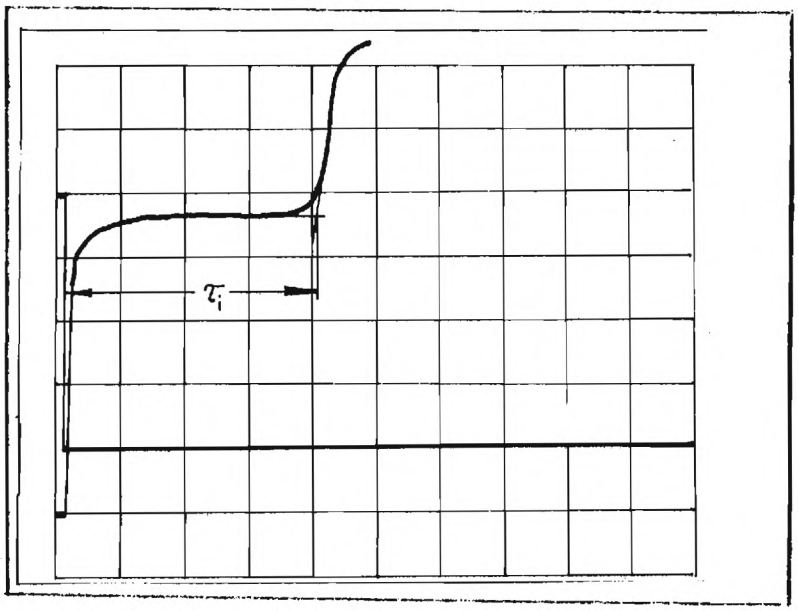

U.B. Sensitivity 20 mV/cm

L.B. Sensitivity 2 V/cm

Sweep Rate 1 s/cm

INFRASCOPE READING:

Ignition time 3.87 cm

Ignition time 3.87 sec

Fourier Number of Ignition

$(N_{Fo})_i$ = 6.20

THERMOELECTRIC HEAT FLUX METER TRACE

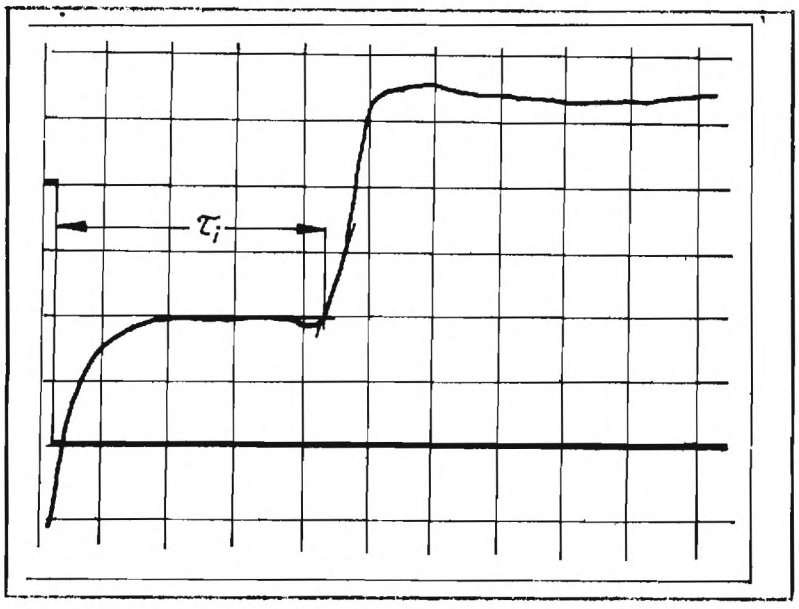

U.B. Sensitivity 0.5 mV/cm

L.B. Sensitivity 2 V/cm

Sweep Rate 1 s/cm

FLUX METER READINGS:

Ignition time 3.93 cm

3.93 sec

Initial Heat Flux 1.33 mV

4.24 Btusec^{-1}ft^{-2}

Heat Flux Prior to Ign 1.532 mV

4.89 Btusec^{-1}ft^{-2}

$(N_{Fo})_i$ = 6.30

Transmittance:

$\tau_{init.}$ = 0.418, τ_{ign} = 0.482

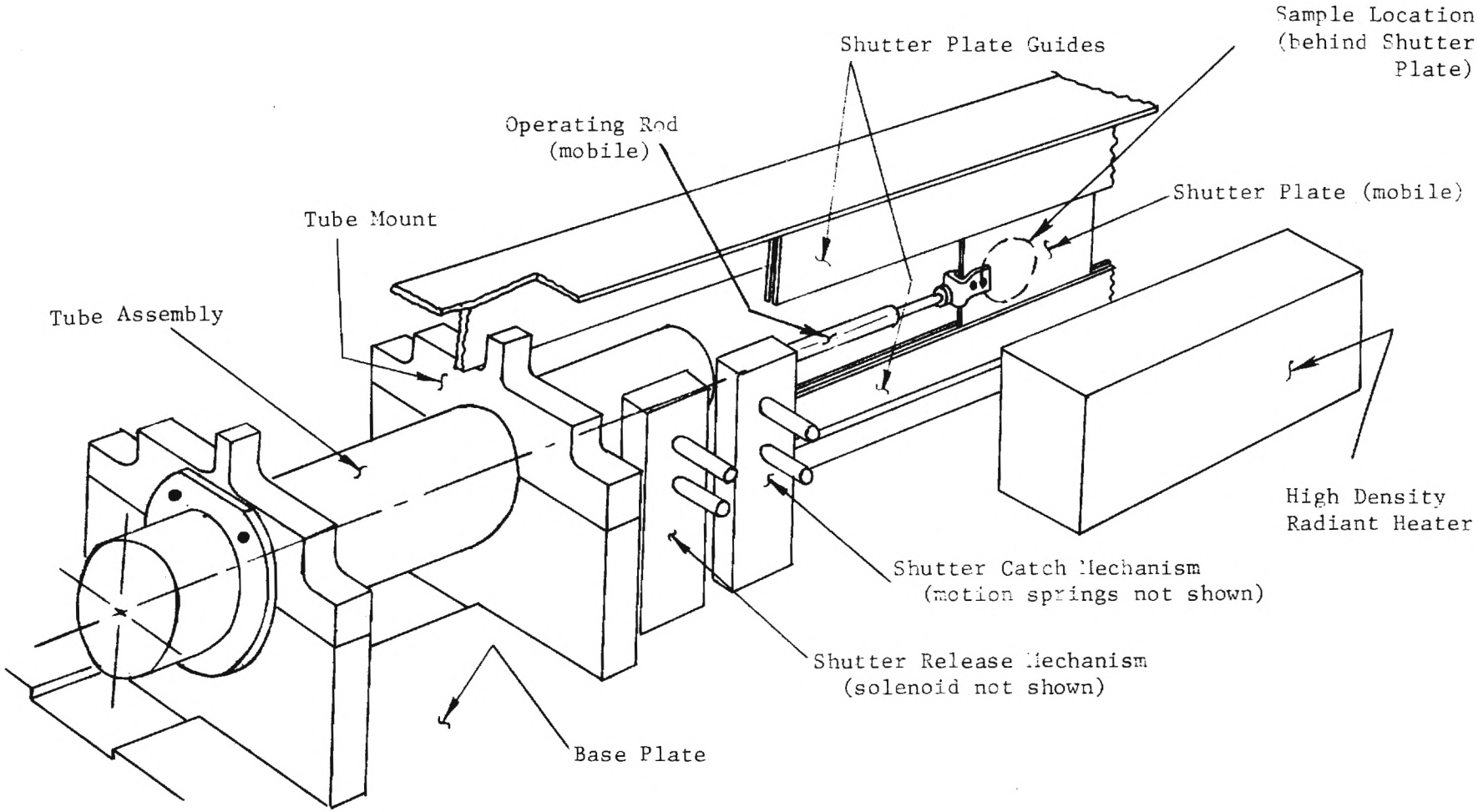

Figure B.1. Schematic of Ignition Time Apparatus

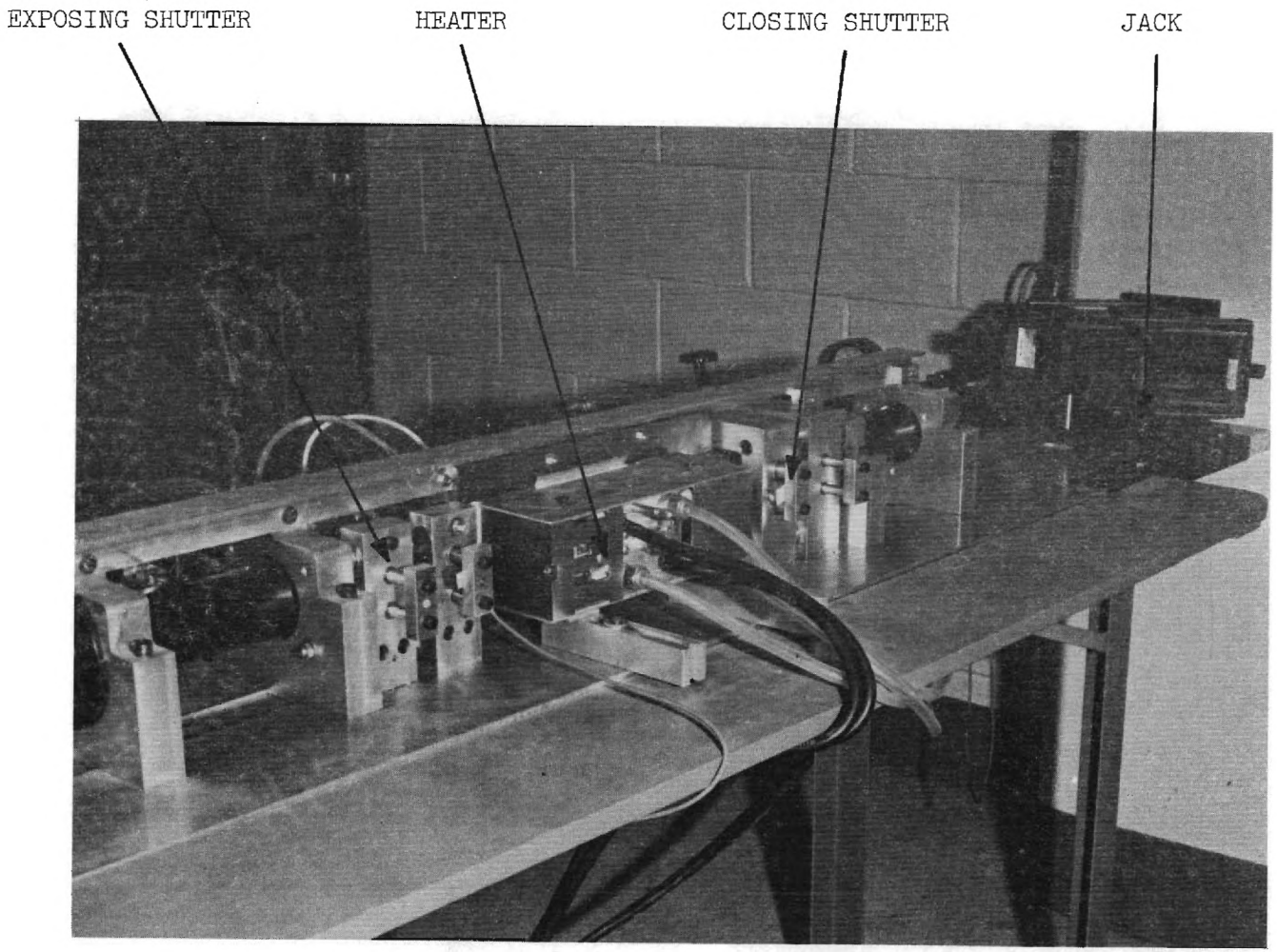

Figure B.2. Ignition Time Apparatus Viewed from Heater Side

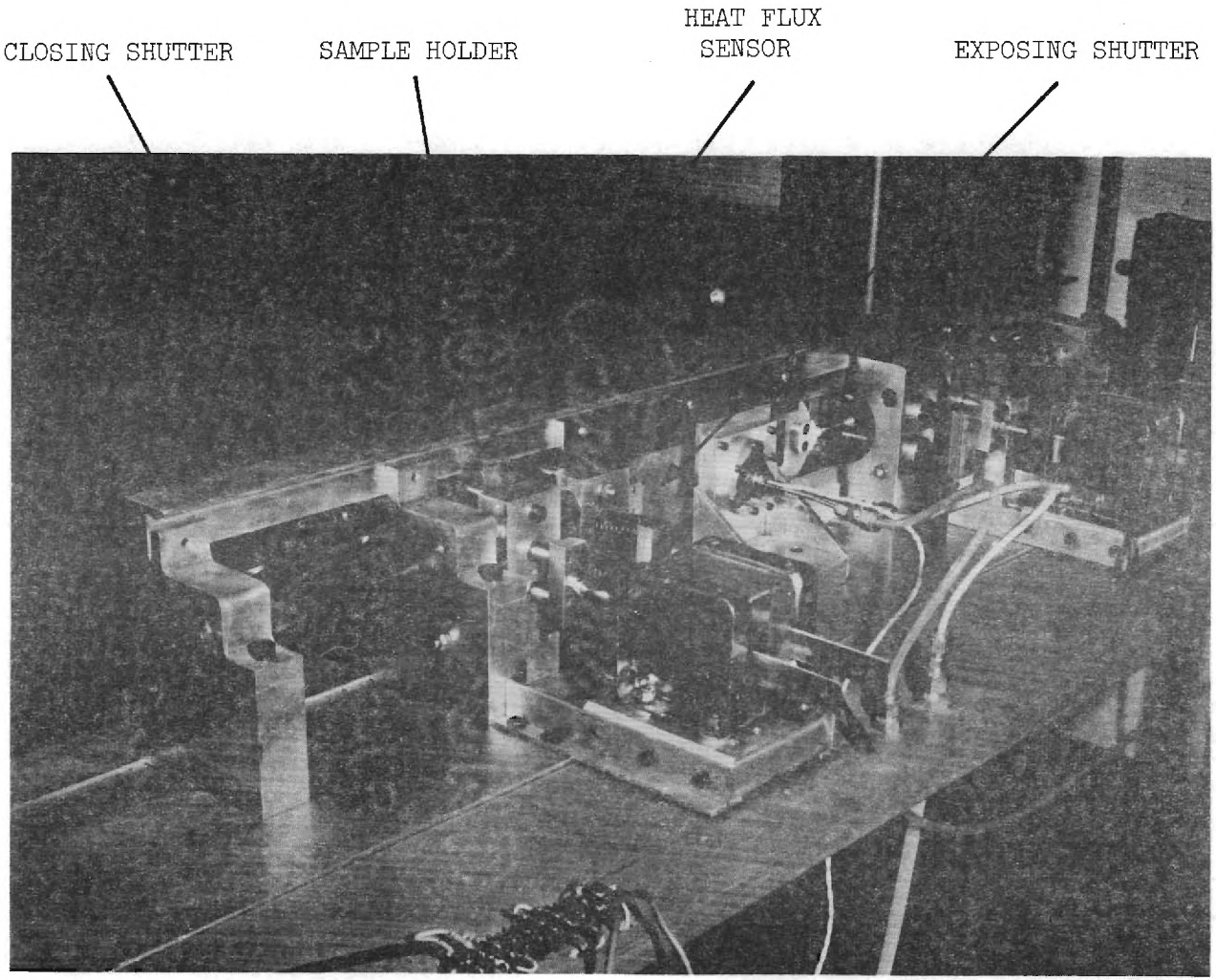

Figure B.3. Ignition Time Apparatus Viewed from Sensor Side

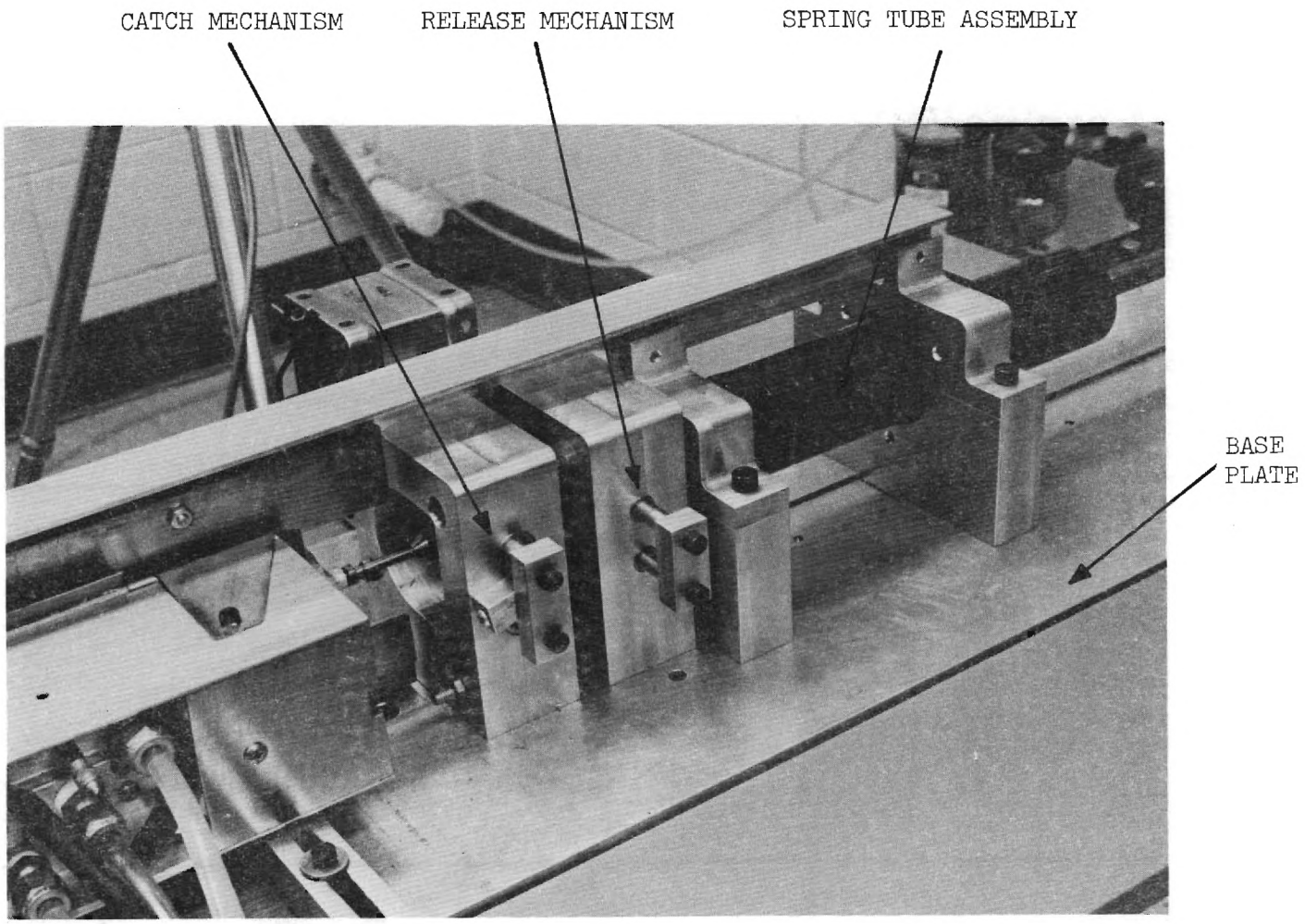

Figure B.4. Shutter Assembly Viewed from Heater Side

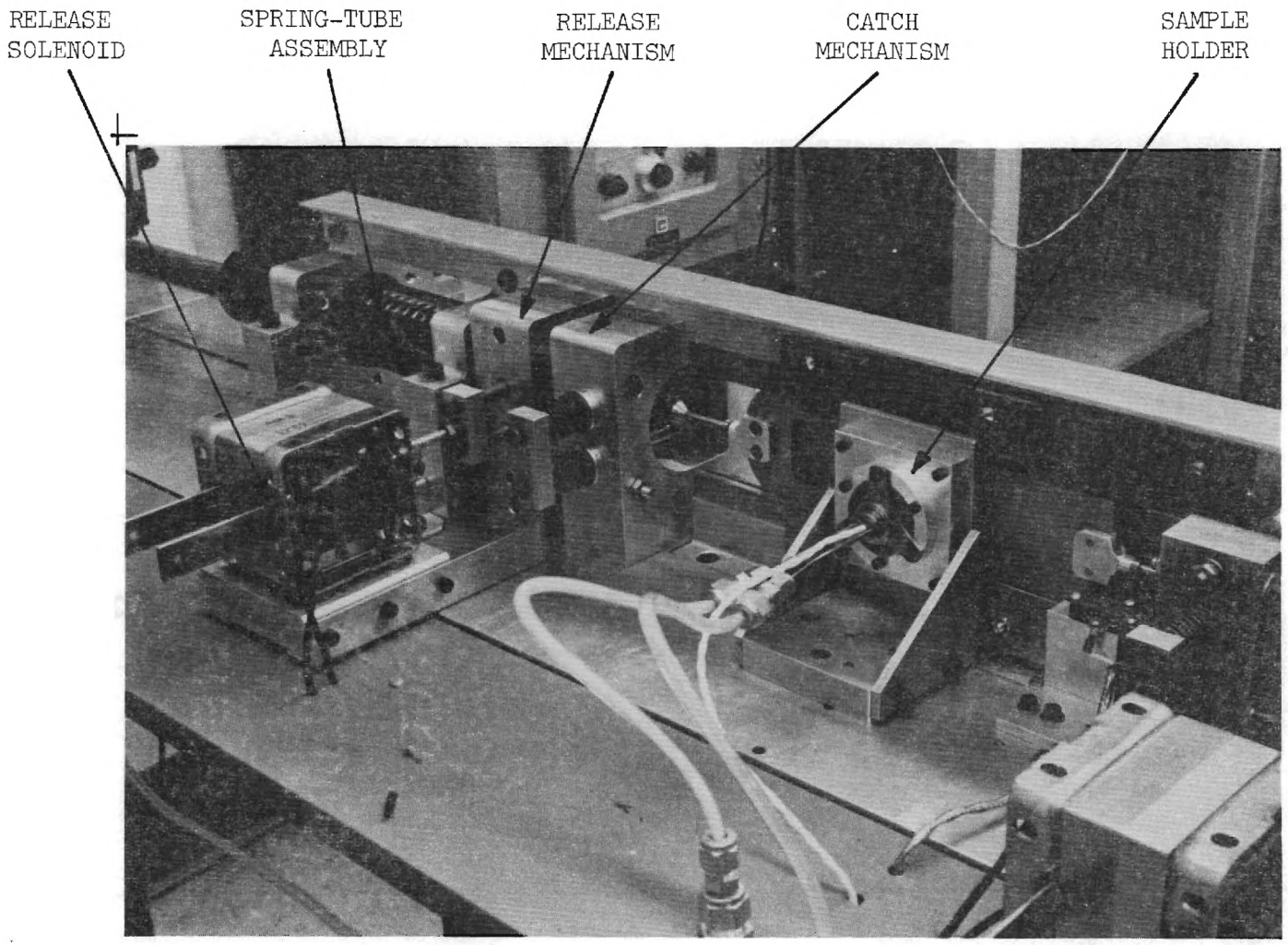

Figure B.5. Shutter Assembly Viewed from Sensor Side

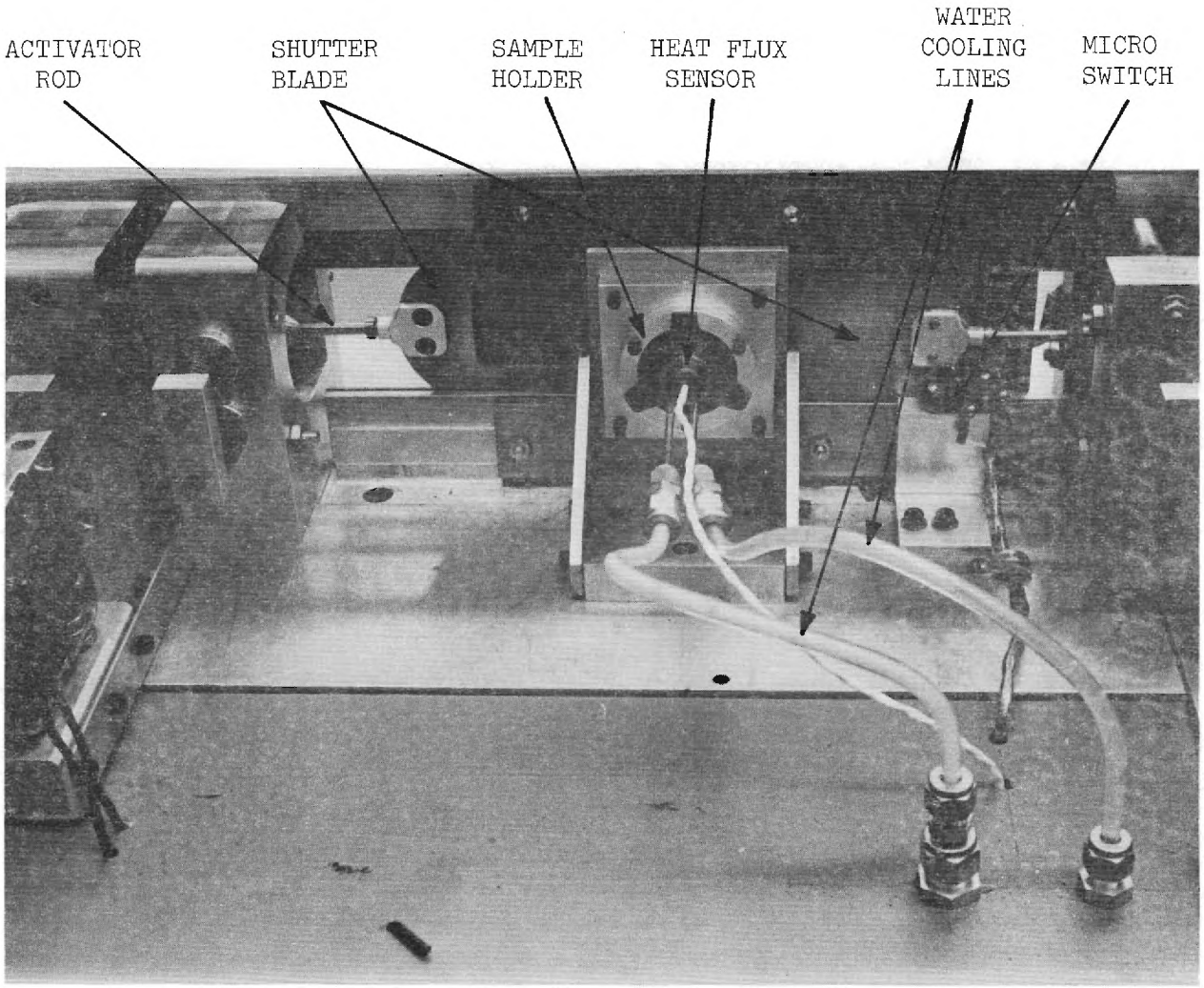

Figure B.6. Sample Support and Heat Flux Sensor

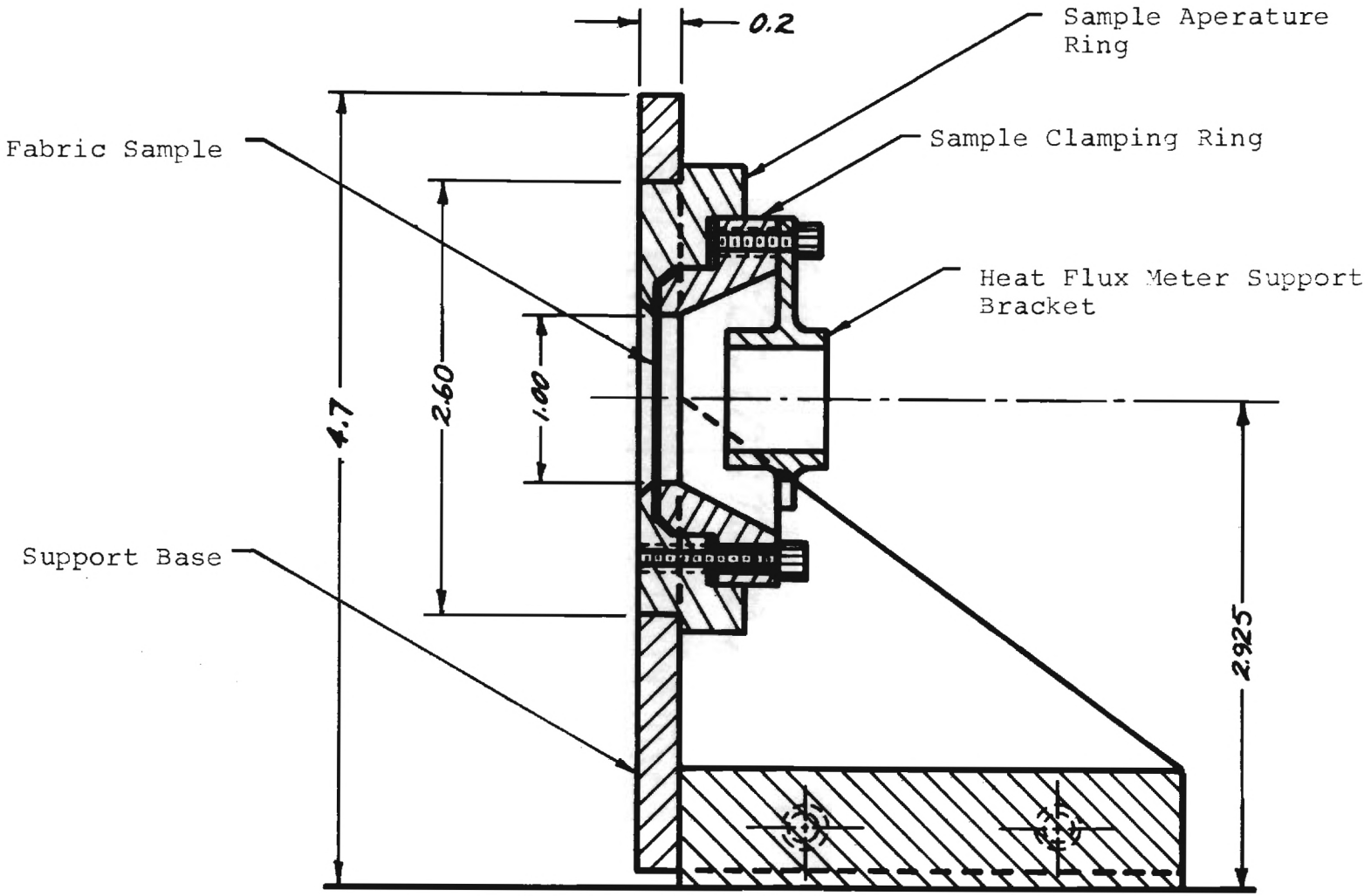

Figure B.7. Sample Holder Assembly (Ignition Time Apparatus)

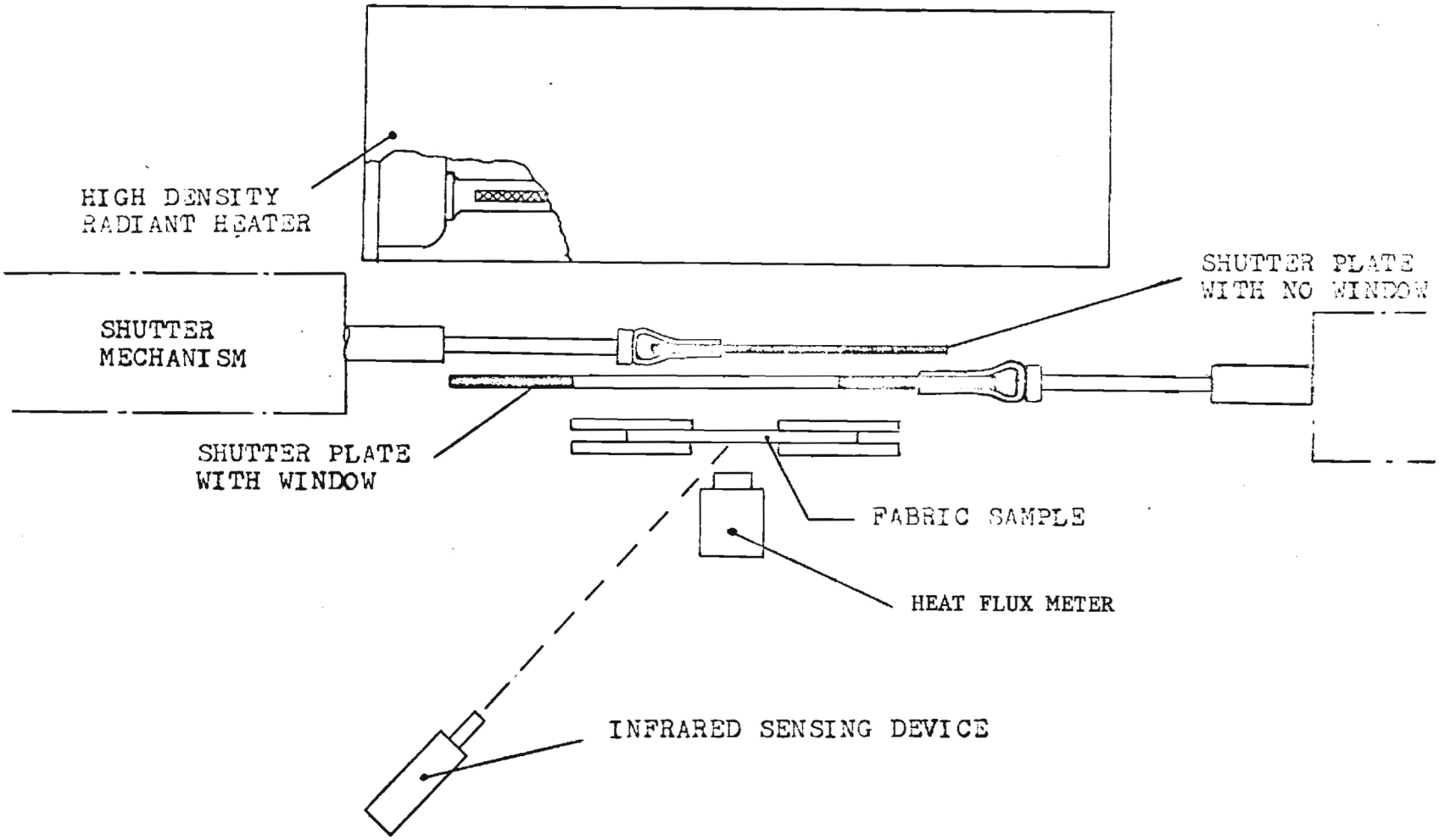

Figure B.8. Arrangement of Heater, Shutter, Sample and Sensors in Ignition Time Apparatus

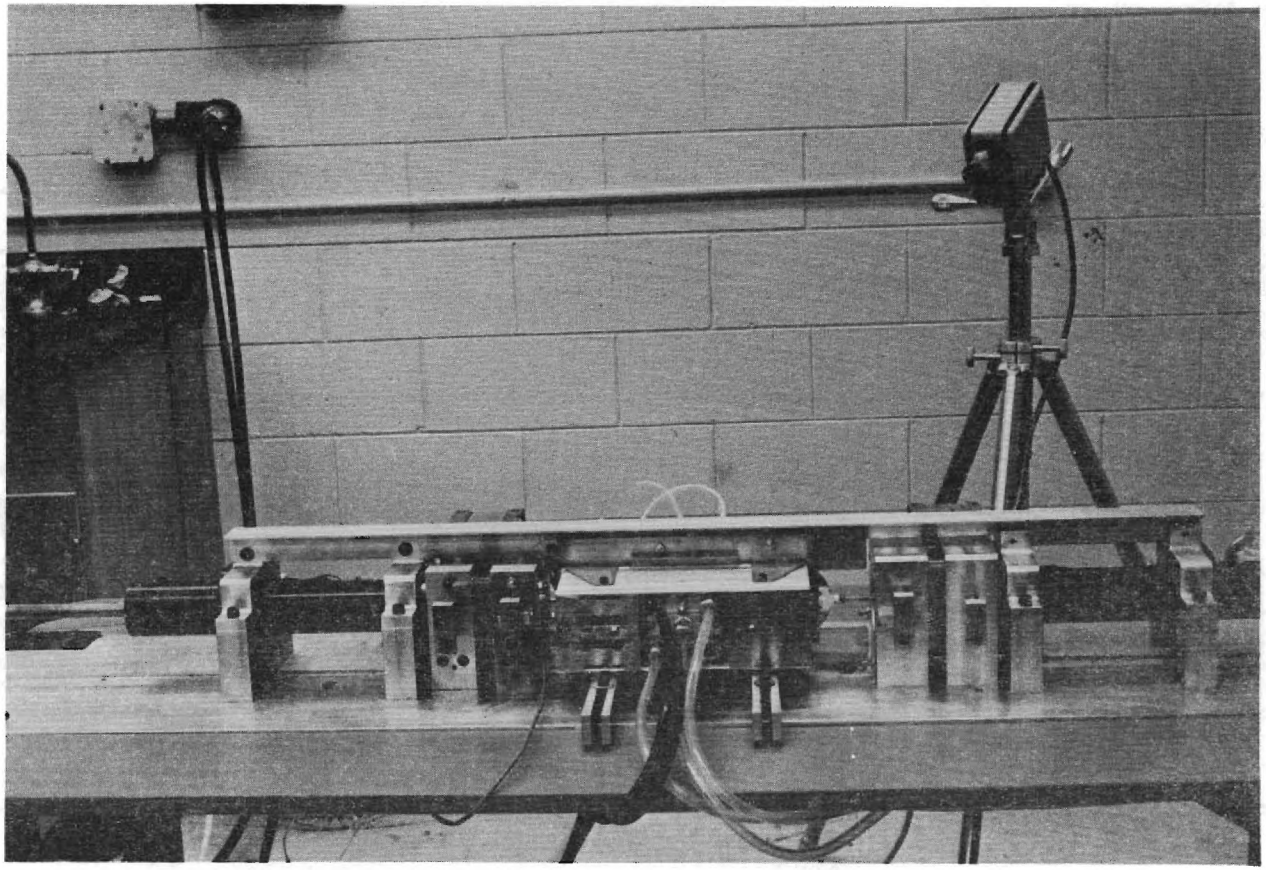

Figure B.9. Ignition Time Apparatus and Infrascope

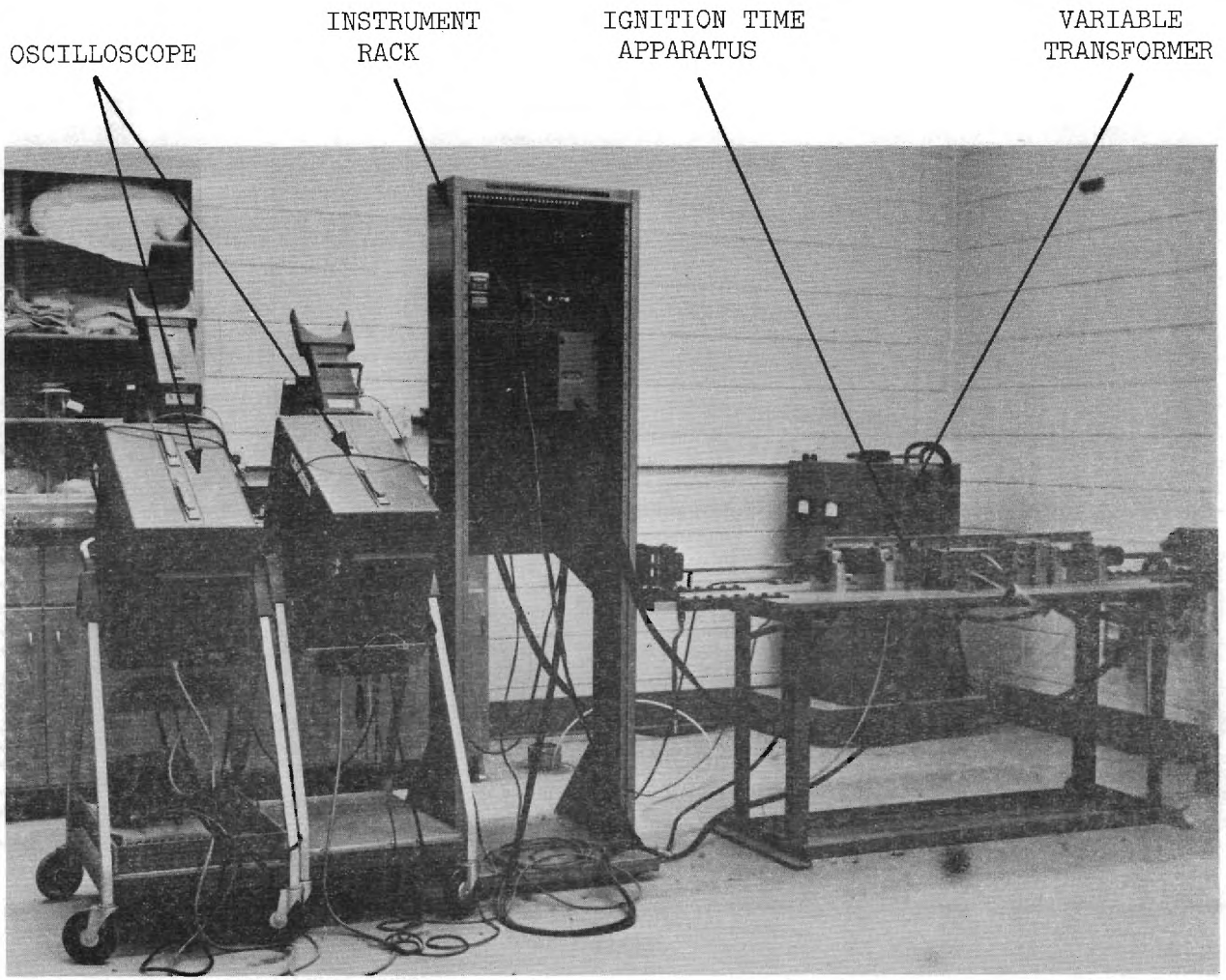

Figure B.10. Ignition Time Measurement Installation

Appendix B.2

Fabric Calorimetry

a. Apparatus Design

The specific heat of fabrics is derived as a function of temperature from enthalpy measurements at various fabric temperatures and subsequent differentiation of enthalpy with respect to temperature. The fabric is heated in the modified Setchkin Furnace (used previously for the measurement of fabric ignition temperatures) until it reaches thermal and chemical equilibrium at the preset furnace temperature. The fabric enthalpy is then measured in a drop calorimeter. Furnace, calorimeter and supporting instrumentation are shown in Figures B-11 through 14.

The Setchkin furnace was fitted with longer legs to accommodate the calorimeter underneath the furnace and with an easily removable, insulating bottom. Its original ceramic liner tube was replaced by a steel tube and the new, removable bottom was clad by aluminum discs to produce a complete inner furnace lining of metal. The aim was to equalize the furnace and fabric sample temperatures. These are monitored by thermocouples.

A stainless steel wire mesh basket of 3 in diameter and 4.25 in length serves to contain the sample in the furnace, to transfer it from the furnace to the calorimeter and to contain it within the calorimeter. The sample size is approximately 80 grams.

The calorimeter consists of the 2,150 cc silvered Dewar flask, the 5 in long sample receiver of 3.125 in diameter, made from copper

and suspended by three hooks from the upper flask edge, further of the copper lid which covers the sample receiver and submerges partially into the water bath, and of the solid foam lid which covers the flask and supports the 100-ohm, four-lead platinum resistance thermometer (Rosemount Engineering). Its electrical resistance is measured by the six decade Guarded Wheatstone Bridge (Leeds and Northrup No. 4737) with external galvanometer (Leeds and Northrup Null Detector Cat. No. 9434).

Environmental temperatures are monitored by a mercury-in-glass thermometer.

b. Operating Procedures

Approximately 80 grams of the sample cloth is rolled up tightly into a cylindrical wad and inserted into the stainless steel basket. Its mass is determined before the heating and after drying in a desiccator following its removal from the calorimeter at the end of a measurement.

A thermocouple is inserted in the center of the wad, and the sample basket is inserted into the furnace. After four hours or more, the thermocouple in the fabric is in thermal equilibrium with the constant internal furnace temperature, monitored by a second thermocouple in contact with the metallic furnace liner. No more evolution of fumes can be detected at this time. The furnace bottom is quickly removed and the sample basket is dropped into the copper sample receiver within the preconditioned calorimeter. The copper lid is placed over the receiver without being touched by the operators hand, and the calorimeter is closed.

The calorimeter is preconditioned by adding precisely 1,250cc of water which has been mixed from hot and cold water to have room temperature $\pm$ 0.2°F. The calorimeter is closed and allowed to reach equilibrium. Then its initial temperature is recorded to an accuracy of $\pm$ 0.002°C, and the sample is inserted as discussed above.

During the equilibration period of between 45 and 90 minutes the calorimeter temperatures are recorded at equally spaced time intervals (for the purpose of heat loss corrections) and the calorimeter bath is manually agitated to prevent thermal stratification. The equilibration period is extended beyond the time of maximum calorimeter temperature until the fabric centerpoint temperature is close enough to the calorimeter temperature that the resulting correcting for the residual enthalpy may be ignored. Finally, the fabric is removed from the calorimeter and weighed.

The specific fabric enthalpy $h_s(t_i)_s$ as a function of fabric temperature $(t_i)_s$ (initially in the furnace) is evaluated in terms of

C	the water equivalent of the calorimeter,
$\Delta t_c = t_n - t_1$	the temperature rise of the calorimeter,
$\bar{t}_c$	the mean calorimeter temperature during
τ_n	the equilibration period,
t_∞	the environmental temperature
C_b	the heat capacity of the basket
t_1, t_n	the initial and final calorimeter temperatures
Δt_{cl}	the residual fabric excess centerline temperature
m_f	the sample mass (after decomposition).

by this relation

$$h_s(t_i)_s = (1 + \delta t_f/\Delta t_s)[C\Delta t_c - (Q_{if} + C_b\Delta t_s)]/m_f \qquad \text{(B-1)}$$

where

$$\delta t_f = [t_n + \Delta t_{cl}/3] - 20°C \cong t_n - 20°C \qquad (B\text{-}2)$$

$$\Delta t_s = (t_i)_s - t_n \qquad (B\text{-}3)$$

$$Q_{if} = 1.6447 \frac{cal}{min°C} (t_\infty - \bar{t}_c)\tau_n \qquad (B\text{-}4)$$

The fabric enthalpy is arbitrarily set equal to zero at 20°C, and the first parentheses in Equation B-1 correct for differences between final fabric temperature and 20°C. The second parentheses constitute the heat lost from the calorimeter and the enthalpy change of the basket.

The correction terms are kept small enough that the overall uncertainty remains less than 2% in most cases so long as $m_f > 70g$ and $\tau_n < 90$ min. Difficulties arise chiefly from the mass loss during the decomposition in the furnace and from the fabrics inability to conduct the heat from within itself to the copper receiver. A typical data collection and evaluation sheet is shown on the following page.

c. Calibration

i. Calorimeter Thermometer

The calorimeter temperature is sensed by a Rosemount Engineering platinum resistance thermometer. The temperature-resistance relationship is given by the Callendar equation

$$R(t) = R_o \{1 + A[\frac{t}{1C} + B\frac{t}{100C}(1 - \frac{t}{100})]\} \qquad (B\text{-}5)$$

SPECIFIC HEAT MEASUREMENT

TEST NO. 10

Date: 8/25/71
Time of drop: 3:00 PM
Experimentor: A.A.

FABRIC No. 11
MASS before m_i = 62.072 g
after m_f = 61.075 g
MASS REDUCTION
$\Delta m = m_i - m_f$ = 0.997 g
$\Delta m/m_i$ = 1.606×10^{-2}

WATER Vol. V_w = 1,250 cm^3

INITAL FABRIC TEMPERATURE $(t_i)_s$ 8.201 mV, 154.01 °C T/C I-C

ENVIRONMENTAL TEMPERATURE t_∞ 75.0 °F, 23.89 °C

CALORIMETER TEMPERATURES

j	time τ min	temperatures $R_t = R_L + R$ Ω	t (chart) °C	t (calc.) °C
1	0	109.614	23.64	23.638
2	10	110.19	25.55	
3	20	.36	.65	
4	30	.41	.85	
5	40	.47	.90	
6	50	.495	.90	
7	60	.501	.95	
8	70	.510	.95	
9	80	.510	.95	
10	90	.506	.94	25.894
11				
12				
13				
14				

n = 10

t_i = 23.638 °C
t_n = 25.894 °C 49.532 °C
$(t_i + t_n)/2$ = 24.766 °C
$\sum_{j=2}^{n-1} t_j$ = 205.90 °C
$(n-1)\bar{t}_c$ = 230.67 °C
$\bar{t}_c$ = 25.63 °C
$t_\infty - \bar{t}_c$ = −1.740 °C

$\Delta t_c = t_n - t_i$ = 2.256 °C
$\Delta t_s = (t_i)_s - t_n$ = 128.116 °C
$\delta t_f = t_n - 20°C$ = 5.894 °C

$C' \cdot \Delta t_c$ = $\Delta t_c \cdot$ 1,620.2 cal °C^{-1} = 3,655.171 cal

Q_{if} = $(t_\infty - \bar{t}_c)\tau_n \cdot 1.611$ cal (min °C)$^{-1}$
= −257.56 cal

$C_b \Delta t_s$ = $\Delta t_s \cdot 7.690$ cal °C^{-1} = 985.21 cal 727.652 cal

$C'\Delta t_c - (Q_{if} + C_b \Delta t_s)$ = 2,927.599 cal

$H_s(t_i) = \left(\frac{\delta t_f}{\Delta t_s} + 1\right)\left[C'\Delta t_c - (Q_{if} + C_b \Delta t_s)\right]$ = 3,062.185 cal

$h_s(t_i) = H_s(t_i)/m_f$ = 50.138 cal g^{-1}

$$A = 3.925 \times 10^3$$

with

$$B = 1.491$$

The constants A and B are obtained by calibration at the steam and antimon points and were furnished by the supplier of the sensor. The resistance R_o at the ice point (OC) was obtained by measuring the resistance R_3 at the triple point of water, produced in an Equiphase Triple Point Cell with t = 0.01 $\pm$ 0.00005 C. R_o was found to be 99.982 ohms.

The constants A and B were verified by calibrating the sensor at slightly above room temperature. The equipment used for this calibration is shown in Figure B-12 and consists of a thermostatically controlled ($\pm$0.01°C) constant temperature bath (Haake NBS Model), a calibrated thermocouple and potentiometer and the Wheatstone bridge used for the calorimetry. The discrepancy between measured and calculated temperature rises was 0.6% and attributed to the axial conduction in the only partially submersed sensor, an effect which is not present in the calorimetric experiment.

ii. Waterequivalent and Convective Heat Losses

The calorimeter was filled with a known amount of hot water with known temperature and was allowed to reach internally thermal equilibrium. From the observed temperature history were derived the water equivalent C and the time-rate of convective heat loss per unit of temperature difference ($A\bar{h}_c$), between calorimeter and environment. The cooling curve gives

$$A\bar{h}_c = (C + C_o)\ \ln[(t_I - t_\infty)/(t_{II} - t_\infty)]/(\tau_{II} - \tau_I) \qquad \text{(B-6)}$$

from two temperatures t_I and t_{II} at two instances τ_I and τ_{II}. The symbols C, C_o and t_∞ represent the waterequivalent C, the heat capacity of the added water and the environmental temperature, respectively. The same energy balance which yields Equation B-7 gives when evaluated in terms of initial and final temperatures t_1 and t_n at times $\tau = 0$ and $\tau = \tau_n$

$$C = C_o \frac{(t_w)_i - t_n + (\bar{t}_c - t_\infty)(A\bar{h}_c)\tau_n}{\Delta t_c - (\bar{t}_c - t_\infty)(A\bar{h}_c)\tau_n} \qquad \text{(B-7)}$$

where $(t_w)_i$ is the known initial temperature of the added water and the other symbols were defined above or in Part b of this section. Substitution of Equation B-7 into Equation B-6 yields first the specific heat loss $(A\bar{h}_c)$ and Equation B-7 gives then the water equivalent C.

The calibration was carried out twice, once with sample basket and once without basket. The two resulting values for C differed by less than 2%.

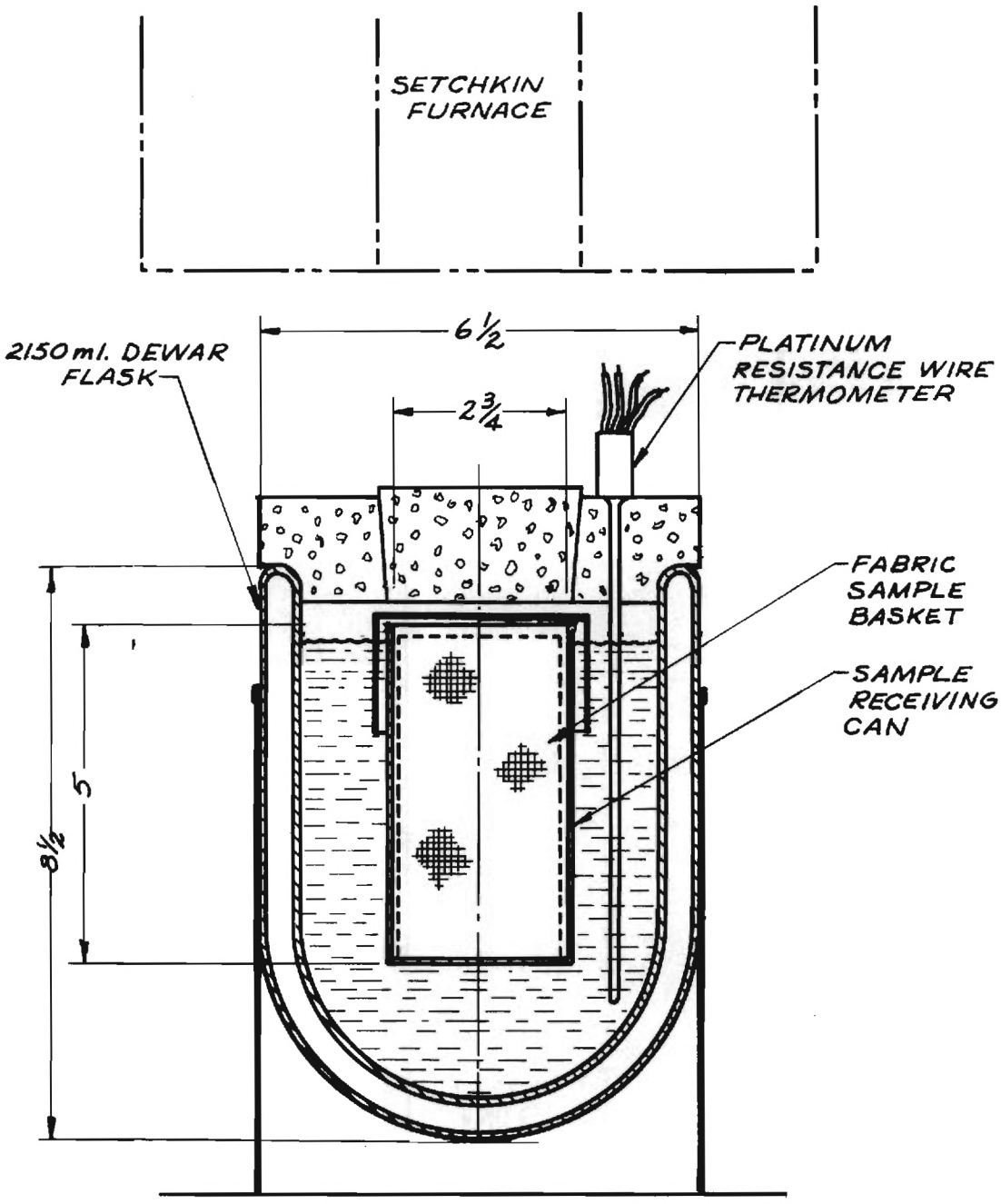

Figure B.11. Drop Calorimeter for Measurement of Fabric Enthalpy

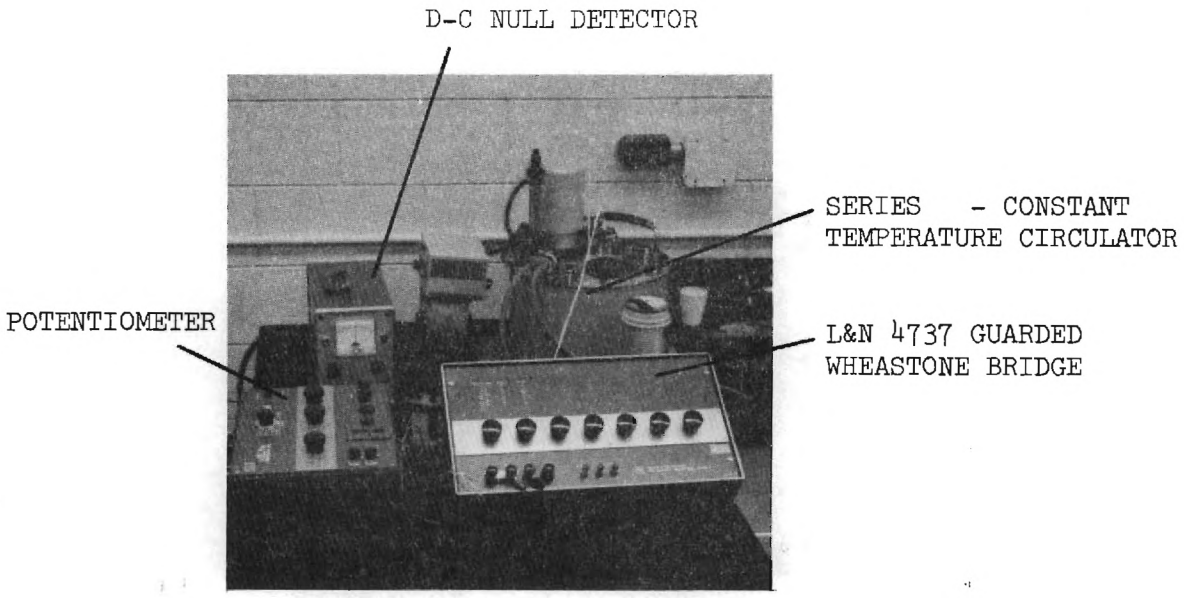

Figure B.12. Apparatus for Calibration of Platinum Resistance Thermometer

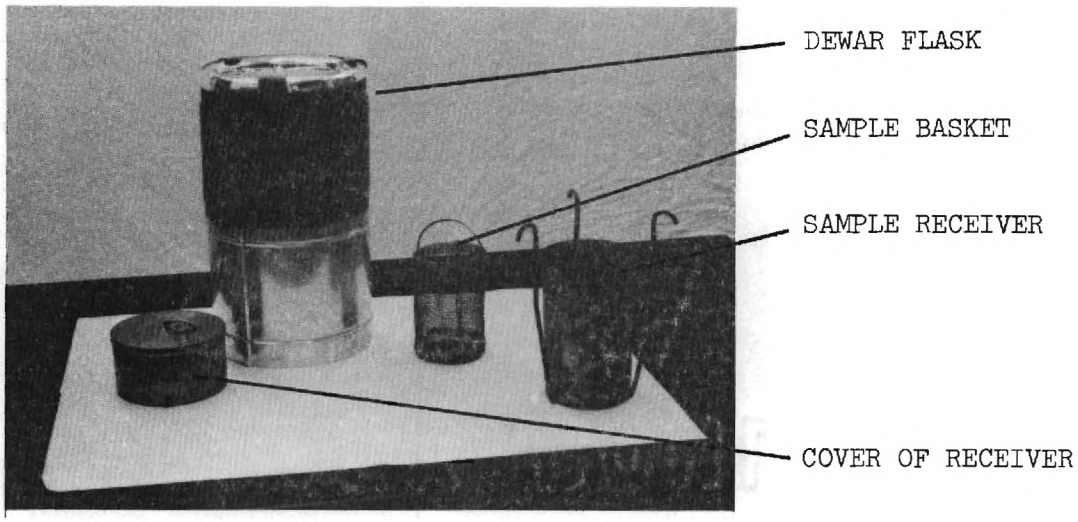

Figure B.13. Calorimeter Components

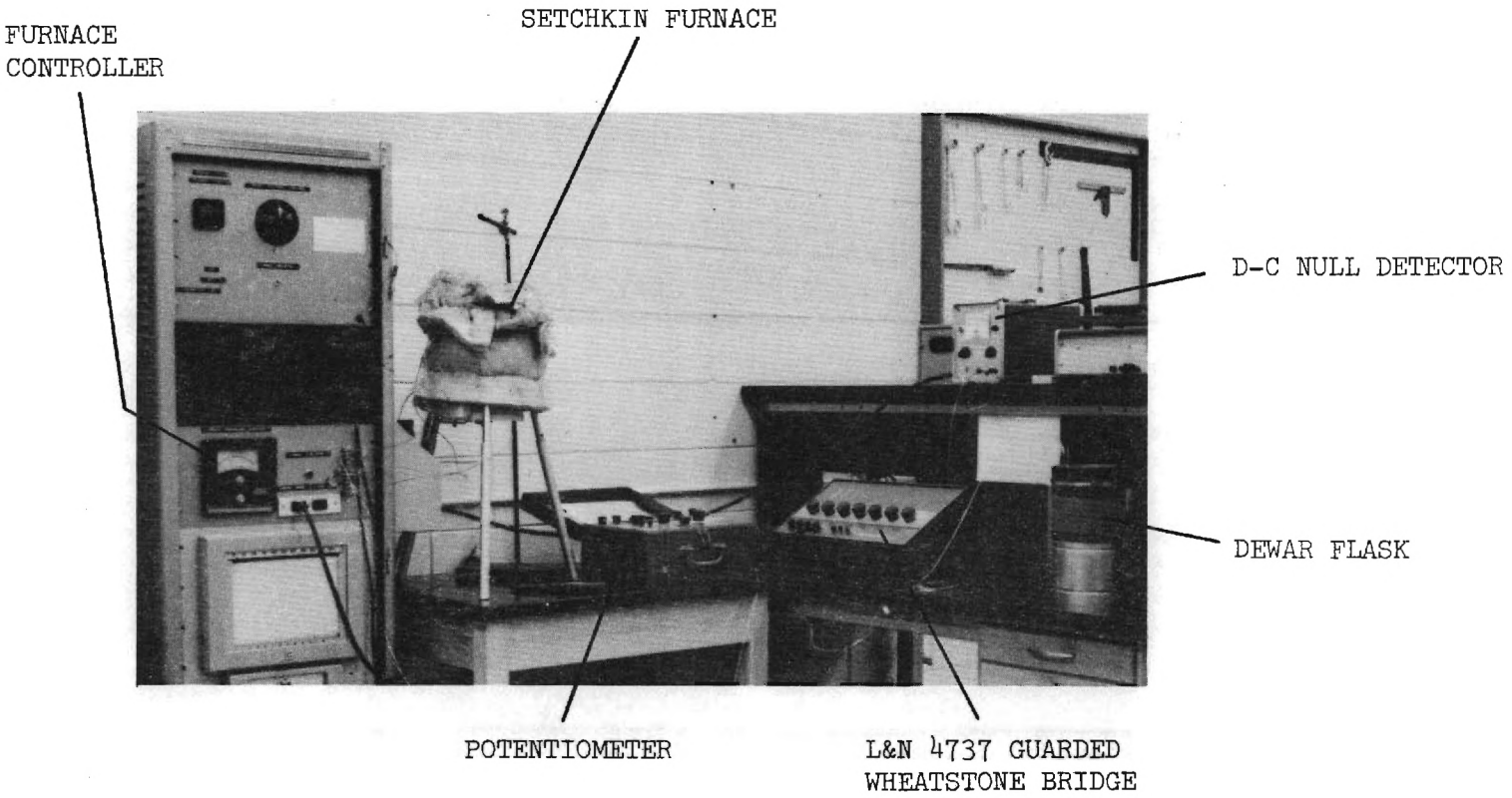

Figure B.14. Specific Heat Apparatus

Appendix B.3

Guarded Hot Plate

a. Apparatus Description

A modification of the traditional guarded hot plate is used to measure fabric thermal conductivity. A carefully metered heat flux is passed through the sample of known thickness and the conductance is inferred from the temperature difference across the sample.

A front sectional view of the single guarded hot plate apparatus designed to measure fabric conductivity is shown in Figure B-15 and the test installation is shown in Figure B-16. The fabric sample is mounted between two 5 in x 5 in naval brass thermal equalizing plates, which are ground and lapped flat to within 0.0005 in and which have a surface roughness of about 16 micro-inches. A 25 watt Watlow silicone rubber heater is mounted below the second equalizing plate. Mounted below the sample heater is a Transite insulation plate sandwiched between two more equalizing plates. The guard heater, located below the bottom equalizinag plate, is used to zero the temperature differential across the insulation plate, thereby assuring that the heat supplied by the sample heater flows up through the fabric sample. Edge losses are similarly minimized by radial guard heaters.

The upper sample plate is constructed to exert a minimum pressure of 528 N/m^2 on the sample. Other test pressures are obtained by adding weights to the upper plate. Electrical power of 5 watts supplied to the sample heater result in a typical temperature

drop across the fabric sample of 3°F. The temperatures in each equalizing plane are measured by 5 thermocouples potted into slots with Eccobond Solder 58C as may be seen in Figure B-17. The apparatus accommodates thick or multiple-layered samples; however, the sample equalizing plate flatness limits the minimum sample thickness to about 0.01 in.

All thermocouples are monitored by a microvolt potentiometer (Leeds and Northrup 755-6-A Potentiometer Facility). Radial heat losses are sensed by monitoring appropriate temperature differences rather than absolute temperatures.

The heat flux through the fabric is derived from the dc-power measurement on the sample heater. A six digit (0.02%-accuracy) differential voltmeter (Hewlett-Packard 3420 B) serves to measure the voltage directly and the current in conjunction with a precision shunt (Leeds and Northrup Cat. No. 4360) whose resistance was measured with a Kelvin Bridge (Leeds and Northrup Model 4287-1) to be 0.10002 ohms. The power supply stability was found to be approximately 0.1%.

b. Test Procedure

Thermal conductivity measurements on the ten primary GIRCFF fabrics were conducted at three temperatures and three pressures. The guarded hot plate apparatus is heated up to a specific temperature and allowed to come to equilibrium. A 5 inch, square sample is inserted and guard heaters are adjusted until radial and axial losses are less than 1% of the power passing through the sample. All thermocouple temperatures and the power supplied to the sample

heater are recorded. (An example of a typical data sheet is shown on the following page). The fabric is removed and the next fabric sample is inserted. The procedure is repeated.

The fabric thicknesses are being measured using a micrometer after the conductivity measurements are made.

The specific conductance (k/δ) is calculated using the following equation:

$$\frac{k}{\delta} = \frac{IU}{T\Delta T} \qquad \text{(B-8)}$$

where
- I Current supplied to sample heater
- U Voltage across sample heater
- A 161.290 cm^2
- ΔT Temperature drop across sample

THERMAL CONDUCTIVITY OF FABRICS

DATE: 9-20

FABRIC NO: 11

OPERATOR A. A. RUN NO. 8 T/C I-C

TIME	HEAT FLUX ΔU		TEMPERATURES (mV)															POWERSTAT SETTINGS			REMARKS
			SAMPLE EQUALIZER PLATES									GUARDS									
			BOTTOM				TOP					AXIAL BOTTOM		AXIAL TOP		RADIAL abs.	RADIAL diff. FRLT	RADIAL diff. RIGT			
	Shunt mV	Voltage V	1-1	1-2	1-3	1-4	2-1	2-2	2-3	2-4	2-5	3-1	3-3	3-6	3-6	1-5	1-6	2-6	DT	FRLT	SKRT	
16:15	26.931	30.736	3.9631				3.5630					4.0545		4.0746		+ 0.083						
16:30			3.9722				3.5654					4.0704		4.0864		+ 0.0314			21	32.5	33.5	
9-21-71																						
10:30			4.0714				3.6510					4.1815		4.1925		+ 0.055			21.5	33	34	
11:00			4.0840				3.6605					4.2032		4.2087		+ 0.0247			22.0	33.5	34.5	
11:30			4.1077				3.6857					4.2315		4.2339		+ 0.0039			22.25	34	35	
12:15	27.049	30.900	4.1302	4.1293	4.1321	4.1261	3.7030	3.6988	3.6977	3.6941	3.6891	4.2600	4.2614	4.2597	4.2586	− 0.0031			22.25	34	35	
13:00			4.1418				3.7121					4.2744		4.2742		+ 0.0128			22.25	34.5	35.5	
13:30			4.1484				3.7183					4.2164		4.2770		− 0.0120			22.25	34.25	35.25	
14:00			4.1560				3.7261					4.2836		4.2839		+ 0.018						
14:35	27.085	30.945	4.1570	4.1546	4.1568	4.1507	3.7184	3.7152	3.7127	3.7079	3.7027	4.2850	4.2841	4.2831	4.2811	+ 0.0081	0.0021	0.0030				

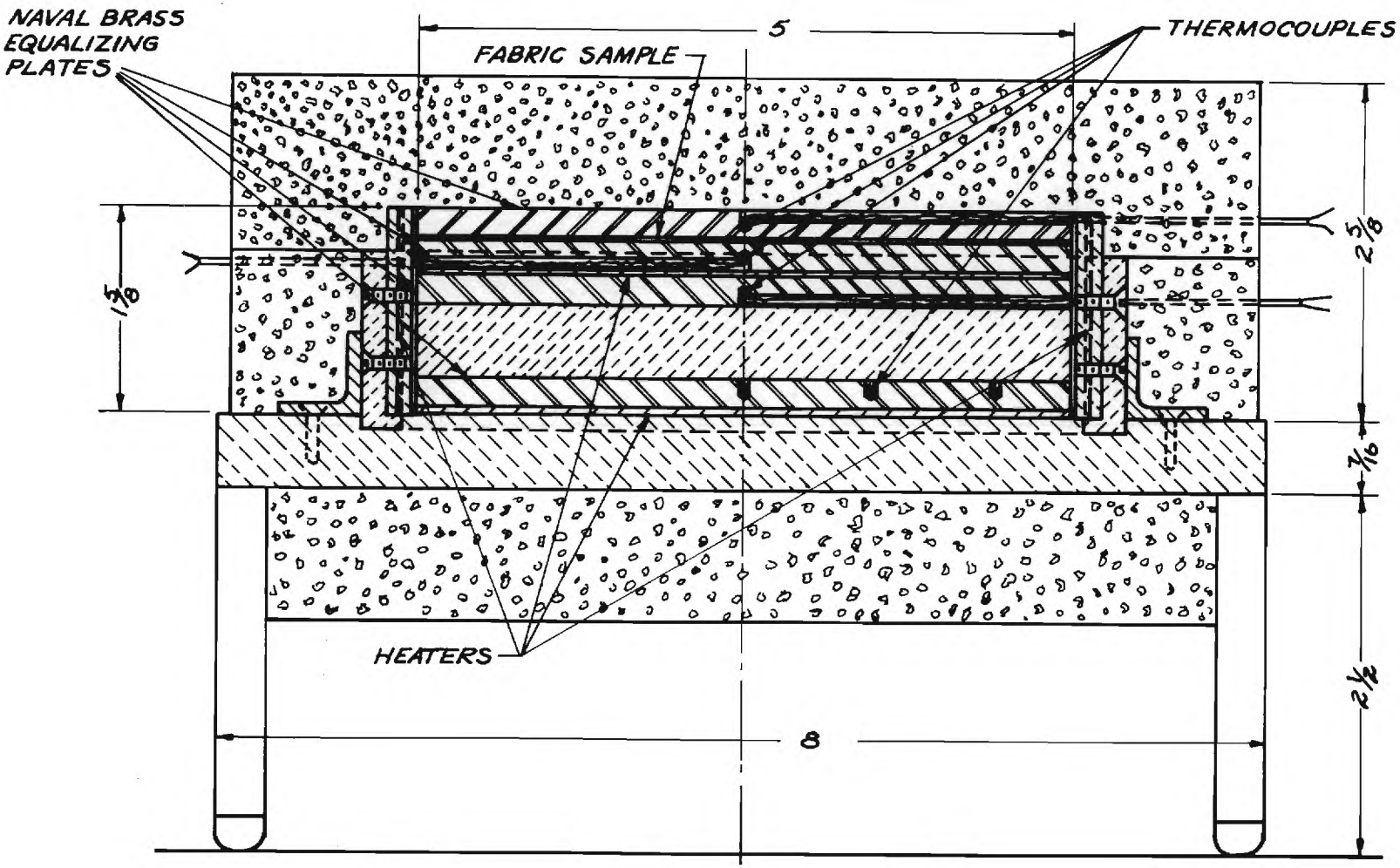

Figure B.15. Guarded Hot Plate

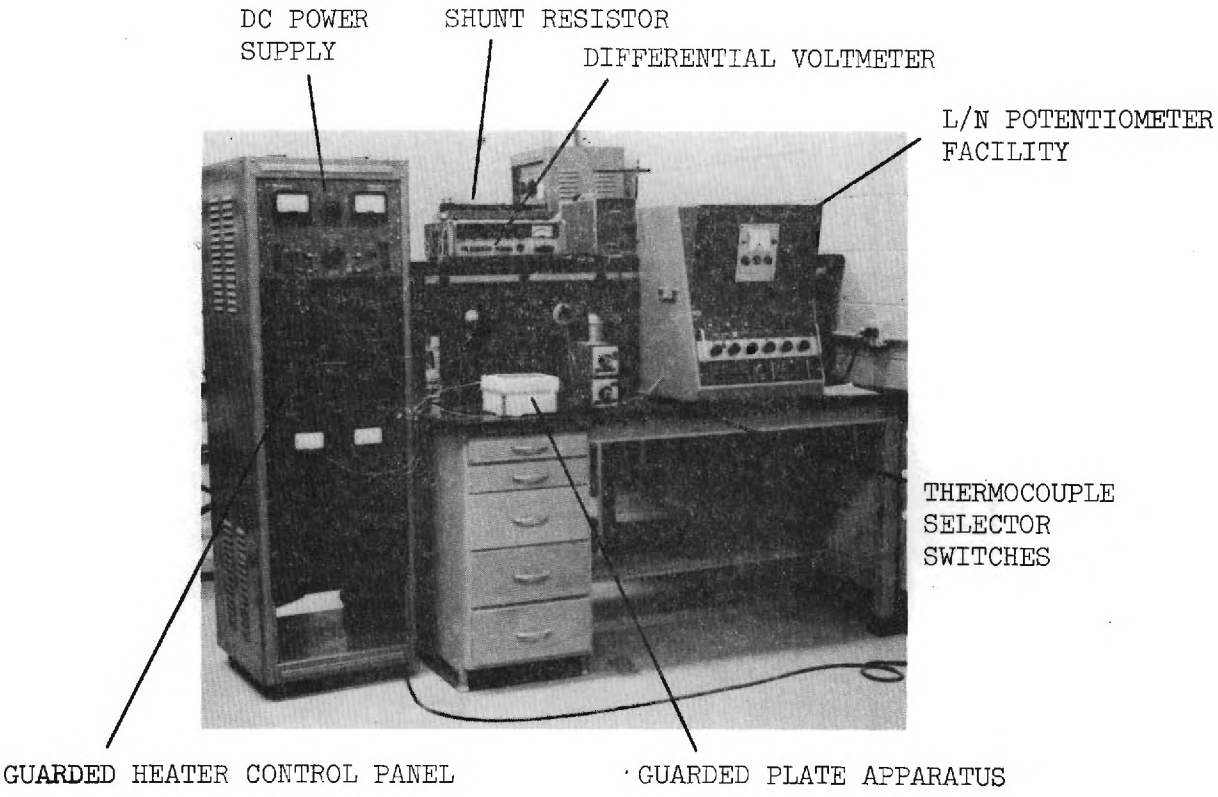

Figure B.16. Thermal Conductivity Test Installation

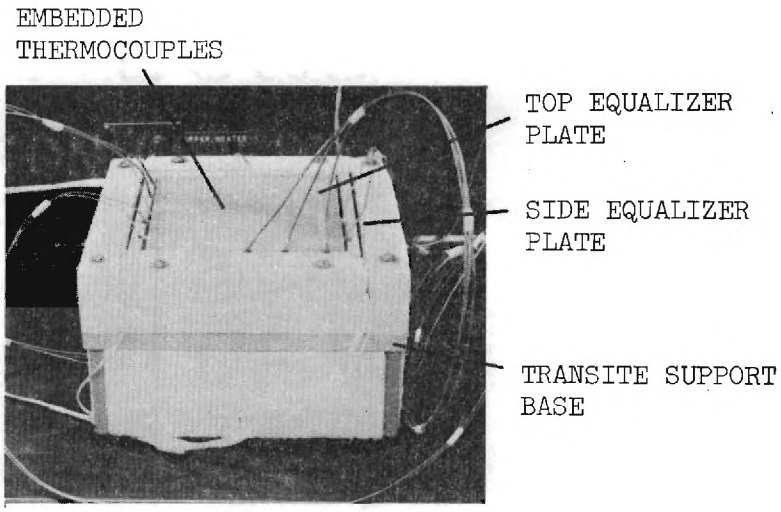

Figure B.17. Guarded Hotplate Apparatus

Appendix B.4

Setchkin Furnace

a. Introduction

The Setchkin Furnace is a thermostatically controlled furnace with controlled air circulation, capable of heating small samples (2 x 2 in) of fabrics at specified heating rates until ignition occurs. The furnace, originally developed by Setchkin [B-1] and later developed as part of the ASTM Standard Test for Ignition Properties of Plastics (ASTM D1929-68) was purchased from Custom Scientific Instruments. The furnace served for ignition and melting temperature measurements and for fabric heating in the enthalpy measurement. The two ignition temperatures measured on ignitable fabrics are defined as follows.

Self-Ignition Temperature: the lowest initial temperature of air passing around the specimen at which, in the absence of an ignition source, ignition occurs of itself, as indicated by an explosion, flame or sustained glow.

Pilot-Ignition Temperature: the lowest temperature of air passing around the specimen at which sufficient combustible gas is evolved to be ignited by a small external pilot flame.

Self-ignition occurs at the onset of spontaneous exothermic reactions between the fabric decomposition products and the oxygen which is present in the boundary layer surrounding the fabric sample. The oxidation gases have reached the activation energy corresponding to the combustible gas composition. The energy imparted on the gases

is the excess energy supplied from the furnace via the air surrounding the sample over the energy absorbed by the sample either as sensible heat or during the endothermic decomposition prior to ignition. Consequently, the self-ignition temperature depends not only on the air flow rate which affects both the gas composition (oxygen index) and the boundary layer temperature profile, but also on the heating rate which dictates the time lag between furnace and fabric temperatures and the degree of decomposition at the time of ignition.

An increase in ignition temperature with increasing air flow is the result of more intensive mixing which yields rather dilute concentrations at first during the heating process until the time rate of decomposition increases with rising fabric temperature. A decrease in ignition temperature with increasing air flow would indicate oxygen deficiency at low air velocities.

Low heating rates for the furnace should result in low self-ignition temperatures as the difference between fabric and air temperatures vanishes with decreasing heating rates. The lowest possible air flow rate of 1.6 m/s was employed during this program. Finally, the flash-ignition temperature is the lowest possible ignition temperature due to the additional energy supplied to the combustion gases by the ignition source.

b. Apparatus Description and Modifications

A schematic of the furnace installation as used for ignition and melting temperature measurements is shown in Figure B-18, the apparatus is shown in the photograph of Figure B-19.

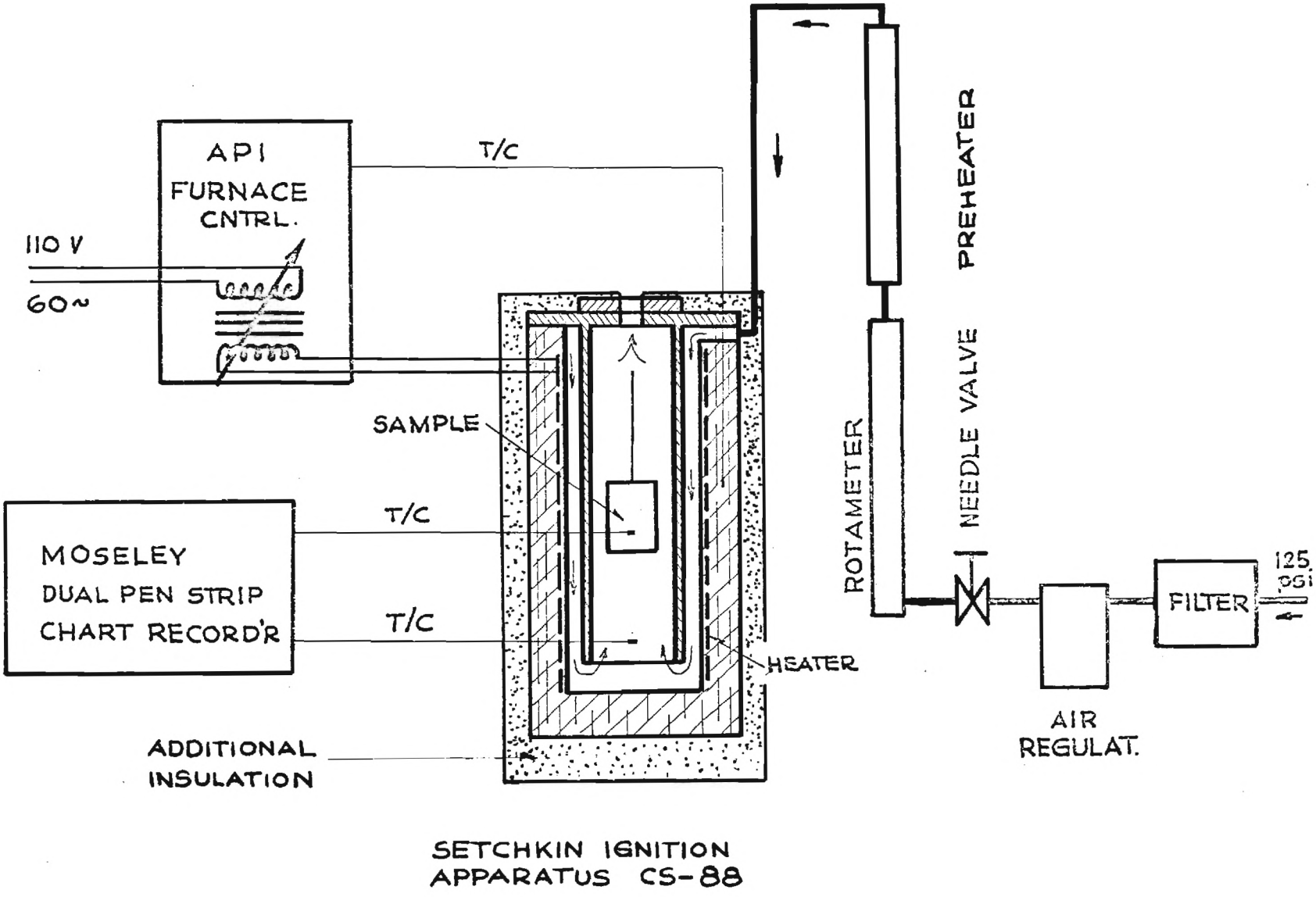

SETCHKIN IGNITION
APPARATUS CS-88

Figure B.18. Ignition Temperature Apparatus (schematic)

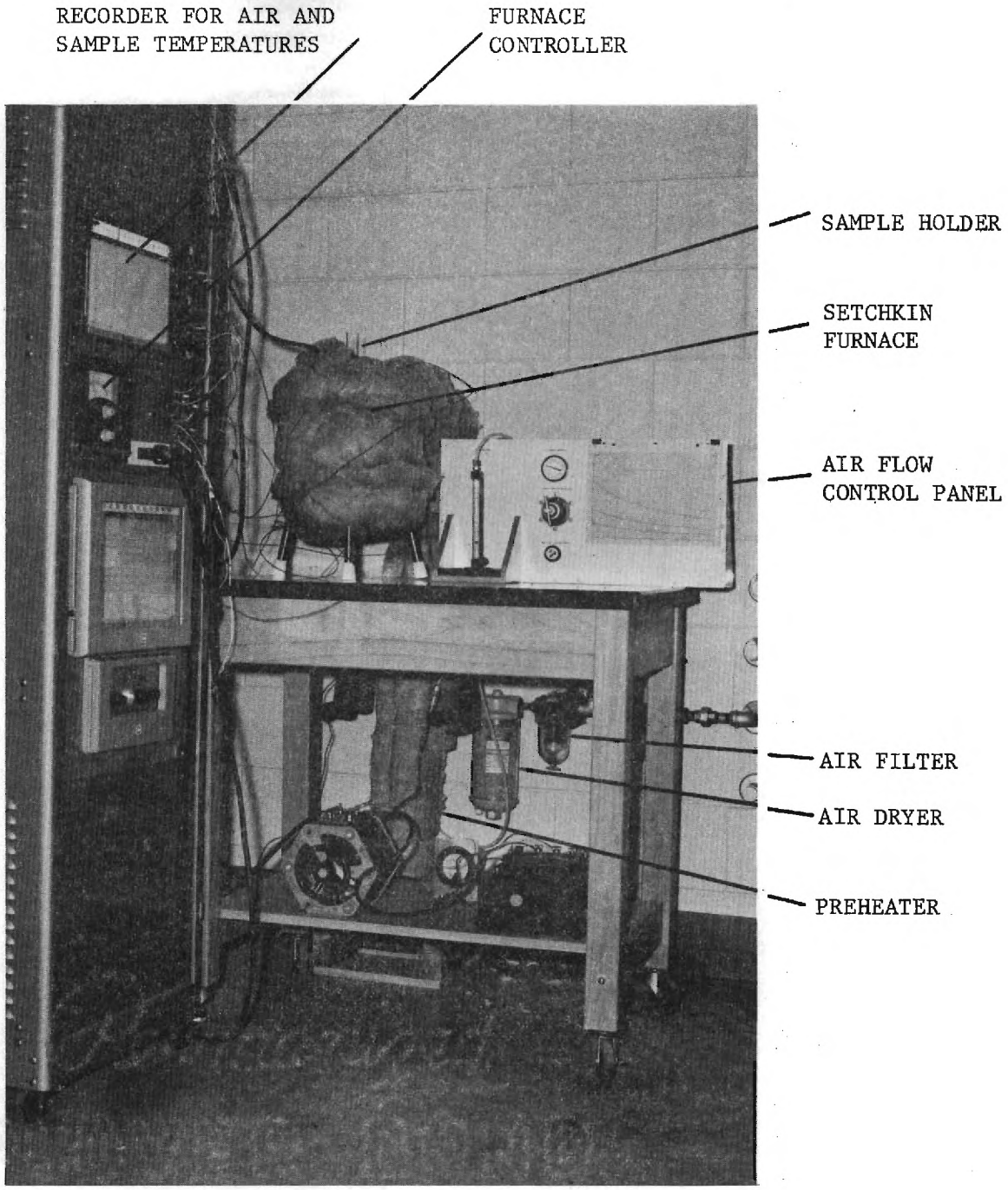

Figure B.19. Ignition Temperature Test Installation

Filtered, and dryed air is metered, through the outer annulus of the furnace core from the top, and passes the fabric from below, to leave the furnace through a small hole in the top cover. The temperature is automatically controlled to a preselected value and recorded, together with the temperature of a thermocouple touching the fabric, on a dual channel strip chart recorder.

Preliminary experiments indicated the need of considerable modifications to improve temperature uniformity within the furnace. The exploratory measurements and modification are summarized as follows:

Temperature profile measurements made in the main core section of the furnace by a five thermocouple rake revealed unexpectedly high temperature differences, up to 50°F from centerline to wall and up to 100°F from bottom to top. The reasons are insufficient heat transfer between purge air and furnace, heat losses to the surroundings and thermometric errors due to radiation.

At the low air flow rate of interest of 5 ft/min the resulting velocity distribution is not expected to be uniform. It was felt that the tangential introduction of air through a small copper tube could accentuate the flow maldistribution in the main chamber.

The 1/4 o.d. copper tubing was removed and replaced by a deadend circular tube of the same size with many small holes at its lower side, emitting the air downward, uniformly over the circumference. To increase the heated air passage the manifold was placed higher than its original position.

As there is insufficient convective heat transfer between the incoming purge air and the outer furnace air passage to achieve uniform temperature it was decided to preheat the purge air. The preheater was made from a 3/4 in galvanized pipe of 3 ft length. A Briskeat, heavy insulated heating tape (768 watts capacity) was wrapped around the steel pipe. The preheater was insulated by a multilayer fiber glass insulation. To improve the effectiveness of the preheater, stainless steel scrubbing pads were inserted into the flow channel.

With this modification, the furnace became simply an enclosure with radial guard heating which also serves for fine control of the air temperature.

The entire furnace was heavily insulated with fiber glass insulation to decrease the heat losses to the surrounding air particularly at either end of the furnace.

The final temperature distribution in the central chamber of the modified furnace was measured with a single thermocouple which could be traversed throughout the furnace. The distribution for typical operating conditions is given in Figure B-20. It can be concluded that the temperature distribution in the region of the fabric is satisfactorily uniform.

c. Sample Holder Design

Considerable effort has been devoted to designing a sample holder which will contain the sparking electrodes for the flash ignition tests. Neither a pilot flame nor a resistance heated wire at the top of the furnace ignited the gases evolved from a

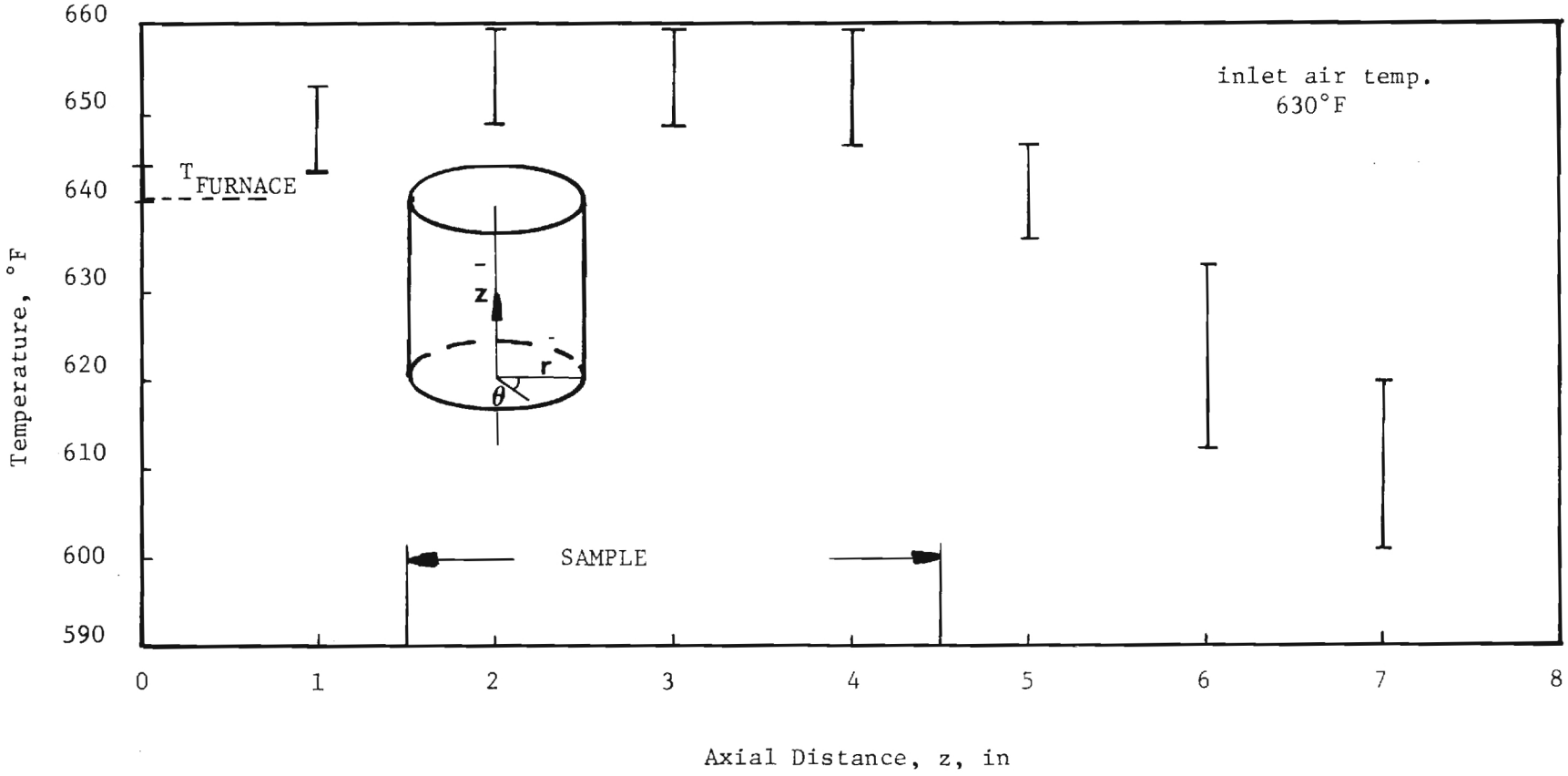

Figure B.20. Temperature Distribution in Setchkin Furnace after Improvement

decomposing fabric because its rate of gas evolution is very low. Spark electrodes were mounted near the fabric and can be intermittently operated so as to avoid fabric heating by the sparks. Sample holders from transite, one of which is shown in Figure B-21, were fabricated. However, when the holders have sufficient mechanical strength, they are bulky, significant flow blockage occurs and long times are required for the holder to reach thermal equilibrium with the air in the furnace.

The sample holder currently in use is fabricated from several wires, which serve as frame and electrodes, as shown in Figure B-22. The arc is produced 1/2 in away from the fabric. Pilot ignition tests have been carried out and the holder has performed satisfactorily throughout the series of self-ignition tests.

d. Test Procedure

The fabric is inserted, after mounting to the holder shown in Figure B-22, into the preconditioned furnace, i.e. the furnace in thermal equilibrium and purged with preheated air at the average core air velocity of 5 ft/sec (1.6 m/s). Ignition either occurs within 5 minutes after insertion and then the furnace temperature is recorded with the previous temperature as ignition temperature interval or does not occur. Then there is a new sample of the same fabric tested at higher temperatures until ignition occurs. For pilot ignition tests the arcing electrodes are intermittently energized for a fraction of a second.

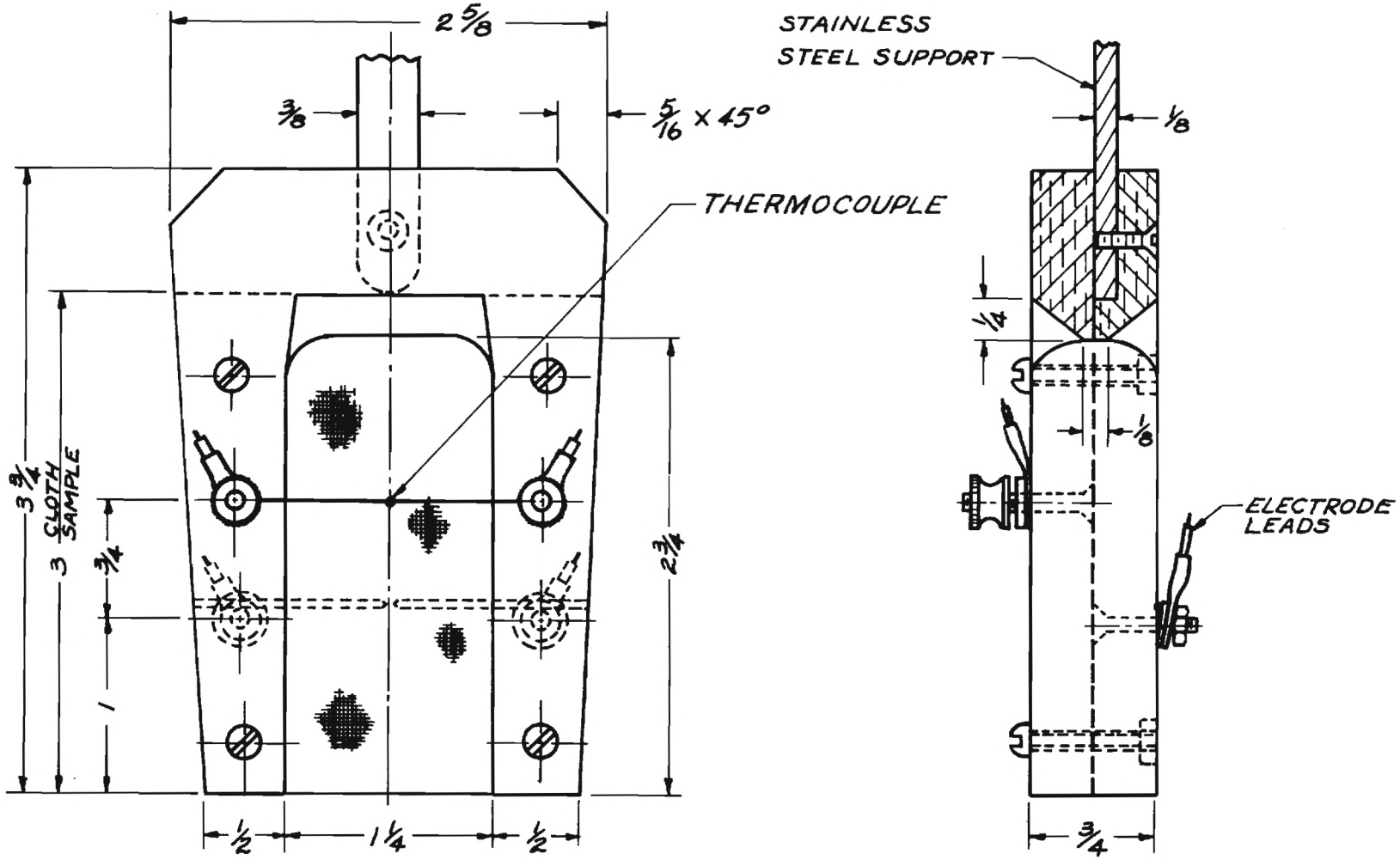

Figure B.21. Transite Sample Holder For Ignition Temperature Test

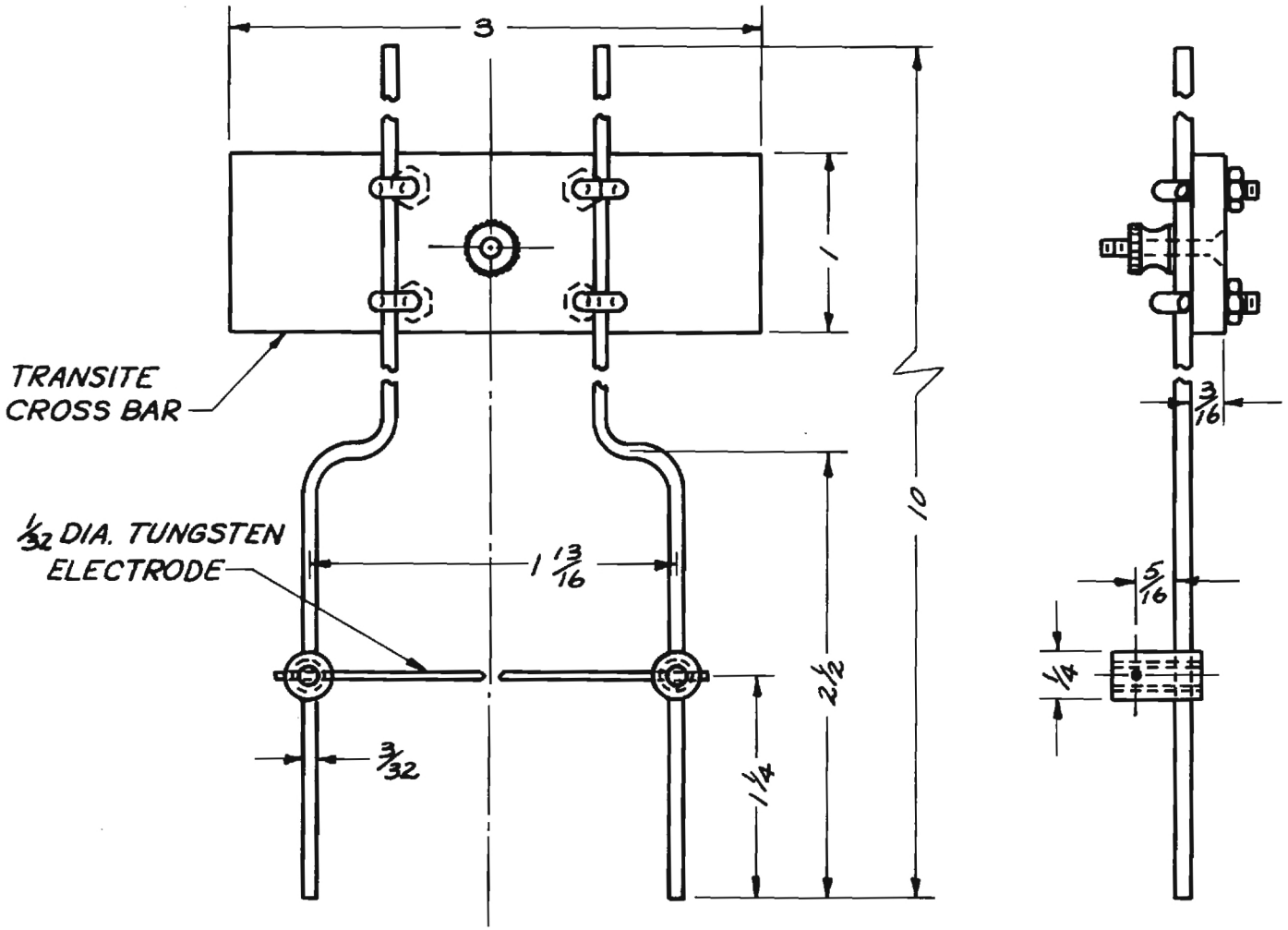

Figure B.22. Metal Sample Holder For Ignition Temperature Test

The drippings of melting fabric are caught in a pan-shaped receiver. Recorded as melting temperature is the lowest temperature at which melting is observed either at the fabric or in the receiver.

Appendix B.5

The Integrating Sphere Reflectometer

a. Introduction

Two fabric properties characterize the fabric interaction with the incident radiative heat flux in the Ignition Time Apparatus: the reflectance ρ and the extinction coefficient κ. In order to properly utilize these properties it is necessary to have the directional and the spectral description of the incident radiative heat flux.

The incident flux is essentially diffuse although slightly retarded at large angles from the fabric surface normal, as a result of apperture effects from the heater-shutter-sample geometry.

At full power production, the tungsten filament temperature in the heating elements is approximately 3,200°K. Aside from the insignificant absorption by the quartz tubes surrounding the filaments, the spectral distribution is such that approximately 12 percent of the energy falls into the ultraviolet and visible regions, 65 percent between the visible spectrum and the 2 μm-wave-length, and the remainder in the far infrared spectrum. At one half power production the corresponding fractions are 4 percent and 63 percent, respectively.

The reflectance ρ depends not only on the fabric geometry, fiber material, and treatment, but also on the source characteristics. The fraction of the incident flux that is reflected by the fabric is the total, hemispherical reflectance, where total

designates the inclusion of spectral variations and hemispherical implies the summation over all directions of both the incoming and the reflected energy fluxes [B-2].

Of the fraction $(1-\rho)$ that enters the fabric, one portion is absorbed and the rest is transmitted by the fabric. If the fractional decrease in intensity of a collimated beam due to its passage through the absorbing fabric is proportional to the distance, i.e. $-dI/I = \kappa\, dx$, where the proportionality constant is the extinction coefficient κ, then the absorbed portion of the diffusely entering fraction $(1-\rho)$ of the incident flux is equal to

$$1-2\int_{0}^{\pi/2} \sin\theta \cos\theta\, e^{-\kappa\delta/\cos\theta} d\theta = 1-2E_3(\kappa\delta) \quad \text{(B-9)}$$

Here, E_3 is called the third exponential integral and is tabulated in standard texts on radiative heat transfer [B-3]. Sometimes $2E_3(z)$ in Equation 1 is approximated by e^{-z}, which is correct for collimated, normal passage of the radiative flux (parallel, normal rays). The difference between $2E_3(z)$ and e^{-z} is 0, 36.8 and 40.4 percent for z equal to 0, 0.5, and 1.0, respectively, with the respective transmittances of τ = 1.00, 0.44, and 0.22. The absorption is assumed to take place in depth. Consistent with Equation B-9 is the fractional absorptance, $-d\tau/dx = 2\kappa\, E_2\,(\kappa x)$, where $E_2(z)$ is called the second exponential integral [B-3].

The transmitted energy $q_o\,(1-\rho)2E_3(\kappa\delta)$ can be measured to evaluate the extinction coefficient κ.

Some wide-mesh fabrics may permit a portion of the radiative flux to pass through the fabric without reflection and absorption. This screening effect, if significant enough, can be isolated by assembling several layers of fabrics since the energy transmitted without interference decays as τ_o^n with increasing numbers n of the fabric layers (τ_o designates the transmittance without interference of a single layer), while the transmittance after in-depth absorption decays as $2E_2(n\kappa L)$.

Both the total hemispherical reflectance and the extinction coefficient have been measured in a 6 in integrating sphere reflectometer. Radiative energy from a tungsten projector lamp, capable of reproducing the spectral characteristics of the radiant heat source in the Ignition Time Apparatus, enters the spherical enclosure of the reflectometer and impinges on the fabric sample at a known angle to its surface normal. The reflected energy reaches, after multiple reflections within the enclosure, a detector at the wall of the enclosure whose output signal is essentially proportional to the reflectance of the sample.

The reflectance is obtained relatively, through comparison of the fluxes reflected from a known reference surface (magnesium oxide) and the unknown fabric surface, and absolutely without reference.

The transmittance is obtained by varying the background behind the sample to either permit the transmitted energy to be reflected by the enclosure, or to be absorbed by a black, opaque diaphragm.

The reflectometer yields the directional-hemispherical, total reflectance which can be integrated to give the hemispherical total reflectance. Filters and filament temperature adjustments have been used to vary the spectral distribution in the range of the heater variations in the ignition time experiments. The expected accuracy of reflectance and transmittance measurements is $\pm$ 0.02.

The optical fabric properties have been measured at room temperature and are expected to be temperature insensitive as are dielectrics in general. However, the effect of discoloration during charring just prior to ignition has been studied on pretreated samples.

b. Apparatus Description

The reflectance measurement apparatus is shown in Figures B-23 and 24 and consist of

(i) the integrating sphere with collimator, thermopile and sample holder

(ii) the light source with constant voltage power supply and rheostat

(iii) the differential voltmeter and the strip chart recorder

These components are described below:

i. The integrating Sphere

The sphere has a 6 inch inside diameter and three, 1-3/4 in diameter ports located in one plane and at 90° from each other. The sample is inserted into the front port, the thermocouple is mounted, flush with the spherical surface, through the second port opposite from the first port and the radiation passes through the third port from the 9 in long collimating tube at the left, between

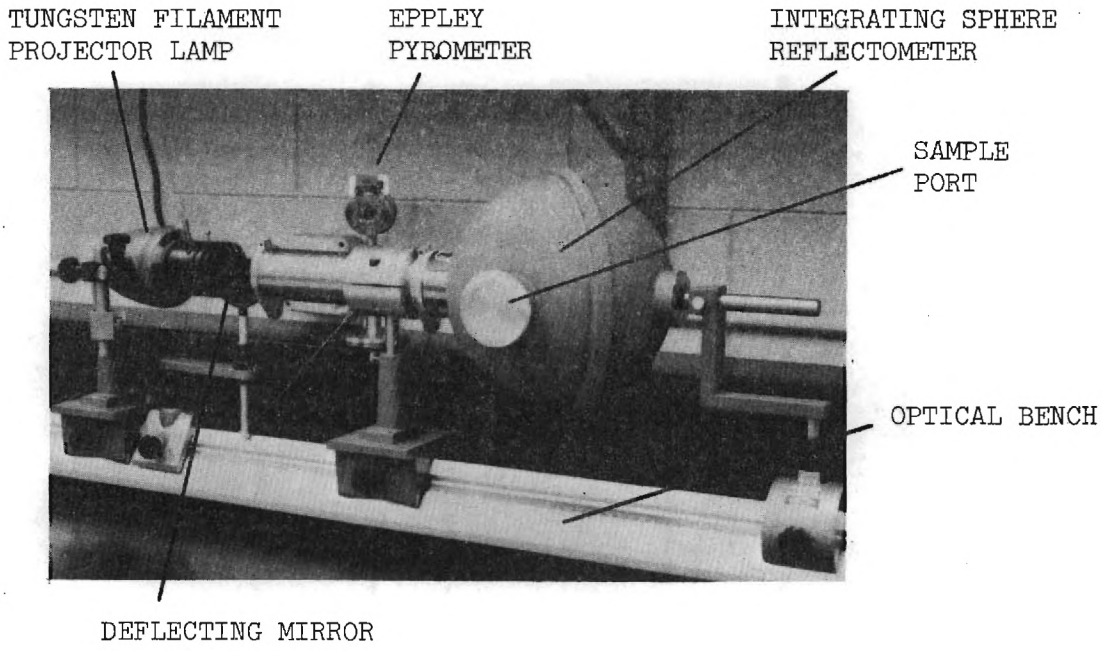

Figure B.23. Reflectance Measurement Apparatus

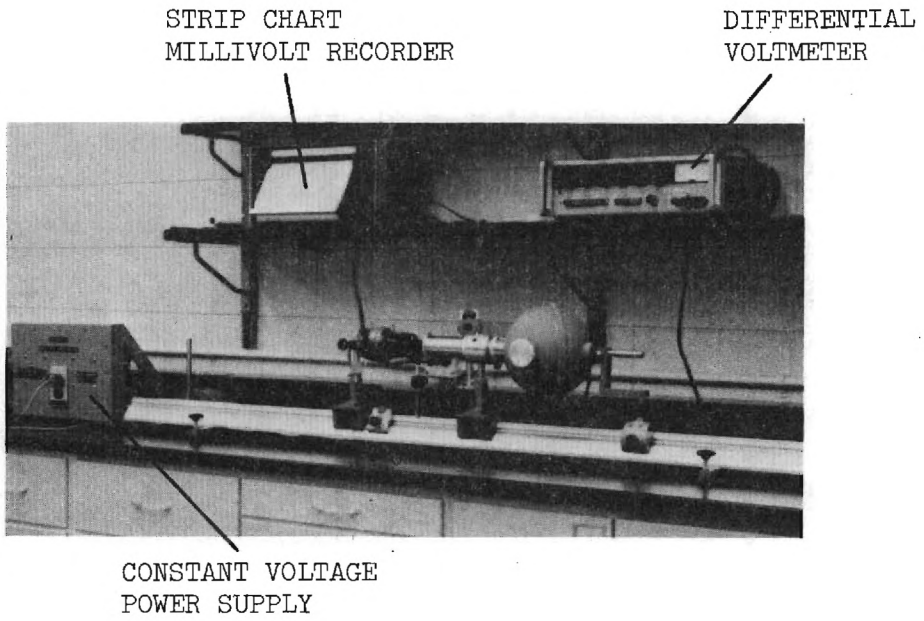

Figure B.24. Reflectance Measurement Installation

the lamp and the sphere. At the lamp end is a 12 mm diameter orifice and at the sphere end is an iris by which to adjust the irradiated area on the sample surface between 1 and 12 mm. The setting is marked on the outside of the tube.

The thermocouple is a 13mm x 35mm rectangular array of 175 copper-constantan wire hot junctions, backed by aluminum foil and mounted flush with the white face of a cylindrical aluminum block. In all experiments the block was mounted in the sphere so that the long axis of the array was parallel to the sample plane to suppress direct sample-to-sensor interaction.

The fabric sample holder design is shown in Figure B-25. The stem, Part No. 4, is inserted into a cylindrical index holder such that when the index holder is inserted into the sphere port, the circular fabric surface is centered in the sphere. The MgO reference holder is identical to the fabric holder except that it cannot be disassembled. The sphere is cooled by a 14 in fan.

ii. The Light Source

A tungsten filament, glass envelope projector lamp provides visible and infrared radiation. The 118 vac lamp voltage supply is regulated within 0.1% by two Sola Type CVS harmonic neutralized constant voltage transformers wired in series and is controlled by a rheostat. The radiation from the lamp is directed through a movable condensor lens and an iris, both mounted on the lamp housing. For all experiments the rheostat was at full setting, the iris at ~ 5mm dia. and the condensor was set to let the light converge slightly.

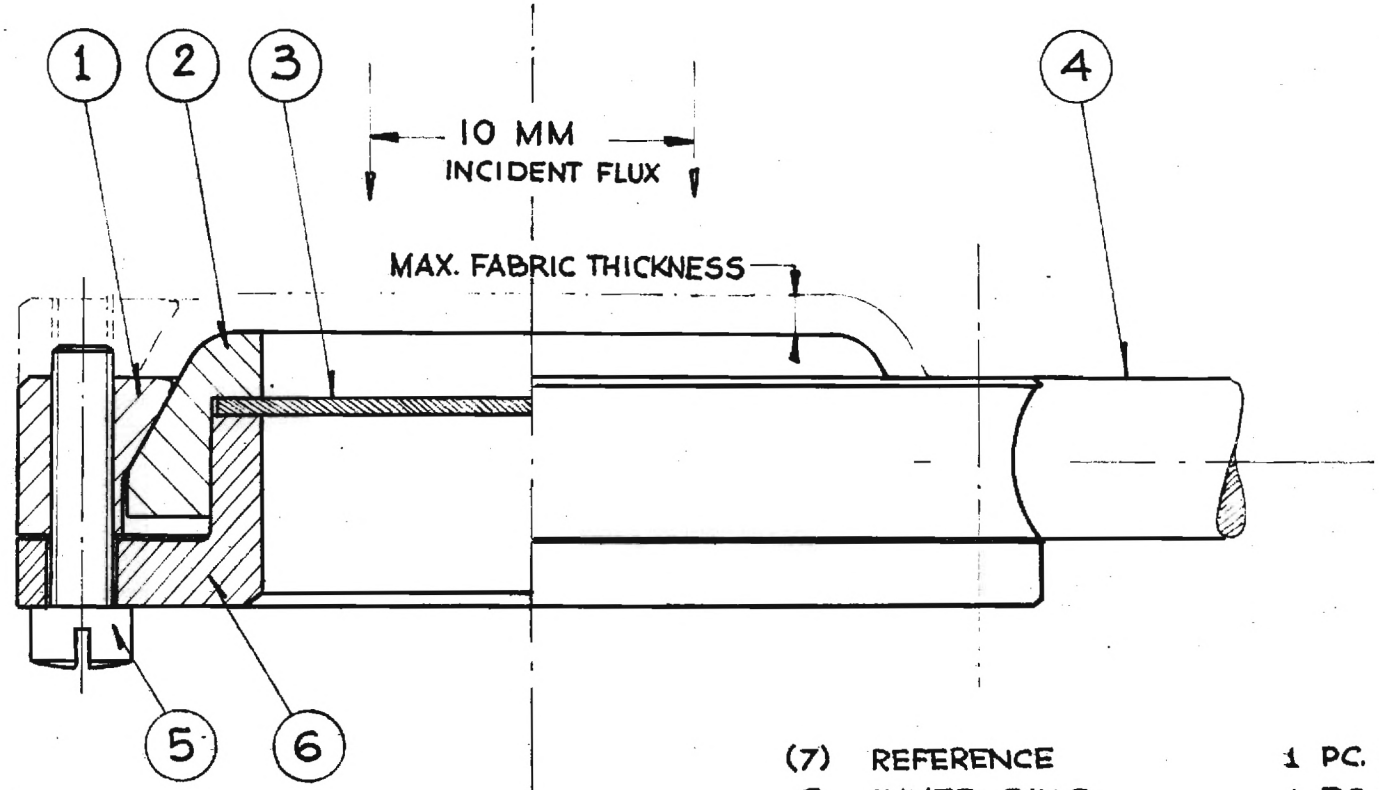

(7)	REFERENCE	1 PC. RQRD.
6	INNER RING	1 PC. RQRD.
5	SCREW 3-48 fillister, 5/16	3 PCS. "
4	STEM	1 PC. "
3	MEMBRANE	2 " "
2	FABRIC SUPPORT	1 " "
1	CLAMP RING	1 " "

SCALE 5:1

B1147 - W01
5-17-71 Lucey

SAMPLE HOLDER REFLECTOMETER

Figure B.25. Sample Holder Assembly

iii. The Optical Bench

An Ealing aluminum optical bench of triangular cross section is used to line up the light source with the reflectometer. Standard supports are used for mounting the components, including an interrupting mirror between light source and reflectometer.

iv. Instrumentation

The signal from the thermopile is transmitted to a Hewlett-Packard differential voltmeter where it is amplified and its initial value subpressed by an opposing voltage. A Moseley two channel strip chart recorder records the amplified thermopile signal.

c. Surface Preparations

The integrating sphere and the white reference sample were painted with a mixture of titanium dioxide and flat lacquer and then lightly sanded to give a flat, rough white surface. The sphere was then coated with magnesium oxide to a thickness of approximately 0.5mm by burning a ribbon of magnesium, fed through a copper tube to the interior of the sphere. The magnesium oxide reference surface was coated by burning magnesium ribbon under an inverted jar until it was filled with smoke and by then placing the mouth of the jar over the reference surface and allowing MgO to settle onto the surface. The white, reflecting fabric background membrane, identified as Part No. 3 in Figure B-25, was painted and smoked with $\tilde{}$ 5mm of MgO, exactly as the reference surface. The black absorbing fabric background membrane was prepared by painting it with 3M NEXTEL Black Velvet paint ($\rho \tilde{} 0.02$) and then coating the surface with soot from an oxygen-free acetylene flame to an

approximate thickness of 0.2mm. The exposed copper-constantan wires of the thermopile were also coated with soot.

d. Test Procedure and Data Evaluation

The original testing procedure [B-4] was to expose the fabric sample to the light source, allow the thermopile to reach its maximum equilibrium value and then to compare the signal to that obtained from a similar exposure of the MgO reference. But this method was discarded because i) the sensor conjunction is drifting before equilibrium is reached, ii) convective eddies develop and distrub the sensor and iii) thermal emission within the sphere is not properly accounted for in the standard procedure.

With the incoming radiation diverted by the mirror, the sphere interior is, after sufficient time, in thermal equilibrium and problems (i) and (ii) above do not exist, and emission is balanced. As soon as radiation enters the sphere the sensor will respond in that the time rate of change of its signal is proportional to the energy reflected by the sample or from the empty sphere. Therefore the recorded slope is measured at time zero, that is when the mirror is swung out of the passage of light from the lamp to the entrance port of the sphere. This method has the advantages of reproducibility and of suppressing the effects of convection currents and thermal emission inside the sphere. The slope is obtained within approximately 4 seconds.

The test procedure consists of the following 3 steps; carried out with both the fabric and the reference:

(i) The (fabric or reference) sample is placed in the sphere and the system is allowed to reach equilibrium while the lamp radiation is deflected from the sphere by the deflecting mirror shown in Figure B-23.

(ii) With the opposing voltage on the voltmeter set at 130μm the recorder is started and the deflecting mirror removed, admitting the lamp radiation into the sphere.

(iii) After approximately 4 seconds the recorder chart is stopped, the deflecting mirror turned to deflect again the radiation, and the sample removed from the sphere.

The above steps are performed for the fabric in front of a white reflecting background then a black background, then the empty sphere, and finally the white reference sample, but not always in this order. The series is repeated for each fabric.

The light source was earlier checked with the Eppley pyrometer as shown in Figure B-23 and found to be stable during a series of tests.

The initial slope of the signal vs time curve is determined by using the second degree (parabolic) collocation approximation with subsequent differentiation

$$(\delta EMF)'_o = \frac{4(\delta EMF)_1 - (\delta EMF)_2}{2\tau_1} \qquad \text{(B-10)}$$

where: τ_1 is some time after $\tau = 0$

$\tau_2 = 2\tau_1$

δEMF is the rise of the amplified sensor signal above the initial signal; the subscripts 1 and 2 refer to τ_1 and τ_2 respectively,

and the subscripts o refers to $\tau = o$. The apparent reflectance ρ_a, resulting from fabric and background reflection is given, firstly by comparison with the MgO reference, by

$$\rho_a = \rho_r \frac{(\delta EMF)'_f}{(\delta EMF)'_r} \qquad \text{(B-11)}$$

where the subscripts f and r refer to the fabric and the reference, respectively. Secondly, by absolute measurement, the apparent reflectance is

$$\rho_a = \frac{(\delta EMF)'_f}{(\delta EMF)'_e} \qquad \text{(B-12)}$$

where subscript e indicates a measurement with the empty sphere. The reference reflectance ρ_r was measured and absolutely found to be 0.901.

The relative and absolute reflectances are measured for each fabric with both a white and a black background. The black background reflectance was determined by comparison of slopes for the black surface, the MgO reference, and the empty sphere and found to be 0.015. For each background an average between the absolute and relative reflectances is computer, and they are called $\rho_{a,1}$ and $\rho_{a,2}$ for the white and black backgrounds respectively.

These average values are reflectances of the system consisting of fabric sample and its background. The effect of air between the fabric and the background is negligible and thus, the system reflection is composed of fabric and background reflectance, the latter being attenuated for each passage of the flux through the fabric:

$$\rho_a = \rho + \tau^2\rho_b + \tau^2\rho_b^2\rho + \tau^2\rho_b^3\rho^2 + \ldots = \rho + \frac{\tau^2\rho_b}{1-\rho\rho_b} \qquad \text{(B-13)}$$

where ρ, τ and ρ_b stand, respectively for reflectance and transmittance of the fabric and for the background reflectance. Writing Equation 17 once for the white ($\rho_{b,1}$) and once for the black ($\rho_{b,2}$) backgrounds one arrives at two equations for the two unknowns ρ, τ, the fabric reflectance and transmittance.

Solving for ρ one finds

$$\rho = \frac{\rho_{b,1}\,\rho_{a,2} - \rho_{b,2}\,\rho_{a,1}}{(\rho_{b,1} - \rho_{b,2}) + \rho_{b,1}\,\rho_{b,2}\,(\rho_{a,2} - \rho_{a,1}} \qquad \text{(B-14)}$$

and for τ:

$$\tau = \frac{\rho_{a,1} - \rho_{a,2}}{\rho_{b,1} - \rho_{b,2}} \left[1 - \rho(\rho_{b,1} + \rho_{b,2}) + \rho^2\rho_{b,1}\,\rho_{b,2}\right]^{1/2} \qquad \text{(B-15)}$$

The fabric absorptance is computed from:

$$\alpha = 1 - \tau - \rho \qquad \text{(B-16)}$$

The optical thickness is found by solving

$$E_3(\kappa^*) = \frac{\tau}{2(1 - \rho)} \qquad \text{(B-17)}$$

for κ^*. The exponential integral $E_3(x)$ is tabulated in standard radiant heat transfer texts.

APPENDIX C

LITERATURE SURVEY

Appendix C.1

Literature Survey on Specific Heat of Fabrics

Specific heat data found in the literature are presented in Figure C-1 for ten different materials, each listed generically without regard to fabric characteristics, methods of measurement, etc. For wool, cotton, rayon, silk, and nylon two sources of information are available. Also, specific heat as a function of temperature is presented for nylon; however, it is improbable that the same temperature variation could be expected for other fabrics. All of the values are greater than those of air and asbestos. The range of values for specific heat is even smaller than that for thermal conductivity, probably due to the specific heat being essentially dependent only on the fiber properties. For approximate design calculations, a value of 0.35 Btu/(lbm F) could be used.

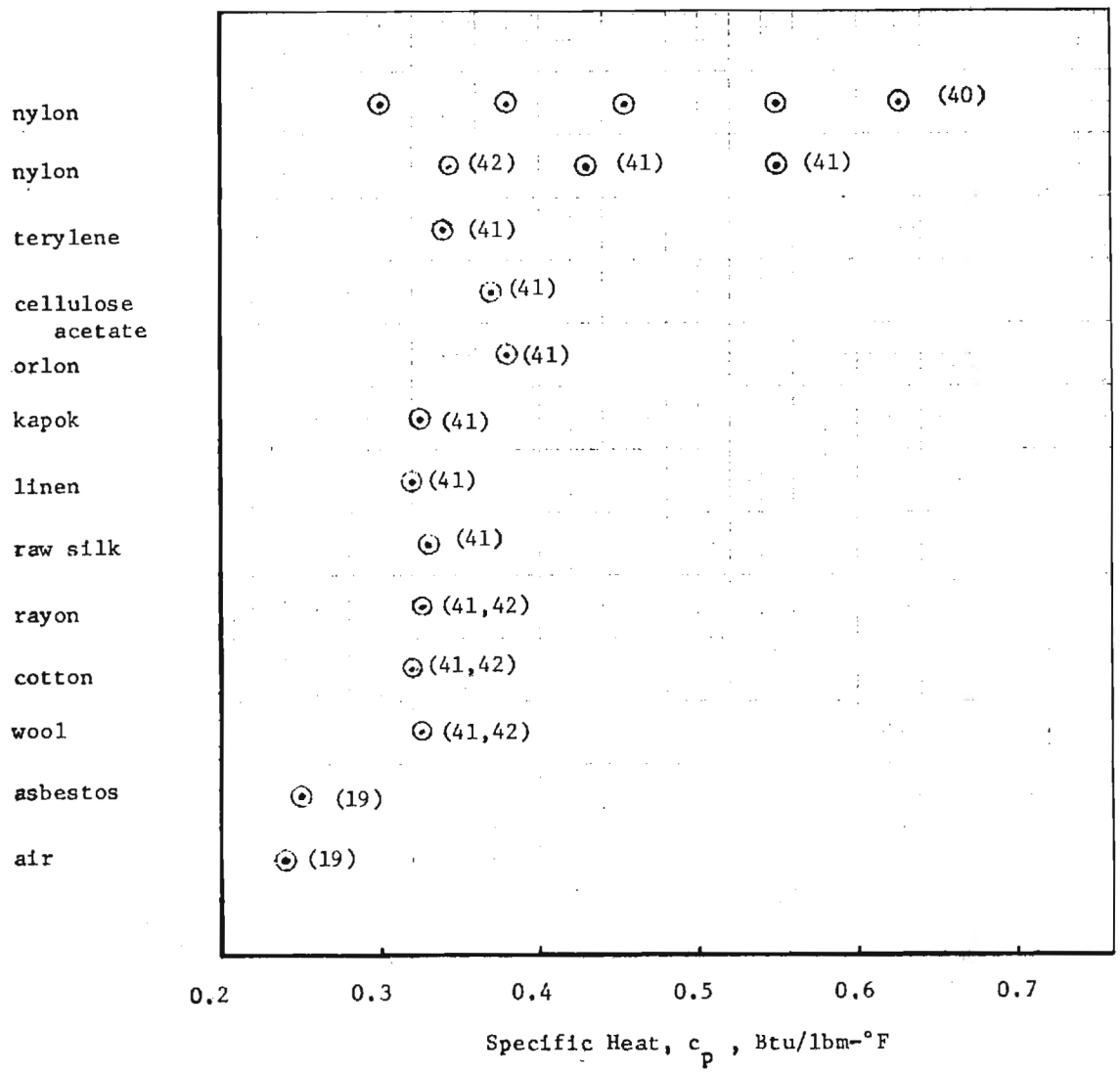

Figure C.1. Composite of Data for Specific Heat of Fabrics

The numbers in parentheses refer to the references with prefix C in the Bibliography.

Appendix C.2

Literature Survey on Thermal Conductivity of Fabrics

It should be emphasized that the following literature survey had been conducted prior to the recognition that thermal conductivity plays a secondary role in the heating process of the ten primary GIRCFF fabrics. However, the information is nevertheless valuable.

1. Background

An extensive literature search for the thermal characteristics of fabrics has revealed considerable research since the early nineteenth century (Rumford presented data as early as 1804). Numerous researchers have measured such quantities as "thermal insulation", "thermal resistance", "warmth" and "heat retention", all of which have something to do with the thermal conductivity. These quantities are presented in such diverse units as:

(1) tog unit: the thermal resistance which will maintain a temperature difference of 0.1°C with a heat flux of 1 watt/m^2

(2) clo unit: the insulation necessary to maintain comfort and a mean skin temperature of 92°F in a room at 70°F with air movement not in excess of 10 ft/min, humidity not over 50%, and with a metabolism of 50 kcal/m^2

(3) T.I.V. (thermal insulating value): the percentage reduction in the heat loss from a hot surface

covered by a fabric, or

$$T.I.V. = \left(1 - \frac{\text{Heat lost from covered hot body}}{\text{Heat lost from uncovered hot body}}\right) \times 100$$

In principle, togs or clos can be converted to thermal conductivity, provided the sample thickness is specified. The problem, however, is that the temperature difference is an overall value and includes other thermal resistances besides that of the fabric. Data reported in the above units are not suitable for the present program.

Characteristic thermophysical properties for transient heat transfer through chemically non-reacting fabrics are density, thermal conductivity, specific heat and thermal diffusivity. Thermal conductivity data found in the literature were usually obtained by a device which establishes and maintains a measurable temperature gradient across the fabric sample with a measurable heat flux through it. Some of the devices used are (1) Lee's disc method, (2) the Cenco-Fitch apparatus, and (3) the Guarded-ring hot plate method. Of the order of 100 studies on thermal conductivity for fabrics were reviewed.

Figure C-2 is a presentation of thermal conductivity data for 25 fabrics and fibers. The full range of available data is shown with the generic terms such as "cotton", "wool", "silk", etc. All data are presented without regard to fabric characteristics, methods of measurement, etc. It is of considerable interest to note that values vary only from 0.013 to 0.08 Btu (hr ft F). Virtually all of the reported fabric thermal conductivity values are greater than that of air (0.014 Btu/(hr ft F)), as expected,

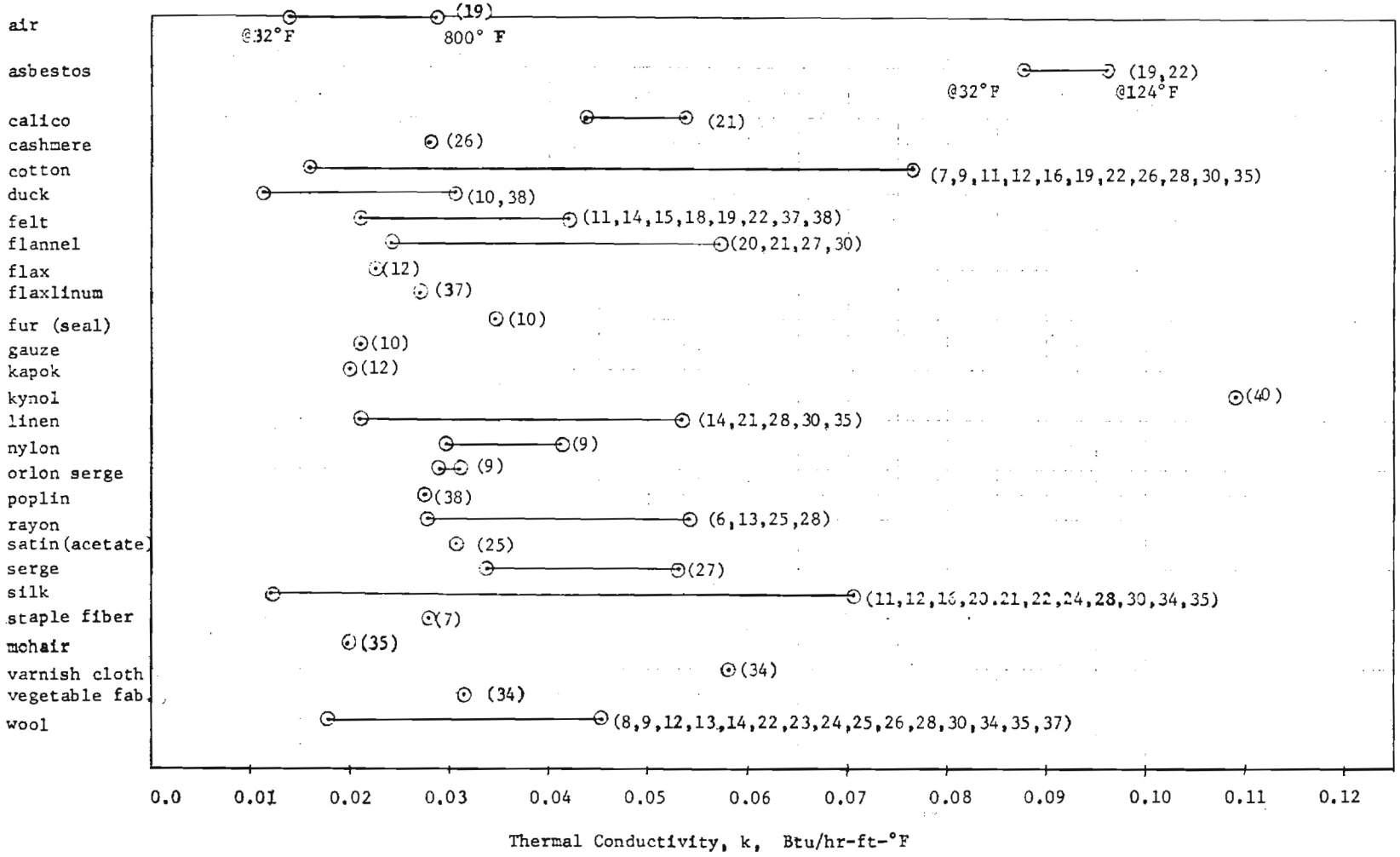

Figure C.2. Thermal Conductivity of Fabrics and Fibers

and less than the thermal conductivity of "fireproof" materials such as asbestos (0.095 Btu/(hr ft F)) and Kynol (0.109 Btu/(hr ft F)). For approximate design calculations a mean value of 0.04 could be used. Eleven of the materials have values from more than one source, and four more materials have two or more values from one source. Particular interest has been shown in cotton and wool, two of the fabrics of interest in the present study, and many researchers have reported results. Their values are summarized in Figures C3 and C4.

Data scatter in the detailed presentations of Figures C-3 and C-4 can be correlated to some extent with a number of variables. It is clear that heat transmission through fabrics is a complicated process involving conduction through the fiber itself, conduction, possibly with convection, in the interstitial air spaces, radiation, and conduction through any absorbed moisture. The thermal conductivity, as applied to a heterogenous system such as a fabric does not have its usual precise meaning. The following parameters, not necessarily independent, were considered in the literature to affect the thermal conductivity of fabrics:

a. fiber material
b. density
c. mechanical pressure
d. moisture content
e. temperature
f. treatment
g. history of utilization
h. multiple layers

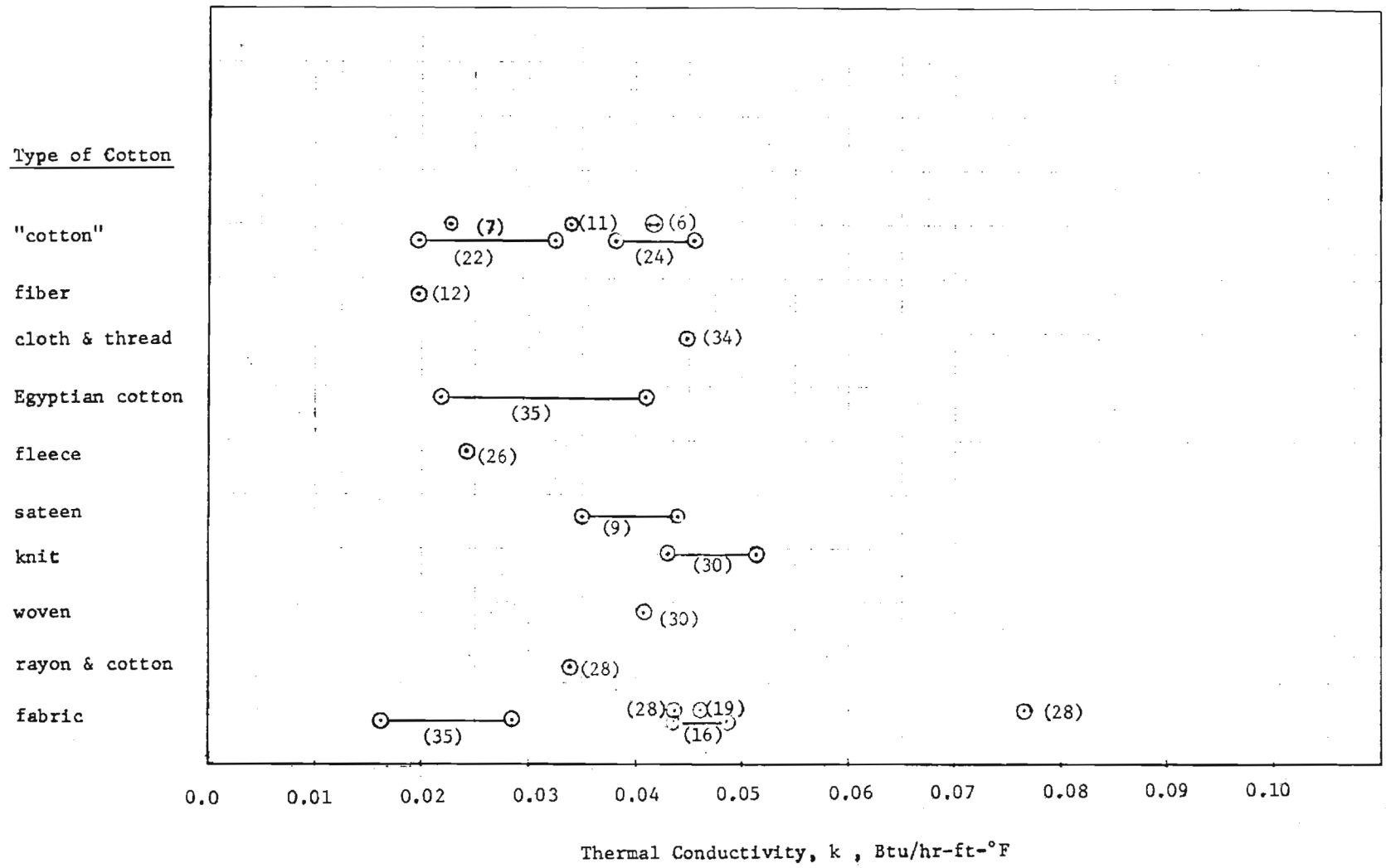

Figure C.3. Thermal Conductivity of Cotton Type Fabrics

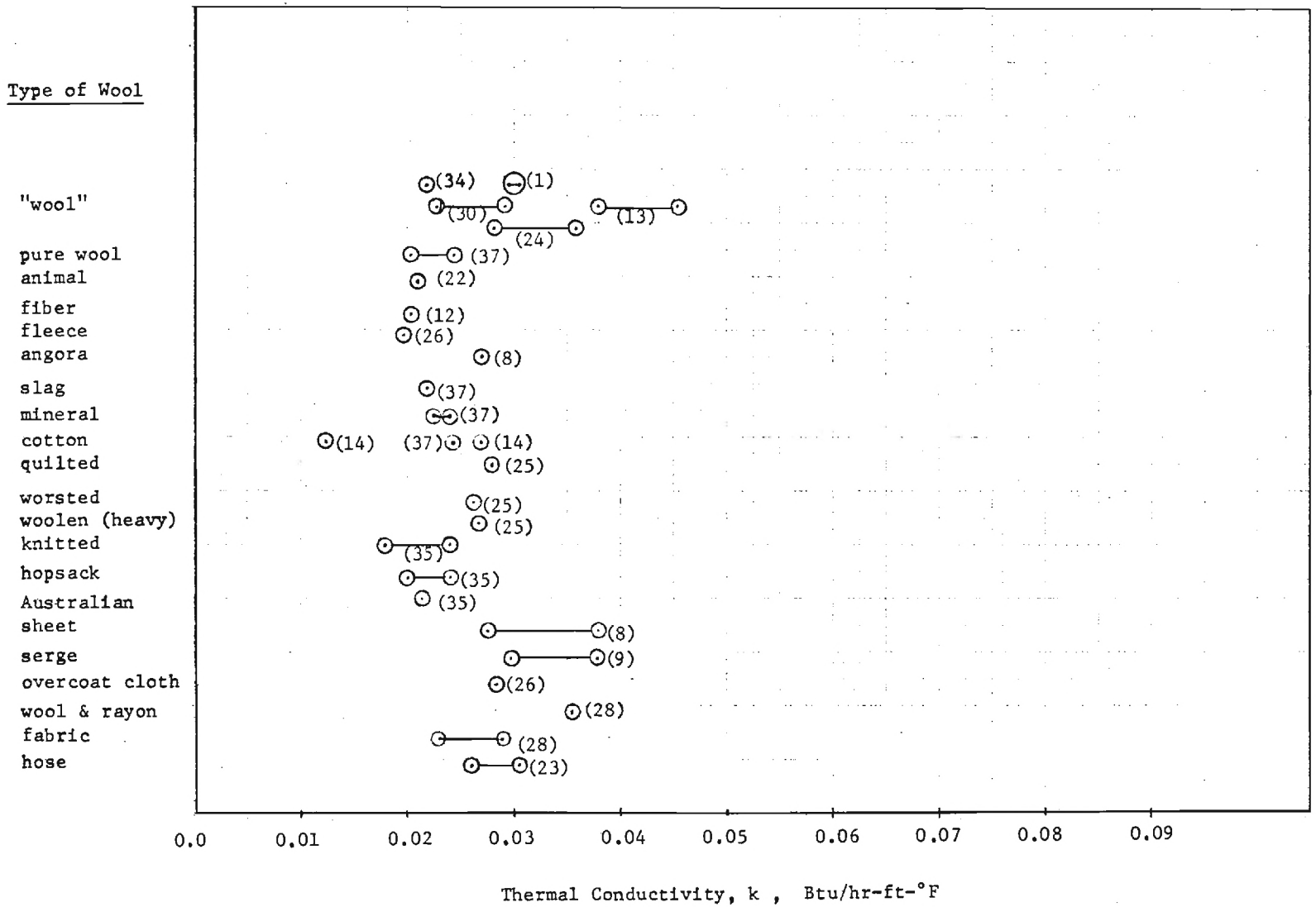

Figure C.4. Thermal Conductivity of Wool Type Fabrics

The effects of these parameters on thermal conductivity are discussed below.

a. Fiber Material. The thermal conductivity of fabrics results from two simultaneous processes (neglecting any absorbed moisture): conduction through the air and conduction through the textile fibers. Since typical fabrics are 70 to 90 percent air, the thermal conductivity of the air will control the thermal conductivity of the fabric, especially of low bulk density fabric.* The fiber material still has an effect on the overall conductivity, however.

Several researchers have determined the thermal conductivity of textile fibers using a matrix model to infer the fiber conductivity from the overall conductivity. Assuming the conductivity of air to be unity, Schuhmeister [C-33] found the relative value for cotton as 37, for wool 12, and for silk 11. Rubner [C-31] using Schuhmeister's method of calculation, gave the conductivity of wool as 6.1, of silk 19.2, and of cotton and linen 29.9, again taking the value of air to be 1. While there is some disagreement on the precise magnitudes, these conductivity values are much higher for the fibers than for fabrics. Peirce and Rees [C-26] state that the effect of fibers on fabric conductivity is due largely to mechanical properties of fibers which characterize thickness and fuzziness of the fabric, rather than to the thermal conductivity of the fiber.

---

*Bulk density refers to density of fabric as opposed to density of fiber.

Artificial fibers can be tested with greater accuracy since the sample can be produced in bulk form. For nylon, the relative conductivity was found to be 10 [C-6].

b. Density. As well as being dependent to some extent on the seven other parameters listed above, density depends on the film or thread size, and weave or fiber arrangement.

Generally the literature indicates that an increase in bulk density results in increase in thermal conductivity, e.g. [C-6,8,30]. Typical results are given in the following table:

Table C. 1. INFLUENCE OF BULK DENSITY ON THERMAL CONDUCTIVITY OF FABRICS

Material	Bulk Density (lbm/ft^3)	Thermal Conductivity (Btu/hr ft °F)
sheet wool [C.5]	8.1	0.0275
sheet wool	10.0	0.0326
wool [C.6]	11.0	0.0227
wool	13.2	0.0291
silk	18.7	0.0244
silk	27.4	0.0268
silk	29.0	0.0296
linen (mesh)	16.6	0.0382
linen (woven)	36.8	0.0406

Speakman and Chamberlain [C-35] suggest that weave structure affects the thermal conductivity only indirectly through the variations which it is able to cause in thickness and density.

Morris [C-25] correlated "thermal insulation" in units ($°C\ sec\ m^2/cal$) with "volume of air" in units (cm^2 air/cm fabric). He found that the dependence of thermal insulation on volume of air was approximately linear with the slope of unity. Bogaty [C-9] considered fiber arrangement in terms of fraction of fibers parallel and perpendicular to the surface of the fabric. He concludes that thermal conductivity is particularly dependent on bulk density as the number of fibers perpendicular to the fabric surface increases. Also, the thermal conductivity of the fabric is more sensitive to fiber arrangement as the fiber conductivity and density are increased. At a fixed density, the fabric conductivity is not very sensitive to the fiber conductivity when the fibers are parallel to the fabric surface, and heat conduction must occur through alternate layers of fiber and air. Bogaty further discusses the effect of mechanical pressure on the fiber arrangement, and hence on thermal conductivity. For smooth-surfaced fabrics such as cotton, nylon, and orlon, a change in pressure produces very little change in fiber arrangement. Thus, thermal conductivity increases with pressure because of the increase in fabric bulk density. For fuzzy-surfaced fabrics such as wool, the rise in pressure causes as increase in density and a change toward more parallel fiber arrangements, with the result that both effects on thermal conductivity counterbalance each other.

c. Mechanical Pressure. Most researchers have determined pressure effects on thermal conductivity indirectly by discussing the thermal insulation value (T.I.V.) or thermal resistance (togs) as a function of thickness which was measured at a specified pressure.

A direct proportionality between these quantities was reported in [C-13,25,26,32,35,39]. McLachlan et al [C-2] mention direct pressure effects for woolen hose. With a pressure of 1/2 psi, the thermal conductivity was found to be 0.0264 Btu/(hr ft F). Doubling this pressure caused the thermal conductivity to increase 10 percent.

Beyond a pressure of 3.55 psi, the conductivity was constant at a value 17 percent higher than the value at 1.2 psi.

d. Moisture Content. In considering this parameter, a general distinction can be made between water vapor, measured as relative humidity of the air surrounding the fabric, and liquid water absorbed by the fibers in the fabric.

Rees [C-28] determined the effect of relative humidity upon heat loss using wool, cotton and rayon blankets in atmospheres of 33, 53, 65, 75 and 88 percent relative humidity. An increase of 55 percent in the relative humidity from 33 to 88 percent, increased the heat loss of the wool blanket by about 10 percent and that of the cotton blanket by about 3 percent. Here "increase in heat loss" can be loosely interpreted as an increase in thermal conductivity.

The literature concerned with absorbed moisture by the fibers is in general agreement that an increase in moisture results in an increase in thermal conductivity, the magnitude of the increase being generally proportional to the bulk density increase [C-6,21, 23,30,36]. Rood [C-30] and Staff [C-3] agree in general that the thermal conductivity of wool and cotton samples increases by 1 to 2 percent for a 1 percent increase in weight of the fabric due to

absorbed moisture. On the other hand, Lees and Chorlton [C-21] record a 10 to 20 percent increase in conductivity for a 1 to 2 percent increase in moisture. In the limit the thermal conductivity of saturated woolen hose (300 percent increase in weight) was found to be 0.221 Btu/(hr ft F) compared to the value of 0.0305 Btu/(hr ft F) at 50 percent relative humidity.

e. Temperature. The variation of thermal conductivity with temperature is shown on Figure C-2 for asbestos and air (see top of graph). The temperature dependence for fabrics, however, is mentioned only by Baxter [C-6] in relation to temperature profiles in multiple layers. He claimed little change in conductivity with increasing number of layers in most cases, where an increase was shown, there was also an increase in temperature. The thermal conductivity of fabrics would be expected to change appreciably over the temperature range of interest for ignition studies but this parameter does not appear to have been evaluated in the literature.

f. Treatment. Fletcher and Sherwood [C-3] show a variation of thermal conductivity with color (or dyeing) for rayon and wool, as shown in the table below.

Table C.2 INFLUENCE OF FABRIC DYE ON THERMAL CONDUCTIVITY [C-3]

Rayon	
Light red	0.0537 Btu/(hr ft F)
Dark red	0.0469
Wool	
Dark blue	0.0452
Light brown	0.0378

g. History of Utilization. Fletcher and Sherwood [C-3] did a limited investigation of the effect of dry cleaning on thermal conductivity and concluded that the effect was negligible. Phelps, Morris, and Lund [C-2] studied extensively the effect of wear and dry cleaning on the thermal conductivity of flannel and serge. As shown in Table C-3, dry cleaning 5 or 10 times decreased the conductivity, however, a slight increase is noted between 10 and 15 dry cleanings.

Table C.3. EFFECT OF DRY CLEANING ON THERMAL CONDUCTIVITY [C-2]

Material	Treatment	k (Btu/(hr ft F))
Flannel - 25 pound new wool	New	0.0290
	Dry clean 5 times	0.0266
	Dry clean 10 times	0.0266
	Dry clean 15 times	0.0290
Serge 14 oz/yd	New	0.0460
	Dry clean 5 times	0.0412
	Dry clean 10 times	0.0339
	Dry clean 15 times	0.0387

Additional experiments indicated a definite effect of combined wear and dry cleaning; however, the trends were not consistent for the two fabrics. These results suggest that wear and dry cleaning affect different fabrics in a variety of ways, causing different effects on the thermal conductivity.

h. Multiple Layer Composition. Several authors discuss the effect of multiple layers on thermal conductivity, but there is little agreement among their results. The disagreement is due to

a great extent to the variability of contact resistance between the layers. Baxter [C-6] and McLachlan et al [C-23] state that the thermal conductivity varies insignificantly with the number of fabric layers. Morris [C-25] compared two methods of determining the thermal insulation (°C sec m^2/cal) of multiple layers by adding the values for individual layers and measuring the combined layers. She found significant differences between the two methods, especially for fabrics with rough surfaces that have poor contacts between fabric layers. Peirce and Rees [C-26], however, found the thermal resistance (togs) of several layers, to be equal to the sum of the resistances of the separate layers, showing that the contact resistance was negligible. Griffiths and Kaye [C-16] compared several layers (up to nine) of silk fabric and found that thermal conductivity increases considerably as the number of layers increases. Rood [C-30] also determined that thermal conductivity increases with the number of layers. The apparent anomaly in these last two investigations is due partially to the reduction in the air gap resistance per layer as the cloth samples were stacked up. Some increase in pressure would also be expected with a large number of layers.

Appendix C.3

Literature Review on Radiative Fabric Properties

Total, hemispherical emittance and absorptance measurements have been reported in the open literature by Hartnett, Eckert and Birkebak [C-46] for solar irradiation and blackbody irradiation at 350°F. Their interest was in parachute materials, nylon and dacron. Solar reflectances range from 0.22 to 0.60, solar absorptivities range from 0.05 to 0.19, while infrared absorptivities vary from 0.72 to 0.90. Table C-5 lists infrared (blackbody temperature of 350°F) radiation properties for some nylon and dacron fabrics.

Table C.4. RADIATION PROPERTIES FOR NORMALLY INCIDENT BLACKBODY RADIATION AT 350°F [C.20]

	Reflectivity	Transmissivity	Absorptivity
Dacron, 100 lb tensile str.	0.08	0.17	0.75
800 lb tensile str.	0.07	0.03	0.90
Nylon rip-stop			
orange 1.1 oz/yd	0.05	0.19	0.76
white 1.1 oz/yd	0.06	0.21	0.73
cloth 14 oz/yd	0.10	0.04	0.86

Spectral fabric characteristics have been measured by Dunkle, Ehrenburg and Gier [C-47] on cotton, linen, wool, silk, acetate, armel, rayon, dacron, orlon and nylon. Spectral reflectance curves are presented for single and multiple fabric layers and show in general several steep peaks in the near infrared spectrum (mostly below 2 μm) but flat trends in the far infrared, fluctuating about 0.20. These results indicate spectral insensitivity for infrared irradiation but strongly increasing reflectivity near the visible spectrum. The screening effect (see Section a above) appears to be insignificant, but color exerts some influence. Aluminized cotton reflects four times as strongly as deep black cotton.

Several reports related to optical fabric properties have been written under Government contracts and are presently being retrieved.

BIBLIOGRAPHY

A. Cited References

I-1. Government-Industry Research Committee on Fabric Flammability, "Study of Hazards from Burning Apparel and the Relation of Hazards to Test Methods." A work statement prepared by the Research Committee, Dr. E. Passaglia, Chairman, National Bureau of Standards, June 5, 1970.

I-2. Tribus, M. "Decision Analysis Approach to Satisfying the Requirements of the Flammable Fabrics Act." Paper presented at the Textile and Needle Trades Division, American Society of Quality Control, Greensboro, North Carolina, February 12, 1970.

I-3. Evans, R. B., Wulff, W. and Zuber, N. "The Study of Hazards from Burning Apparel and the Relation of Hazards to Test Methods," research proposal submitted by the School of Mechanical Engineering, Georgia Institute of Technology, to the Government Research Committee, July 1970.

II-1. Alkidas, A., Hess, R. W., Kirkpatrick, C. S., Kirkpatrick, M. J., Bergles, A. E., Wulff, W. and Zuber, N., "Study of Hazards from Burning Apparel and the Relation of Hazards to Test Methods," Progress Report No. 1, Georgia Institute of Technology, April 1, 1971.

II-2. Alkidas, A., Hess, R. W., Kirkpatrick, C. S., Bergles, A. E., Wulff, W., and Zuber, N., "Study of Hazards from Burning Apparel and the Relation of Hazards to Test Methods," Progress Report No. 2, Georgia Institute of Technology, July 1, 1971.

II-3. Kalekar, A. S. and Kung, H. C., "A Study of Pre-Ignition Heat Transfer Through a Fabric-Skin System Subjected to a Heat Source," Third Progress Report, Factory Mutual Research Corporation, March 31, 1971.

II-4. Goldsmith, A., Waterman, T. E. and Hirschorn, H. J. Handbook of Thermophysical Properties of Solid Materials, McMillan, 1961.

III-1. Frank, R. Steward, "Ignition Characteristics of Cellulosic Materials," presented at the Eastern States Section Meeting of the Combustion Institute, August 30-31, (1971), University of Waterloo, Ontario, Canada.

III-2. Martin, S., "Diffusion-Controlled Ignition of Cellulosic Materials by Intense Radiant Energy," Tenth Symposium (International) on Combustion, the Combustion Institute, Pittsburgh, 877-896, (1965).

III-3. Lawson, D. I. and Simms, D. L., "The Ignition of Wood by Radiation," Journal of Applied Physics, 3, 288-292, (1952).

III-4. Alvares, N. J., Blackshear, P. L. and Murty, Kanury, A., "The Influence of Free Convection on Ignition of Vertical Cellulosic Panels by Thermal Radiation," Combustion Science and Technology, 1, 407-413, (1970).

III-5. Carslaw, H. S. and Jaeger, J. C., Conduction of Heat in Solids, Second Edition, Oxford University Press, London, 1959.

III-6. Alkidas, A., Hess, R. W., Kirkpatrick, C. S., Bergles, A. E., Wulff, W. and Zuber, N., "Study of Hazards from Burning Apparel and the Relation of Hazards to Test Methods," Progress Report No. 2, Georgia Institute of Technology, July 1, 1971.

III-7. Akita, K. and Kase, M., "Determination of Kinetic Parameters for Pyrolysis of Cellulose and Cellulose Treated with Ammonium Phosphate by Differential Thermal Analysis and Thermal Gravimetric Analysis," Journal of Polymer Science, Part A-1, Volume 5, 833-884, (1967).

III-8. Kalekar, A. S. and Kung, H. C., "A Study of Pre-Ignition Heat Transfer Through a Fabric-Skin System Subjected to a Heat Source," Third Progress Report, Factory Mutual Research Corporation, March 31, 1971.

B-1. Setchkin, N. P., "A Method and Apparatus for Determining the Ignition Characteristics of Plastics," Journal of Research of the National Bureau of Standards, Research Paper RP 2052, Vol. 43, (1949), 591-605.

B-2. Siegel, R. and Howell, J. R., Thermal Radiation Heat Transfer, NASA SP-164, Vol. I.

B-3. Kourganoff, V., Basic Methods in Transfer Problems, Dover, New York, 1963.

B-4. Heat Transfer Laboratories, Inc., St. Paul, Minnesota, "Integrating Sphere Radiometer," a Manual for Model No. ISR-1A.

C-1. Spalding, D. B., "The Art of Partial Modeling," Ninth Symposium (International) on Combustion, The Combustion Institute, Academic Press, (1963).

C-2. Williams, F. A., "Scaling Mass Fires," Fire Research Abstracts and Reviews, Vol. 11, No. 1, (1969), 1-23.

C-3. Newman, A. B. and Green, L., "The Temperature History and Rate of Heat Loss of an Electrically Heated Slab," Trans. Electrochemical Soc., Vol. 66, 1934, 345-358.

C-4. Carslaw, H. S. and Jaeger, J. C., Conduction of Heat in Solids, Oxford at the Clarendon Press, London, (1959).

C-5. Schneider, P. J., Temperature Response Charts, John Wiley & Sons, Inc., New York, (1963).

C-6. Baxter, S., "Thermal Conductivity of Textiles," Proc. Phys. Soc., Vol. 58, (1946), 105-707.

C-7. Baxter, S. and Cassie, A. B. D., "Thermal Insulating Properties of Clothing," J. Textile Inst. Trans., Vol. 34 (July 1943), 141-154.

C-8. Bettini, T. M., "Ricerche Preliminari Sulla Resistenza Termica Della Lana Angora," Ric. Sci., Vol. 20, No. 4, (April 1950), 464-466.

C-9. Bogaty, H. N., Hollies, R. S. and Harris, M., "Some Thermal Properties of Fabrics," Textile Research Journal, (January 1957), 445-449.

C-10. Freedman, E., "Thermal Transmission of Fabrics," The Melliand, Vol. 2, No. 5, (August 1930), 701-707.

C-11. Eckert, E. R. G., Introduction to the Transfer of Heat and Mass, McGraw-Hill Book Company, Inc., 1950.

C-12. Elliot, A. N., "Heat Insulators," Textile World, Vol. 84, (January 1934), 84.

C-13. Fletcher, H. M. and Sherwood, H. M. S., "Wool and Rayon Gabardines," American Dyestuff Reporter, Vol. 32, (1943), 280-296.

C-14. Forbes, G., "On the Thermal Conductivity of Ice, and a New Method of Determining the Conductivity of Different Substances," Royal.Soc. of Edinburgh Proc., Vol. 8, (November 1872-July 1875), 62-68.

C-15. Gebhart, B., Heat Transfer, McGraw-Hill Company, Inc., New York, (1961).

C-16. Griffiths, E., and Kaye, G. W. C., "The Measurement of Thermal Conductivity," Proc. Roy. Soc. (London) 104A, (1923), 71-98.

C-17. Hoffman, R. N. and Beste, L. F., "Some Relations of Fiber Properties to Fabric Handling," Textile Research Journal, Vol. 21, No. 1, (January 1951), 66-77.

C-18. Holman, J. P., Heat Transfer, Second Edition, McGraw-Hill Book Company, New York (1968).

C-19. Kreith, F., Principles of Heat Transfer, Second Edition, International Textbook Company, (1965).

C-20. Lees, C. H., "On the Thermal Conductivities of Crystals and Bad Conductors," Phil Trans. Soc. London, Vol. 183, (1892), 481-509.

C-21. Lees, C. H. and Chorlton, J. D., "On a Simple Apparatus for Determining the Thermal Conductivities of Cements and Other Substances used in the Arts," Phil. Mag. Vol. 41, (1896), 495-503.

C-22. McAdams, W. H., Heat Transmission, 3rd Edition, McGraw-Hill Book Company, Inc., New York, (1954).

C-23. McLachlan, N. W., Goodfellow, H. and Cushnie, H. C., "Thermal Conductivity of Shoe Materials," Journal of the International Society of Leather Trades' Chemists, Vol. 26, (February 1942), 23-43.

C-24. Anonymous, Melliand Textilber, "The Heat Conductivity of Textile Fibers," Vol. 18, (1937), 684-687.

C-25. Morris, M. A., "Thermal Insulation of Single and Multiple Layers of Fabrics," Textile Research Journal, Vol. 25, No. 1, (January 1955), 766-773.

C-26. Peirce, F. T. and Rees, W. H., "The Transmission of Heat Through Textile Fabrics-Part II," The Journal Textile Institute Trans., Vol. 37, (1946).

C-27. Phelps, E. L., Morris, M. A. and Lund, L. O., "The Thermal Conductivity of Selected Flannel and Serge Fabrics Before and After Wear," American Dyestuff Reporter, Vol. 45, No. 7, (March 26, 1956), 181-183.

C-28. Rees, W. H., "The Transmission of Heat Through Textile Fabrics," Journal of the Textile Institute Trans., Vol. 32, (August 1941), 148-165.

C-29. Rohsenow, W. M. and Choi, H., Sea, Mass and Momentum Transfer, Prentice-Hall, Inc., Englewood Cliffs, New Jersey, (1961).

C-30. Rood, E. S., "Thermal Conductivity of Some Wearing Materials," The Physical Review, Vol. 18, Series II, 1921, 356.

C-31. Rubner, M., "Das Wärmeleitungsvermögen der Grundstoffe unserer Kleidung," Archiv fuer Hygiene und Bakteriologie, Vol. 24, (1895), 265-345.

C-32. Sale, P. D. and Hedrick, A. F., "Measurement of Heat Insulation and Related-Properties of Blankets," National B. S. Technolog. Papers, No. 266, Vol. 18, (1924), 529-546.

C-33. Schumeister, Ber. K. Akad. Wien (Math-Naturn. Klasse), Vol. 76, (1877), 283.

C-34. Shimizn, S. and Nisihuzi, I., "Thermal Properties of Electric Materials," Denki-Kagaku Kyokai or in English: J. Electrochem. Assoc. Japan, Vol. 8, (1940), 94-101.

C-35. Speakman, J. B. and Chamberlain, N. H., "Thermal Conductivity of Textile Materials and Fabrics," Journal Textile Inst. Trans., Vol. 21, (1930), 29-56.

C-36. Staff, H., "The Effect of Humidity on the Thermal Conductivity of Wool and Cotton," Abstract, The Phys.Review, Vol. 25, (January-June 1925), 252.

C-37. Van Dusen, M. S., "The Thermal Conductivity of Heat Insulators," American Society of Heating and Vent. Eng. Trans., Vol. 26, No. 566, (1920), 385-414.

C-38. Wing, P. and Monego, C. J., "Thermal Insulation Measurement on Textiles - A Comparison of Two Methods," ASTM Bulletin, (October 1959), 29-33.

C-39. Winston, G. and Backer, S., "Measurement of the Thermal Transmission of Textile Fabrics," ASTM Bulletin, (December 1949), 62-67.

C-40. Brochure by the Carborundum Company, Polymer Systems Dept, Sanborn, New York.

C-41. Bates, J. J., and Monahan, T. I., "Research Report on Thermal Radiation Damage to Cloths as a Function of Time of Exposure, Rectangular Pulses," Laboratory Project 5046-3, Part 74, Final Report, Material Laboratory, New York Naval Shipyard, June 1950.

C-42. Patten, G. A., "Ignition Temperatures of Plastics," Modern Plastics, July 1961, 119.

C-43. Setchkin, N. P., "A Method and Apparatus for Determining the Ignition Characteristics of Plastics," Journal of Research of the National Bureau of Standards, Research Paper RP 2052, Vol. 43, (1949), 591-605.

C-44. Kuchta, J. M., et al, "Flammability of Fabrics and Other Materials on Oxygen - Enriched Atmospheres: Part I-Ignition Temperatures and Flame Spread Rates," Fire Technology, Vol. 1, (1969), 203-216.

C-45. Shimizu, S. and Nisihuzi, I., "Thermal Properties of Electric Materials," The Journal of the Electrochemical Association of Japan, (December 1940), 94-101.

C-46. Hartnett, J. P., Eckert, E. R. G., and Birkebak, R., "The Emissivity and Absorptivity of Parachute Fabrics," Journal of Heat Transfer, Vol. 81, No. 3, August 1959.

C-47. Dunkle, R. V., Ehrenburg, F. and Gier, J. T., "Spectral Characteristics of Fabrics," Journal of Heat Transfer, Vol. 82, No. 1, February 1960.

B. Related References

1. Bates, J. J. and Monahan, T. I., "Research Report on Thermal Radiation Damage to Cloths as a Function of Time of Exposure, Rectangular Pulses," Lab Project 5046-3, Part 74, Final Report, Material Laboratory, New York Naval Shipyard, June 1950.

2. Kuchta, J. M., et al, "Flammability of Fabrics and other Materials on Oxygen - Enriched Atmospheres: Part I Ignition Temperatures and Flame Spread Rates," Fire Technology, Vol. 1, (1969), 203-216.

3. Patten, G. A., "Ignition Temperatures of Plastics," Modern Plastics, July (1961), 119.

4. Hoffman, R. N. and Beste, L. F., "Some Relations of Fiber Properties to Fabric Handling," Textile Research Journal, Vol. 21, No. 1, (January 1951), 66-77.

5. Elliott, A. N., "Heat Insulators," Textile World, Vol. 84, (January 1934), 84.

6. Freedman, E., "Thermal Transmission of Fabrics," The Melliand, Vol. 2, No. 5, August 1930, 701-707.

7. Wing, P. and Monego, C. J., "Thermal Insulation Measurement on Textiles - A Comparison of Two Methods," ASTM Bulletin, (October 1959), 29-33.

8. Spalding, D. B., "The Art of Partial Modeling," Ninth Symposium (Internationally) on Combustion, The Combustion Institute, Academic Press, 1963.

9. Williams, F. A., "Scaling Mass Fires," Fire Research Abstracts and Reviews, Vol. 11, No. 1, (1969), 1-23.

10. Alkidas, A., Hess, R. W., Kirkpatrick, C. S., Mays, R. L., Wulff, W. and Zuber, N., "Study of Hazards from Burning Apparel and the Relation of Hazards to Test Methods," Progress Report No. 3, Georgia Institute of Technology, October 1, 1971.